

NAVAL POSTGRADUATE SCHOOL MONTEREY, CALIFORNIA



THESIS

**INVESTIGATION OF THE EFFECT OF
REYNOLDS NUMBER ON LAMINAR
SEPARATION BUBBLES ON CONTROLLED-
DIFFUSION COMPRESSOR BLADES IN
CASCADE**

by

David G. Schnorenberg

June, 1996

Thesis Advisor:

Garth V. Hobson

Thesis
S337975

Approved for public release; distribution is unlimited.

UDLEY KNOX LIBRARY
NAVAL POSTGRADUATE SCHOOL
MONTEREY CA 93943-5101

REPORT DOCUMENTATION PAGE

Form Approved OMB No. 0704-0188

Public reporting burden for this collection of information is estimated to average 1 hour per response, including the time for reviewing instruction, searching existing data sources, gathering and maintaining the data needed, and completing and reviewing the collection of information. Send comments regarding this burden estimate or any other aspect of this collection of information, including suggestions for reducing this burden, to Washington Headquarters Services, Directorate for Information Operations and Reports, 1215 Jefferson Davis Highway, Suite 1204, Arlington, VA 22202-4302, and to the Office of Management and Budget, Paperwork Reduction Project (0704-0188) Washington DC 20503.

1. AGENCY USE ONLY (Leave blank)		2. REPORT DATE June 1996		3. REPORT TYPE AND DATES COVERED Master's Thesis	
4. INVESTIGATION OF THE EFFECT OF REYNOLDS NUMBER ON LAMINAR SEPARATION BUBBLES ON CONTROLLED-DIFFUSION COMPRESSOR BLADES IN CASCADE.				5. FUNDING NUMBERS	
6. AUTHOR(S) David G. Schnorenberg					
7. PERFORMING ORGANIZATION NAME(S) AND ADDRESS(ES) Naval Postgraduate School Monterey CA 93943-5000				8. PERFORMING ORGANIZATION REPORT NUMBER	
9. SPONSORING/MONITORING AGENCY NAME(S) AND ADDRESS(ES)				10. SPONSORING/MONITORING AGENCY REPORT NUMBER	
11. SUPPLEMENTARY NOTES The views expressed in this thesis are those of the author and do not reflect the official policy or position of the Department of Defense or the U.S. Government.					
12a. DISTRIBUTION/AVAILABILITY STATEMENT Approved for public release; distribution is unlimited.				12b. DISTRIBUTION CODE	
<p>13. ABSTRACT (maximum 200 words)</p> <p>Detailed experimental investigation of second-generation, controlled-diffusion, compressor-stator blades at an off-design inlet-flow angle was performed in a low-speed cascade wind tunnel using various experimental procedures. The objective of the study was the characterization of the off-design flow and the detailed investigation of flow separation which occurred near mid-chord. When it was found that the flow separation behavior was strongly influenced by the Reynolds number, the effect of Reynolds number variation on flow separation was investigated. Surface flow visualization was performed to gain general insight into the flow behavior. Blade surface pressure measurements were obtained using instrumented blades, from which coefficients of pressure were calculated. Laser-Doppler velocimetry (LDV) was used to characterize the off-design flow upstream, in the passage between two blades, in the boundary layer on the suction side of the blades, and in the wake region.</p> <p>Overall, good comparisons between blade surface pressure measurements, LDV data and flow visualization were obtained for the separation region. At the highest Reynolds number, separation was turbulent and three-dimensional and at the low Reynolds number the separation was predominately laminar and two-dimensional.</p>					
14. SUBJECT TERMS Controlled-Diffusion, Compressor, Stator, Cascade, Turbomachinery				15. NUMBER OF PAGES 141	
				16. PRICE CODE	
17. SECURITY CLASSIFICATION OF REPORT Unclassified	18. SECURITY CLASSIFICATION OF THIS PAGE Unclassified	19. SECURITY CLASSIFICATION OF ABSTRACT Unclassified	20. LIMITATION OF ABSTRACT UL		

Approved for public release; distribution is unlimited.

**INVESTIGATION OF THE EFFECT OF REYNOLDS NUMBER ON
LAMINAR SEPARATION BUBBLES ON CONTROLLED-DIFFUSION
COMPRESSOR BLADES IN CASCADE**

David G. Schnorenberg
Captain, United States Marine Corps
B.S.A.E., University of Minnesota, 1987

Submitted in partial fulfillment
of the requirements for the degree of

MASTER OF SCIENCE IN AERONAUTICAL ENGINEERING

from the

**NAVAL POSTGRADUATE SCHOOL
June 1996**

ABSTRACT

Detailed experimental investigation of second-generation, controlled-diffusion, compressor-stator blades at an off-design inlet-flow angle was performed in a low-speed cascade wind tunnel using various experimental procedures. The objective of the study was the characterization of the off-design flow and the detailed investigation of flow separation which occurred near mid-chord. When it was found that the flow separation behavior was strongly influenced by the Reynolds number, the effect of Reynolds number variation on flow separation was investigated. Surface flow visualization was performed to gain general insight into the flow behavior. Blade surface pressure measurements were obtained using instrumented blades, from which coefficients of pressure were calculated. Laser-Doppler velocimetry (LDV) was used to characterize the off-design flow upstream, in the passage between two blades, in the boundary layer on the suction side of the blades, and in the wake region.

Overall, good comparisons between blade surface pressure measurements, LDV data and flow visualization were obtained for the separation region. At the highest Reynolds number, separation was turbulent and three-dimensional and at the low Reynolds number the separation was predominately laminar and two-dimensional.

TABLE OF CONTENTS

I. INTRODUCTION	1
A. BACKGROUND	1
B. PURPOSE	2
II. EXPERIMENTAL SETUP	3
A. LOW-SPEED CASCADE WIND TUNNEL.....	3
B. INSTRUMENTATION.....	4
III. EXPERIMENTAL PROCEDURE	9
A. BLADE SURFACE PRESSURE DISTRIBUTIONS	9
B. SURFACE FLOW VISUALIZATION.....	9
C. LDV MEASUREMENTS	10
1. LDV Probe Volume Alignment.....	10
2. Inlet Guide Vanes Adjustment.....	10
3. LDV Surveys	10
a. Inlet Surveys.....	11
b. Passage Surveys.....	11
c. Boundary Layer Surveys.....	12
d. Wake Surveys	12
IV. RESULTS AND DISCUSSION.....	15
A. PRELIMINARY INVESTIGATION AT DESIGN INCIDENCE	15
B. MEASUREMENTS AT OFF-DESIGN INCIDENCE	15
1. Blade Surface Pressure Distribution	15
2. Flow Visualization	16
3. LDV Measurements at Reynolds Number of 640,000.....	17
a. Inlet Surveys.....	17
b. Passage Surveys.....	18

c. Boundary Layer Surveys.....	19
d. Wake Surveys	21
4. LDV Measurements at Reynolds Number of 380,000.....	21
5. LDV Measurements at Reynolds Number of 210,000.....	22
a. Inlet Surveys.....	22
b. Boundary Layer Surveys.....	23
c. Wake Surveys.....	26
C. SUMMARY	26
V. CONCLUSIONS AND RECOMMENDATIONS	61
A. CONCLUSIONS.....	61
B. RECOMMENDATIONS	62
APPENDIX A. LDV SUMMARY AND REDUCED DATA	63
APPENDIX B. REFERENCE VELOCITY INPUT AND OUTPUT DATA	101
APPENDIX C. INVESTIGATION AT DESIGN INCIDENCE.....	105
APPENDIX D. LDV MEASUREMENTS AT $Re=380,000$	113
LIST OF REFERENCES	123
INITIAL DISTRIBUTION LIST.....	125

LIST OF FIGURES

1. NPS Low-Speed Cascade Wind Tunnel	5
2. Stator 67B Blade Profile	6
3. Fully-Instrumented Blade Pressure Tap Locations	6
4. Survey Station Numbering and Position.....	7
5. LDV System.....	13
6. LDV Survey Locations	14
7. Experimental Cp Distribution at $Re=640,000$	27
8. Experimental Cp Distribution at $Re=380,000$	28
9. Experimental Cp Distribution at $Re=210,000$	29
10. Experimental Cp Distributions	30
11. Blade Surface Flow Visualization at $Re=640,000$	31
12. Blade Surface Flow Visualization at $Re=380,000$	32
13. Blade Surface Flow Visualization at $Re=210,000$	33
14. Station 1 Inlet Survey Results at $Re=640,000$	34
15. Station 1 Inlet Survey Results at 3000 Data Points	35
16. Station 3 Inlet Survey Results at $Re=640,000$	36
17. Station 5 Passage Survey Results at $Re=640,000$	37
18. Station 8 Passage Survey Results at $Re=640,000$	38
19. Station 10 Passage Survey Results at $Re=640,000$	39
20. Station 5 Boundary Layer Survey Results at $Re=640,000$	40
21. Station 7 Boundary Layer Survey Results at $Re=640,000$	41
22. Station 9 Boundary Layer Survey at Results at $Re=640,000$	42
23. Station 13 Wake Survey Results at $Re=640,000$	43
24a. Station 13 Wake Flow Angle Distribution at Design Indidence	44
24b. Station 13 Wake Flow Angle Distribution at Off-Design Incidence	44
25. Station 1 Inlet Survey Results at $Re=210,000$	45

26. Station 3 Inlet Survey Results at $Re=210,000$	46
27. Station 5 Boundary Layer Survey Results at $Re=210,000$	47
28. Station 6 Boundary Layer Survey Results at $Re=210,000$	48
29a. Station 7 Boundary Layer Survey Results at $Re=210,000$	49
29b. Station 7 Boundary Layer Survey Results at $Re=210,000$	50
29c. Station 7 Axial Velocity Histograms	51
30a. Station 7.25 Boundary Layer Survey Results at $Re=210,000$	52
30b. Station 7.25 Axial Velocity Histograms	53
31a. Station 7.5 Boundary Layer Survey Results at $Re=210,000$	54
31b. Station 7.5 Axial Velocity Histograms	55
32. Station 7.75 Boundary Layer Survey Results at $Re=210,000$	56
33. Station 8 Boundary Layer Survey Results at $Re=210,000$	57
34. Station 9 Boundary Layer Survey Results at $Re=210,000$	58
35. Station 13 Wake Survey Results at $Re=210,000$	59
36. Flow Structure Variation with Reynolds Number	60
37a. Station 7 Boundary Layer Survey Results at Design Incidence (Present study)	107
37b. Station 7 Boundary Layer Survey Results at Design Incidence (Fron Ref. 3)	108
38. Station 7.5 Boundary Layer Survey Results at Design Incidence	109
39. Station 6 Boundary Layer Survey Results at Design Incidence	110
40. Station 8 Boundary Layer Survey Results at Design Incidence	111
41. Station 1 Inlet Survey Results at $Re=380,000$	115
42. Station 3 Inlet Survey Results at $Re=380,000$	116
43. Station 5 Boundary Layer Survey Results at $Re=380,000$	117
44. Station 6 Boundary Layer Survey Results at $Re=380,000$	118
45. Station 7 Boundary Layer Survey Results at $Re=380,000$	119
46. Station 8 Boundary Layer Survey Results at $Re=380,000$	120
47. Station 9 Boundary Layer Survey Results at $Re=380,000$	121
48. Station 13 Wake Survey Results at $Re=380,000$	122

LIST OF SYMBOLS

c	blade chord
$c_{uv} = \frac{\overline{u'v'}}{\sqrt{\overline{u'^2}} \sqrt{\overline{v'^2}}}$	correlation coefficient
c_{ac}	blade axial chord
C_p	coefficient of pressure
d	distance from the blade surface
P_s	Prandtl static pressure
P_t	Prandtl total pressure
Re	Reynolds number
S	blade pitch/spacing
$T_u = \frac{\sqrt{\overline{u'^2}}}{V_{ref}}$	axial turbulence intensity
$T_v = \frac{\sqrt{\overline{v'^2}}}{V_{ref}}$	tangential turbulence intensity
U	axial velocity component
u'	axial fluctuating velocity
$\overline{u'v'}$	Reynolds stress
V	tangential velocity component
V_{ref}	reference velocity
v'	tangential fluctuating velocity
$W = \sqrt{U^2 + V^2}$	total velocity
x	axial direction
y	tangential direction
β_1	tunnel inlet flow angle

β_{1w}	tunnel sidewall setting angle
β_2	tunnel outlet angle
β_{2w}	tunnel tailboard setting angle
$\sigma = \frac{c}{S}$	blade solidity
η	axis normal to blade chord
ξ	axis tangent to blade chord

ACKNOWLEDGMENTS

I would like to acknowledge the financial support of NAVAIR, which sponsored this work as part of the fan and compressor stall project.

I wish to thank Professor Garth Hobson for his friendship, patience and endless enthusiasm towards my project. I am grateful to Professor Raymond Shreeve for his guidance and motivation which inspired me throughout. Also thanks to Rick Still and Thad Best for their continuous support and technical expertise. Finally, I thank Jennifer, my wife and best friend, for her understanding, encouragement and patience during the past year.

I. INTRODUCTION

A. BACKGROUND

Compressor stall and off-design performance behavior limit the performance attainable in aircraft gas turbine engines. Compressor stall can lead to degradation in engine performance to the point of total loss of engine power. Advances in compressor technology in general, and compressor blade design specifically, have benefited from ongoing gas turbine engine research and development. Compressor blade designs have progressed over the years with the overall goals of increased blade loading with high efficiency at the design point, and a wide stall-free range at off-design conditions. Towards this end, Controlled-Diffusion (CD) blading was developed.

Controlled-Diffusion blading is shaped such that the adverse pressure gradient, which must occur on the suction surface of the blading, is controlled so that the boundary layer will not separate. This approach allowed the blading to be more highly loaded, giving more turning for a given number of blades (or solidity), or the same turning with fewer blades (lower solidity). In either case, fewer blades were required for the same compressor pressure ratio leading to a reduction in total engine weight.

The CD compressor blades investigated in the current study were designed by Thomas F. Gelder of NASA Lewis Research Center [Ref. 1]. The compressor stator profiles were Stator 67B blades, which, together with Rotor 67, comprised Compressor Stage 67B. The Stator 67B blades were second generation CD blades which were designed as an improvement over Stator 67A, a first generation CD blade designed by Nelson Sanger [Ref. 2]. Previous to the current study, ten midspan Stator 67B blades were machined from aluminum and installed in the Naval Postgraduate School (NPS) Turbopropulsion Laboratory (TPL) Low-Speed Cascade Wind Tunnel (LSCWT). Hansen [Ref. 3] examined the flow through the blading at the design inlet-flow angle of

36.3 degrees using laser-Doppler velocimetry (LDV) and pressure probe measurements, with the goal being the characterization of the flow at the design inlet-flow angle and the validation of the design itself.

B. PURPOSE

The objective of the current study was the characterization the flow at an off-design inlet-flow angle of 38 degrees. An initial investigation of the growth of a suspected separation region detected by Hansen [Ref. 3] near-mid chord was also performed. Throughout the progression of the current study, it was noted that the flow separation behavior was strongly influenced by Reynolds number. Therefore, the effect of Reynolds number variation on flow separation was investigated. LDV measurements, flow visualization and blade surface pressure measurements were the primary experimental measurement techniques.

II. EXPERIMENTAL SETUP

A. LOW-SPEED CASCADE WIND TUNNEL

The subsonic cascade wind tunnel contained 10 Stator 67B controlled-diffusion blades. A schematic of the cascade is shown in Figure 1. A detailed description of the test facility and test section was fully documented in Reference 3. Elazar [Ref. 4] thoroughly documented the uniformity of tunnel flow conditions and the flow periodicity in the cascade test section with 20 Stator 67A blades at approximately 40 (design), 43 and 46 degrees inlet-flow angle. The tunnel was initially configured for a design inlet-flow angle (β_1) of 36.3 degrees, and later reconfigured for an inlet-flow angle of 38 degrees. Reference 3 contains a description of the procedure utilized to configure the inlet flow angle.

Each blade was 254 mm in span, 127.25 mm in chord and separated by 152.4 mm in the pitchwise direction. Reference 3 contains the machine coordinates used to manufacture the blades as well as a detailed description of the blade alignment procedure. Figure 2 shows the Stator 67B blade profile. Two partially instrumented blades containing eight pressure taps each were installed at blade locations 2 and 8 (Figure 1). A fully-instrumented blade containing 42 pressure taps was installed at blade location 6. Figure 3 shows the pressure tap locations of the fully instrumented blade. Additionally, blades 3 and 4 were anodized black to minimize light scatter during LDV measurements. The LDV test section between blades 3 and 4 is shown in Figure 4, with the locations of the 13 survey locations indicated as fractions of the axial chord (C_{ac}).

B. INSTRUMENTATION

Blade surface pressure measurements were recorded using a 48-channel Scanivalve system controlled by a HP-9000 computer. A full description of the data acquisition system is given in Reference 5.

Surface flow visualization results were photographed using a 8 mm video camera and a 35 mm SLR camera.

A two-component, four-beam TSI model 9100-7 LDV system was used for all flow field measurements. Elazar [Ref. 4] thoroughly documented the LDV setup, including laser type, optics, atomizer and seeding. Murray [Ref. 6] discussed the traverse mechanism and data acquisition system. The LDV and traverse mechanism were controlled by a personal computer. All experimental data were acquired and processed using TSI FIND software. The LDV and traverse systems are shown in Figure 5.

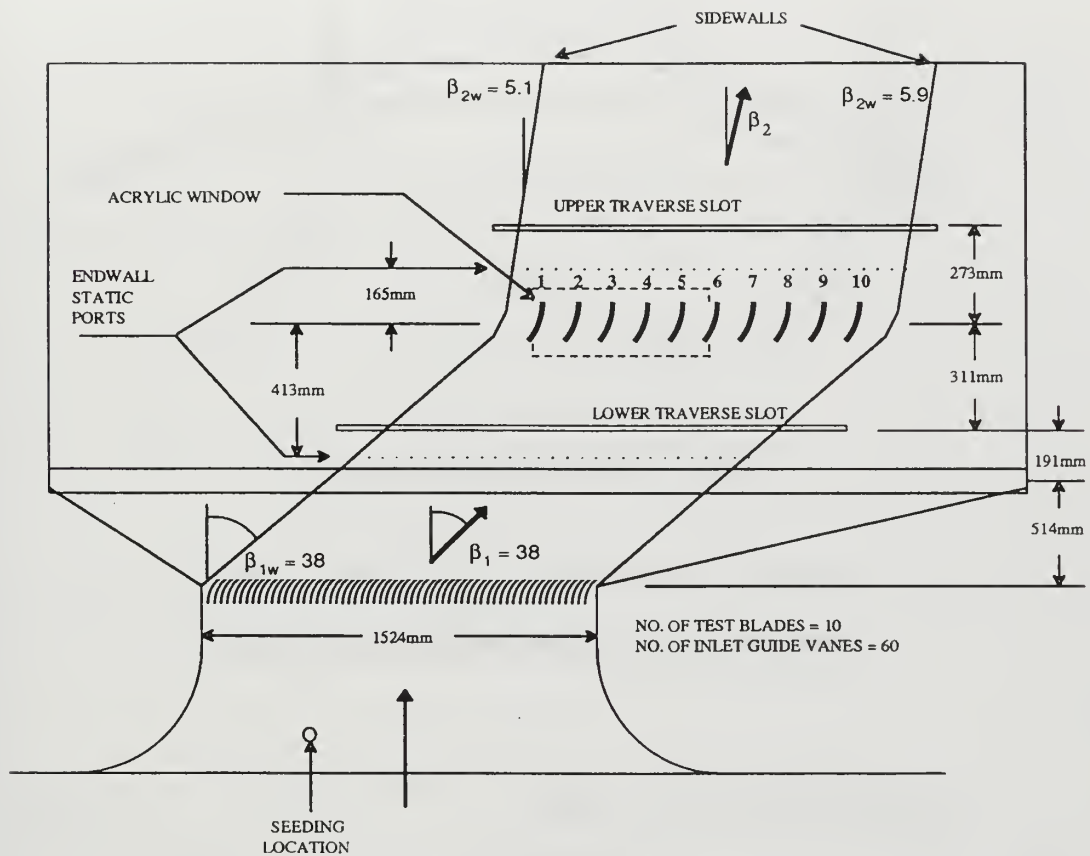


Figure 1. NPS Low-Speed Cascade Wind Tunnel

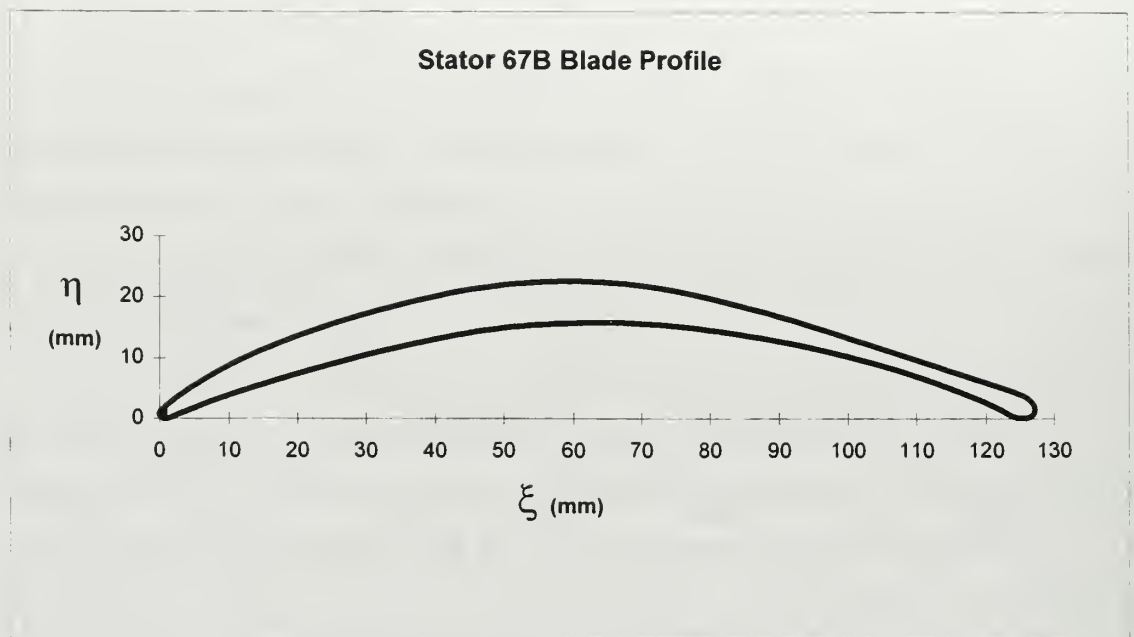


Figure 2. Stator 67B Blade Profile.

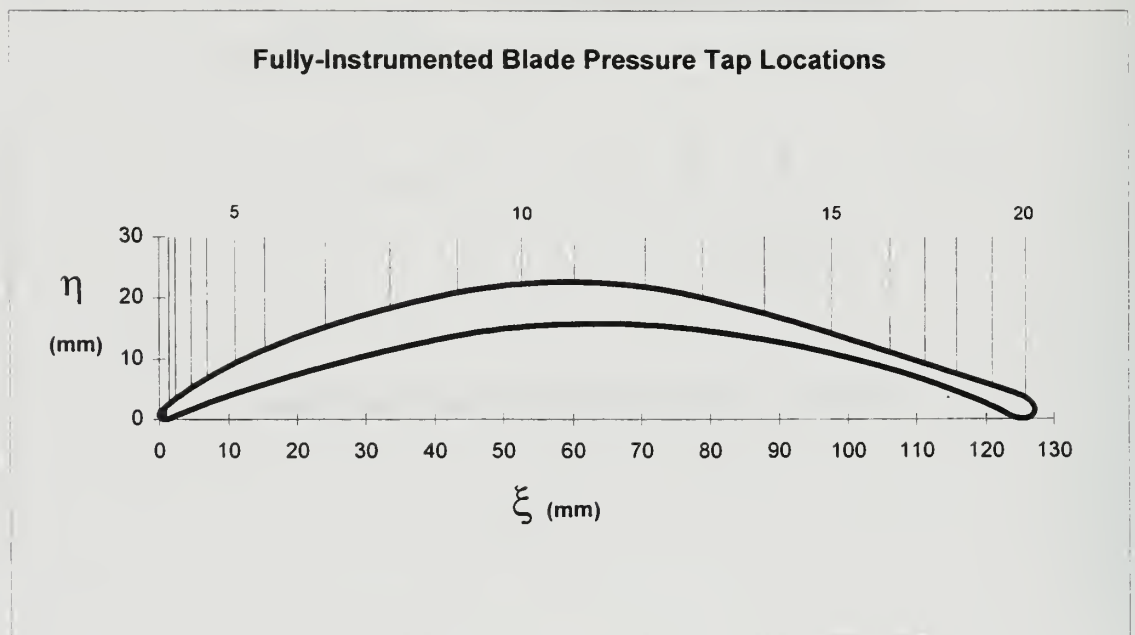


Figure 3. Fully-Instrumented Blade Pressure Tap Locations.

Survey Station Numbering and Location in Terms of Axial Chord

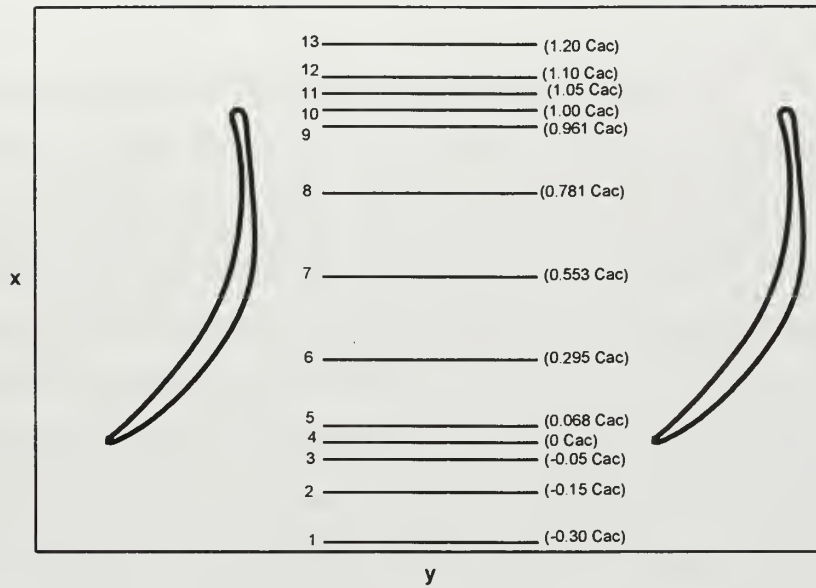


Figure 4. Survey Station Numbering and Position.

Blade Type	Stator 67B Controlled-Diffusion
Number of Blades	10
Blade Spacing	152.4 mm
Chord	127.14 mm
Solidity	0.834
Thickness/Chord	0.05
Setting Angle	16.3° +/- 0.1°
Span	254.0 mm

Table 1. Test Section Data.

III. EXPERIMENTAL PROCEDURE

A. BLADE SURFACE PRESSURE DISTRIBUTIONS

The cascade tunnel was allowed to reach an equilibrium plenum temperature prior to all surveys. Blade surface pressure measurements were taken using the HP Automated Data Acquisition System as described in Appendix B of Reference 5. Inlet total and static pressures were recorded to non-dimensionalize the blade surface pressure measurements as a coefficient of pressure; i.e., $C_p = (p_{\text{local}} - p_{\infty}) / (p_{\text{t}\infty} - p_{\infty})$. Pressure distributions were recorded at three different cascade settings to investigate the effects of varying Reynolds number. The cascade was run at a plenum chamber gage pressure of 305 mm (12 inches) H₂O for comparison with the previous design incidence measurements (Reference 2). The 305 mm setting yielded a free stream Mach number of 0.22 and a Reynolds number of 640,000. Measurements were also performed at an intermediate tunnel setting, corresponding to a plenum gage pressure of approximately 102 mm (4 inches) H₂O, and a slow tunnel setting corresponding to a plenum gage pressure of approximately 38 mm (1.5 inches) H₂O. The intermediate tunnel setting yielded a Mach number of 0.13 and a Reynolds number of 380,000 and the slow tunnel setting yielded a Mach number of 0.07 and a Reynolds number of 210,000.

B. SURFACE FLOW VISUALIZATION

Surface flow visualization was performed using a titanium oxide (TiO₂) and kerosene mixture. With the tunnel off and the acrylic window removed, blades 3 and 4 were coated with the TiO₂ mixture. The acrylic window was immediately replaced and the tunnel was brought up to speed. The evolution of surface streamlines was recorded using a tripod mounted VHS camera from the initiation of the run to equilibrium conditions. Still photographs were also recorded throughout the run using a hand-held

35mm camera. Surface flow visualization was performed at the three Reynolds number settings (210,000, 380,000 and 640,000).

C. LDV MEASUREMENTS

1. LDV Probe Volume Alignment

LDV probe volume alignment was performed using an alignment tool as outlined in Reference 3. The alignment process was performed prior to each survey. All LDV surveys were performed at the midspan of the blades.

2. Inlet Guide Vanes Adjustment

The cascade wind tunnel was configured for an off-design incidence of 38 degrees. LDV inlet surveys were performed over a 254 mm distance, corresponding to two blade passage widths, at station 1 to allow calculation of a mean inlet flow angle. Inlet guide vanes were adjusted until the mean inlet-flow angle was within 0.1 degrees of the desired 38 degrees.

3. LDV Surveys

A total of 34 LDV surveys were completed with the initial four at the design incidence and the remaining at the off-design incidence. At the off-design incidence, at least one survey was completed at each station as well as boundary layer surveys performed at various locations between stations 4 and 9. Off-design surveys were performed at tunnel settings corresponding to the three Reynolds numbers (210,000, 380,000 and 640,000). All surveys were performed by collecting 1000 data points, with station 1 and 4 surveys also taken with 3000 data points. Figure 6 illustrates the location of the surveys. Appendix A contains a listing of all surveys performed.

The laser optics were configured identically throughout this experiment, with the 514.5 nm (green) beam measuring the axial (vertical) velocity component, U , and the 488

nm (blue) beam measuring the tangential (horizontal) velocity component, V . Frequency shifting of 5 Mhz was performed to detect reverse flow velocities.

Ambient pressure, plenum total pressure and plenum total temperature were recorded for each survey. The velocity at the inlet of the test section was measured for each survey and used as the reference velocity, V_{ref} , for purposes of non-dimensionalizing the data. A FORTRAN code, CALIB1 [Ref. 3], was used to calculate V_{ref} for each survey using atmospheric pressure, plenum total pressure and plenum total temperature. A summary of the V_{ref} for each survey is listed in Appendix A. A listing of the input and output data files for each survey is contained in Appendix B.

TSI Flow Information Display (FIND) Version 4.0 software was used to acquire and analyze all LDV data. Axial and tangential velocities and turbulence intensities, Reynolds stress and Reynolds stress correlation coefficient information were processed using FIND, and the information was further non-dimensionalized using the inlet flow reference velocity, V_{ref} , to allow surveys to be compared.

a. Inlet Surveys

The inlet flow region was surveyed at stations 1, 2 and 3, covering the far to near upstream regions. All three stations were surveyed over a region encompassing blades 3 and 4 of the test section. The laser was positioned horizontally for each inlet survey.

b. Passage Surveys

Passage surveys were performed at stations 4 through 10. Stations 4 and 10 were surveyed over a two blade pitch region, and stations 5 through 9 were surveyed over a single blade pitch region. The laser was positioned horizontally for the majority of the surveys. Survey boundaries were selected to exclude regions of interference between the blade surface and laser beams. One survey at station 4 was performed with the laser pitched up 4 degrees to minimize blade tip interference with the vertical laser beam.

Potential problems associated with pitching and yawing of the LDV system were discussed by Hobson and Shreeve in Reference 8. Their analysis showed a maximum spatial error from probe volume orientation to be 0.3 mm, which corresponded to the probe volume minimum diameter.

c. Boundary Layer Surveys

Boundary layer surveys were performed at stations 5 through 9 on the suction side of blade 3. Additional surveys were performed at station 8 on blade 4 to check for periodicity. All surveys were performed with the laser positioned horizontally and yawed left 4 degrees. All boundary layer surveys were performed along a line perpendicular to the blade surface at the selected station.

d. Wake Surveys

Wake surveys were performed at stations 11 through 13 covering the near to far wake region. Station 11 was initially surveyed with the laser positioned horizontally. Two additional surveys were performed at station 11, one with the laser horizontal and pitched down 2 degrees, and another with the laser yawed 2 degrees left and pitched 2 degrees down, to minimize blade trailing edge interference with the vertical laser beam. Stations 12 and 13 surveys were both performed with the laser positioned horizontally.

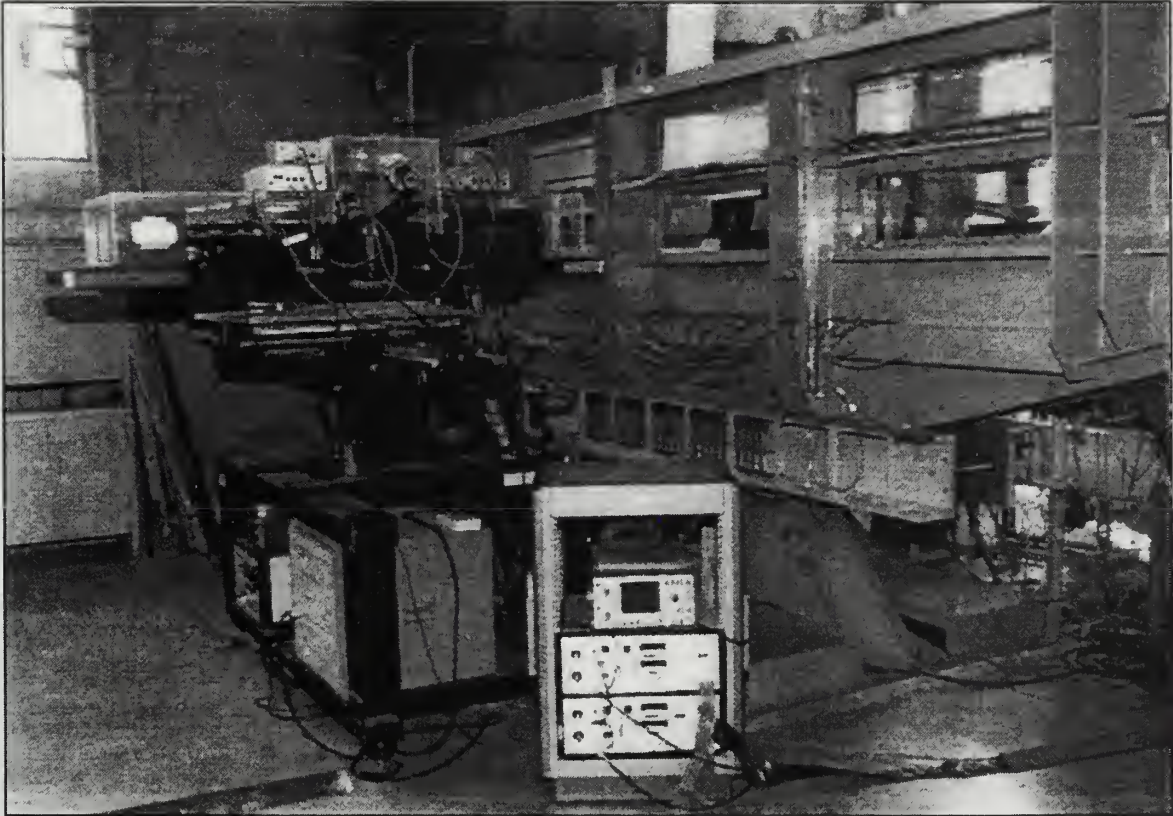


Figure 5. LDV System.

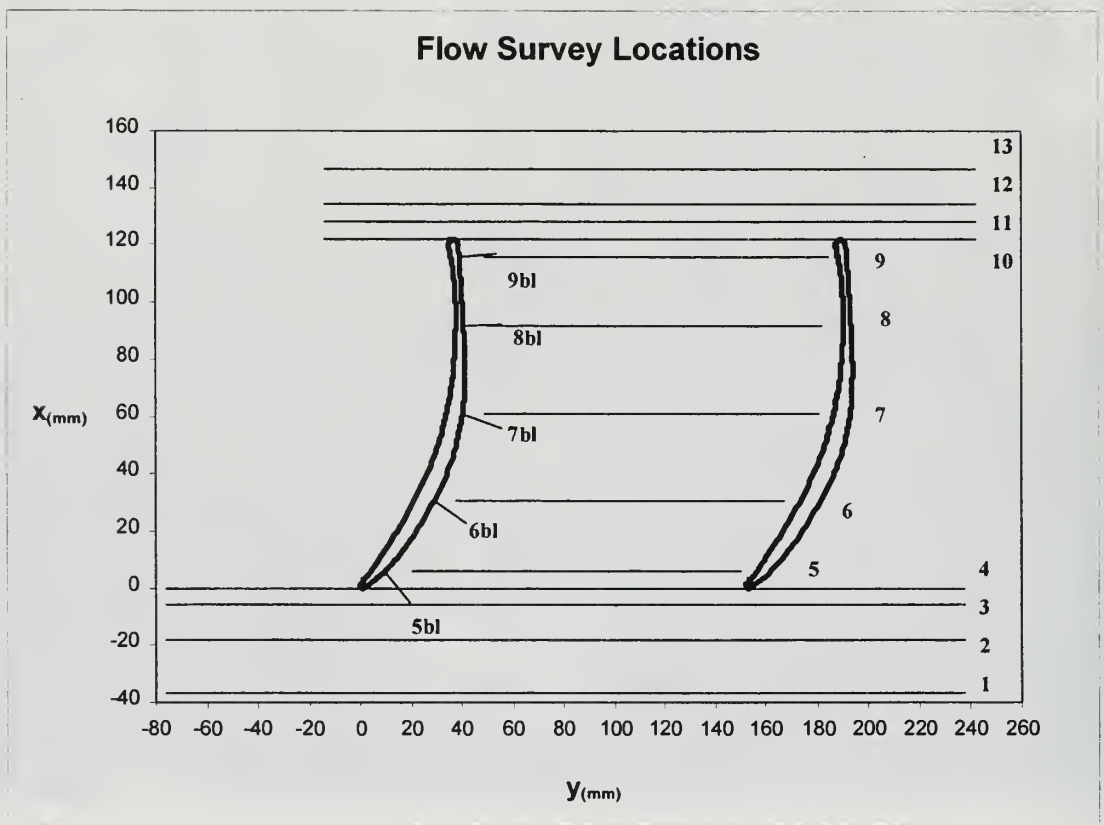


Figure 6. LDV Survey Locations.

IV. RESULTS AND DISCUSSION

A. PRELIMINARY INVESTIGATION AT DESIGN INCIDENCE

A preliminary investigation at design incidence was performed in the vicinity of the blade mid-chord to confirm the initiation of flow separation at station 7 as reported in Reference 3. The results are contained in Appendix C.

B. MEASUREMENTS AT OFF-DESIGN INCIDENCE

1. Blade Surface Pressure Distribution

Blade surface pressure measurements were taken on blade 6, the fully instrumented blade, at Reynolds numbers of 210,000, 380,000 and 640,000. The results are presented in terms of the coefficient of pressure, C_p , plotted along the blade chord at various positions given by the ratio ξ/c .

The C_p distribution at the high Reynolds number (640,000) is shown in Figure 7. The C_p distribution on the suction side of the blade rose continuously from the minimum pressure location at $0.4 C_{ac}$, and thus showed no indication of flow separation.

The C_p distribution at the intermediate Reynolds number (380,000) is shown in Figure 8. The distribution implied a separation region between approximately 0.50 and $0.65 C_{ac}$.

The C_p distribution at the low Reynolds number (210,000) is shown in Figure 9. The distribution implied a separation region between approximately 0.45 and $0.70 C_{ac}$ because of the plateau type perturbation in the mid chord region of the suction surface. The separation region had moved forward with decreasing Reynolds number. The separation bubble had also affected the minimum suction peak by decreasing its magnitude. The observed separation bubble behavior with Reynolds number was consistent with earlier separation bubble studies as reported in Reference 9.

In summary, all the pressure distributions are overplotted in Figure 10, which clearly shows the location of the separation bubble with variation in Reynolds number.

2. Flow Visualization

Surface flow visualization was performed on blades 3 and 4 at the three Reynolds numbers.

The flow visualization at the high Reynolds number, shown in Figure 11, revealed that the flow was three-dimensional in the trailing edge region due to the formation of corner vortices in the vicinity of the cascade end walls. In addition, the flow was non-symmetric due to the different boundary layer thickness between the two end walls [Ref. 10] which resulted in asymmetric vortices on the blades. Thus, two-dimensional measurements were obtained in a flow which was three-dimensional over most of the blade surface. However, comparison between blades 3 and 4 indicated reasonable periodicity at midspan.

The flow visualization at the intermediate Reynolds number, shown in Figure 12, indicated two dimensional flow along most of the midspan section as well as good periodicity between the two blades. A region of transitional separation was noted and measured at a position corresponding to $0.43 C_{ac}$ with a re-attachment point corresponding to approximately $0.57 C_{ac}$. By transitional separation is meant that where the boundary layer had transitioned to turbulent flow, separation had not yet occurred. This gave rise to the regions where no TiO_2 was present, i.e. the three vertical black streaks on the blade at midspan (Figure 12). The actual separation position without the fluid was probably farther downstream due to the gravitational effects associated with the mass of fluid. The measured separation region correlated well with the C_p distribution, which indicated a separation region between approximately 0.50 and $0.65 C_{ac}$.

The flow visualization at the low Reynolds number, shown in Figure 13, indicated two-dimensional flow along most of the midspan section. A region of laminar separation was noted and measured at a position corresponding to $0.37 C_{ac}$ with a re-attachment

point at approximately $0.63 C_{ac}$. A small amount of the TiO_2 /kerosene fluid, approximately 1 cm in length, was suspended in this region. Again, taking into account the gravitational effects associated with the suspended fluid, the measured separation region correlated well with the C_p distribution, which indicated a separation region between approximately 0.45 and $0.70 C_{ac}$.

3. LDV Measurements at Reynolds Number of 640,000

From the surface flow visualization, it was determined that the flow was neither symmetrical nor two-dimensional along the blade midspan. LDV surveys were performed throughout the test section at midspan for purpose of comparison with previous design incidence measurements.

a. Inlet Surveys

Inlet surveys were performed at stations 1, 2 and 3. Surveys were performed throughout a region corresponding to two blade spacings encompassing blades 3 and 4 of the test section. Stations 1 and 3 will be discussed to characterize the test section inlet flow conditions in both the near and far fields.

Station 1 ($0.3 C_{ac}$ upstream) surveys were performed taking both 1,000 and 3,000 data points per measurement. The initial survey at 1,000 data points, shown in Figure 14, indicated a nearly uniform total velocity ratio, W/V_{ref} . Both the axial and tangential turbulence were slightly higher than expected, ranging from 2 to 3%. Repeating the survey at 3,000 data points reduced the turbulence to a maximum of 2%, thus verifying uniform inlet flow conditions. Reference 8 showed that more data points gave a more conservative measure of turbulence levels. The Reynolds stress correlation coefficient remained below approximately 0.15 throughout the survey, indicating a random or uncorrelated flow. The results of this survey are shown in Figure 15.

The station 3 ($0.05 C_{ac}$ upstream) survey results are shown in Figure 16. The total velocity ratio, W/V_{ref} , decreased as the survey approached the blade leading

edge, and then drastically increased as the flow progressed around the suction side of the blade leading edge. The axial turbulence remained constant at approximately 2% while the tangential turbulence was nearly constant at 2.5% on the pressure side and increased just past the blade leading edge to in excess of 3% before settling down to 2.5% near midspan. The correlation coefficient remained below 0.2 throughout the survey.

Both inlet surveys matched well with those at design incidence.

b. Passage Surveys

Passage surveys were conducted at stations 4 through 9 over a single blade spacing region between blades 3 and 4, and at station 10 over two blade spacings. Surveys at stations 5, 8 and 10 will be discussed.

The station 5 passage survey results are shown in Figure 17. The velocity ratios indicated a smooth decrease in velocity from suction side to pressure side of the passage. The axial and tangential turbulence both ranged from 2 to 3%, and the correlation coefficient remained below 0.2 throughout the passage. The first survey point on the suction side showed an increased turbulence level which was most likely at the edge of the blade surface boundary layer. The station 5 passage survey matched well with that at design incidence.

The station 8 passage survey results are shown in Figure 18. The velocity ratios indicated that the first few points of the survey were inside the boundary layer on the suction side of the blade. The turbulence remained consistent at approximately 2% from 0.2 to 0.9 y/s but increased to a maximum of approximately 25% in the axial direction and 10% in the tangential direction inside the boundary layer. Once again, the results matched well with those at design incidence.

The station 10 passage survey results are shown in Figure 19. The velocity ratios indicated a recirculation region of reversed flow at the trailing edge of the blade and displaced from the suction surface. This region of reversed flow resulted from the mixing of the corner vortices and was therefore a result of the three dimensionality of

the flow at that Reynolds number (Figure 11). As the flow transitioned to freestream, the total velocity ratio decreased slightly near the middle of the passage and began to increase again as the pressure side of the blade was approached. The axial and tangential turbulence both peaked near the blade, which corresponded to the region of reversed flow, with the axial turbulence peaking at 25 to 30% and the tangential turbulence peaking at 15%. As the flow approached freestream, the turbulence settled to approximately 2% throughout the remainder of the survey. The correlation coefficient indicated a negative spike near the suction side blade and ranged from 0 to 0.25 in the freestream portion of the passage.

c. Boundary Layer Surveys

Boundary layer surveys were performed at stations 5 through 9. Yawing the laser 4 degrees left was found to work best for positioning the laser probe volume as close to the blade surface as possible while minimizing interference due to beam reflections off the blade surface and cascade back wall. All boundary layer data are presented in terms of a non-dimensional perpendicular distance (d/c) from the blade surface. Boundary layer surveys at stations 5, 7 and 9 will be discussed and compared to those at design incidence.

The station 5 boundary layer results are shown in Figure 20. The velocity ratios indicated only a slight decrease for the first survey point, which corresponded to the edge of the boundary layer, and then remained relatively constant throughout the survey. The axial turbulence peaked at 4% and the tangential at 14% for the first survey point and then remained relatively constant at 2% throughout the freestream. The correlation coefficient reached a maximum of 0.25 near the edge of the boundary layer and then decreased to less than 0.2 in the freestream. The results matched closely to those at design incidence.

Station 7 boundary layer results are shown in Figure 21. The velocity ratio profiles indicated more than four survey points in the boundary layer with a

relatively steep velocity gradient throughout. The boundary layer extended out to a d/c of approximately 0.02. The off-design profiles did not match well with those at design incidence, which indicated a relatively flat velocity profile out to a d/c of approximately 0.08. This comparison nullified the initial speculation of a separation region in the vicinity of station 7 at the design incidence. The reason that the previous measurement anomaly did not appear for this set of measurements is unexplained. The turbulence profiles indicated a peak of 16% for the axial turbulence and a peak of 6% for the tangential turbulence, both occurring in the boundary layer region closest to the blade. Both turbulence profiles decreased to approximately 2% in the freestream. The off-design turbulence profiles also did not match those at design incidence which indicated an axial turbulence of 15% from a d/c of 0.01 to 0.08 and then peaked at 40% near the boundary layer to freestream transition. The correlation coefficient ranged from 0 to -0.5 within the boundary layer and -0.5 to -0.1 throughout the freestream.

Station 9 boundary layer results are shown in Figure 22. The velocity ratios indicated several survey points with mean reversed flow for the axial velocity component. Freestream velocity did not occur until a d/c of approximately 0.20, which indicated a large region of separated flow in the vicinity of the blade trailing edge. This recirculation region was a result of the three-dimensionality of the flow due to the mixing of the corner vortices (Figure 11). The design incidence results indicated attached flow in this region, indicating that the three-dimensional effect is amplified at the off-design incidence. The axial turbulence profile gradually increased from 5% near the blade to 30% on the edge of the separation region (d/c of 0.16) before decreasing to 5% in the freestream. The tangential turbulence increased from 5% to 20% (at d/c of 0.12) before decreasing to 3% at the edge of the boundary layer. The correlation coefficient ranged between -0.1 to 0.30 throughout the separation region.

d. Wake Surveys

Wake surveys were performed at stations 11, 12 and 13 over two blade spacings. The station 13 far wake survey will be discussed.

Station 13 wake survey results are shown in Figure 23. The velocity profiles indicated a minimum on the suction side of the blade trailing edge. In the freestream region, the velocity ratios indicated a slight decrease as the wake was traversed, followed by an increase as the pressure side of the blade was approached. The axial wake turbulence showed two peaks, with a maximum magnitude of 28%. Double peaks correspond to the maximum mean velocity gradient on either side of the wake. The tangential turbulence showed a single peak of magnitude 20%. The correlation coefficient varied between -0.4 and 0.3. The off-design wake profiles matched well with those at design incidence, with the primary difference being larger magnitudes of turbulence for the off-design incidence.

The wake flow angle distributions at design [Ref. 3] and off-design incidence are shown in Figures 24a and 24b. Comparison of the two distributions indicated an increase from approximately 2 degrees for the design incidence to 10 degrees for the off-design incidence. The large increase was due to the growth of the recirculation region in the vicinity of the blade trailing edge as the flow incidence angle was increased from design to off-design, resulting in a large deviation angle.

4. LDV Measurements at Reynolds Number of 380,000

LDV surveys were performed to characterize the flow in general and the behavior of the separation region as Reynolds number was decreased. Similarities between the flow measurements at the intermediate and low Reynolds number were noted. More detailed measurements were performed at the low Reynolds number, therefore those results follow. The results at the intermediate Reynolds number as compared to the low Reynolds number are summarized in Appendix D.

5. LDV Measurements at Reynolds Number of 210,000

From the surface flow visualization, it was determined that the flow was two-dimensional along most of the blade span for the low Reynolds number. LDV surveys were performed to characterize the off-design incidence flow in general and the separation region as noted in the C_p distribution.

a. Inlet Surveys

Inlet surveys were performed at stations 1, 2 and 3. The station 1 and 3 surveys will be discussed in detail.

Station 1 inlet survey results are shown in Figure 25. The velocity profiles were nearly uniform throughout the survey. The axial turbulence ranged from 2 to 3% and the tangential turbulence ranged from 2.5 to 4%, with a few survey points above 4%. The turbulence was slightly higher than that at the 305 mm (12 inch) tunnel setting, as was expected for a lower Reynolds number. The correlation coefficient remained below 0.2, which indicated generally random flow.

Station 3 results are shown in Figure 26. The velocity profiles were similar to those at the high Reynolds number. The velocity decreased as the blade leading edge was approached and then sharply increased as the flow progressed around the suction side of the blade. The axial turbulence ranged from 2 to 3%. The tangential turbulence fluctuated between 2 and 8% on the pressure side of blade 3 and remained fairly steady between 2 and 4% for the rest of the survey region. The non-uniform tangential turbulence on the pressure side of blade 3 was attributed to inlet guide vane effects associated with the tunnel. The singular point which corresponded to the peak in axial turbulence and correlation coefficient was a result of the laser beam hitting the blade leading edge. The correlation coefficient remained fairly steady between 0 and 0.2.

b. Boundary Layer Surveys

Boundary layer surveys were performed at stations 5 through 9. Since the C_p distribution at this Reynolds number indicated a separation region between approximately 0.45 and 0.70 C_{ac} , three additional surveys were performed between station 7 (0.55 C_{ac}) and station 8 (0.78 C_{ac}) in an attempt to further characterize the separation region.

Station 5 boundary layer results are shown in Figure 27. The velocity profiles indicated a slight decrease for the first point of the survey, corresponding to the outer edge of the boundary layer. The axial turbulence remained steady throughout the survey with the tangential turbulence spiking at the edge of the boundary layer, due to the large gradient associated with the shear layer, and then remained constant thereafter. The correlation coefficient ranged from 0 to 0.1 throughout the survey.

Station 6 boundary layer results are shown in Figure 28. The boundary layer profiles all behaved similarly to those at station 5. Both station 5 and station 6 boundary layer profiles confirmed attached laminar flow.

Station 7 (0.55 C_{ac}) boundary layer results are shown in Figure 29a. The velocity profiles showed at least two survey points within the boundary layer. The turbulence profiles showed a peak in the axial turbulence of magnitude 10% and a peak in the tangential turbulence of 30% for the first survey point, again associated with the shear layer, and then relatively steady turbulence between 2 and 3% in the freestream. The correlation coefficients for the two points within the boundary layer were -0.2 and 0.1, respectively, and the remaining points remained between 0 and 0.1.

A finer boundary layer survey at station 7 was performed with the results shown in Figure 29b. The axial velocity histograms for the first 3 points of the survey are shown in Figure 29c. The velocity profiles showed six survey points within the boundary layer, and the general shape of the profiles indicated the initiation of flow separation. The boundary layer thickness was approximately 0.012 d/c. The mean axial velocity ratios were all positive therefore mean reversed flow was detected. The histograms for

the first three survey points indicated no data points with a negative axial velocity. The turbulence profiles matched those of the previous station 7 survey. The first two points showed levels of turbulence of less than 2% which seem to indicate that laminar separation had occurred as these levels were below free stream values. The correlation coefficient for the first point was approximately 0.8 which indicated a fairly correlated flow close to the blade.

Station 7.25 ($0.61 C_{ac}$) boundary layer results are shown in Figure 30a. The axial velocity histograms for the first three points of the survey are shown in Figure 30b. The velocity profiles showed eight survey points within the boundary layer, with the boundary layer thickness approximately $0.017 d/c$. The axial velocity profile showed two survey points with a mean negative velocity, thus indicating mean reversed flow. The histograms for the first two survey points indicated several data points with a negative axial velocity, which resulted in the mean reversed flow. The velocity profiles indicated a general growth of the separation region. The turbulence profiles showed peaks of 44% in the axial turbulence and 20% in the tangential turbulence. The turbulence inside the bubble had risen to approximately 10%, as shown by the first two points, which indicated that transition to turbulent flow had occurred inside the bubble as these levels were above freestream values. The correlation coefficient for the first survey point was approximately 0.6, which indicated fairly correlated flow near the blade surface, as was indicated by the station 7 survey.

Referencing figures 29b and 30a, based on the assumption that the maximum turbulence intensity corresponds to the location of the encompassing streamline [Ref. 9], an estimate of the flow separation point can be made. Since laminar flow was detected at station 7, the actual separation point must be forward of this location as the separation point would correspond to the location where the encompassing streamline was coincident with the blade surface. Based on the flow visualization results and C_p distribution, it is believed that the actual separation point lies somewhere between $0.37 C_{ac}$ and $0.45 C_{ac}$.

Station 7.5 ($0.67 C_{ac}$) boundary layer results are shown in Figure 31a. The axial velocity histograms for the first three points of the survey are shown in Figure 31b. The velocity profiles showed 12 points in the boundary layer, none with a mean negative axial velocity, indicating that the mean reversed flow has ceased. The axial velocity histograms for the first three survey points all showed some data points with a negative axial velocity; however, the mean axial velocities were positive. The boundary layer thickness was approximately 0.022 d/c and the general boundary layer profile suggested that the separation bubble had reattached or was about to reattach.. The turbulence profiles showed peaks of 35% in the axial turbulence and 25% in the tangential turbulence. The correlation coefficients ranged between -0.4 and 0.

Station 7.75 ($0.73 C_{ac}$) boundary layer results are shown in Figure 32. The general boundary layer profiles indicated that the boundary layer had reattached at this location. The velocity profiles showed 16 survey points within the boundary layer with a thickness of 0.027 d/c, and the turbulence profiles showed peaks of 25% in the axial turbulence and 20% in the tangential turbulence. The correlation coefficient for the first point was 0.4 with the remaining points between -0.3 and -0.1.

Station 8 ($0.78 C_{ac}$) boundary layer results are shown in Figure 33. The velocity profiles indicated a boundary layer thickness of approximately 0.035 d/c and the turbulence profiles showed peaks of 19% in the axial turbulence and 16% in the tangential turbulence. The shape of the boundary layer profile suggested that the flow was fully turbulent and attached by this position. The correlation coefficients ranged between -0.2 and 0.2.

Station 9 ($0.96 C_{ac}$) boundary layer results are shown in Figure 34. The boundary layer thickness is approximately 0.06 d/c and the turbulence profiles showed peaks of 15% and 11% for the axial and tangential turbulence, respectively. The correlation coefficient ranged between -0.2 and 0.2. The boundary layer profiles indicated attached turbulent flow.

In general, the boundary layer profiles correlated well with the C_p distribution. Specifically, the boundary layer profiles indicated a transitional separation bubble, as per References 9 and 11. A laminar separation bubble began in the vicinity of station 7, with a corresponding separated laminar free shear layer. A short recirculation region developed near station 7.25. The recirculation region corresponded to the thickest part of the separation bubble which is normally the point of laminar to turbulent transition. By station 7.5, the separation bubble and free shear layer were fully turbulent, and by station 8 the fully turbulent flow had reattached.

c. Wake Surveys

Wake surveys were performed at stations 11, 12 and 13. The station 13 farfield wake results are shown in Figure 35. The velocity profiles were uniform in the freestream, with depressions in the vicinity of the blade trailing edge position. The turbulence profiles were also relatively constant in the freestream, ranging between 2 and 4%, with peaks of 12 and 13% for the axial and tangential turbulence, respectively, at the trailing edge position. The turbulence was slightly higher for blade 4 than blade 3, which indicated a slight degradation in periodicity across the survey region.

C. SUMMARY

In summary, Figure 36 shows the approximate flow structure for the three Reynolds numbers. The experimentally determined separation and reattachment locations for the low and intermediate Reynolds number cases are indicated. The region of reverse flow determined from flow visualization and LDV measured separation for the high Reynolds number case are also shown with the vortex structure on the blade suction surface. The three measurement techniques (surface pressure measurements, flow visualization and LDV) all agree reasonably well giving confidence in the proposed flow structure.

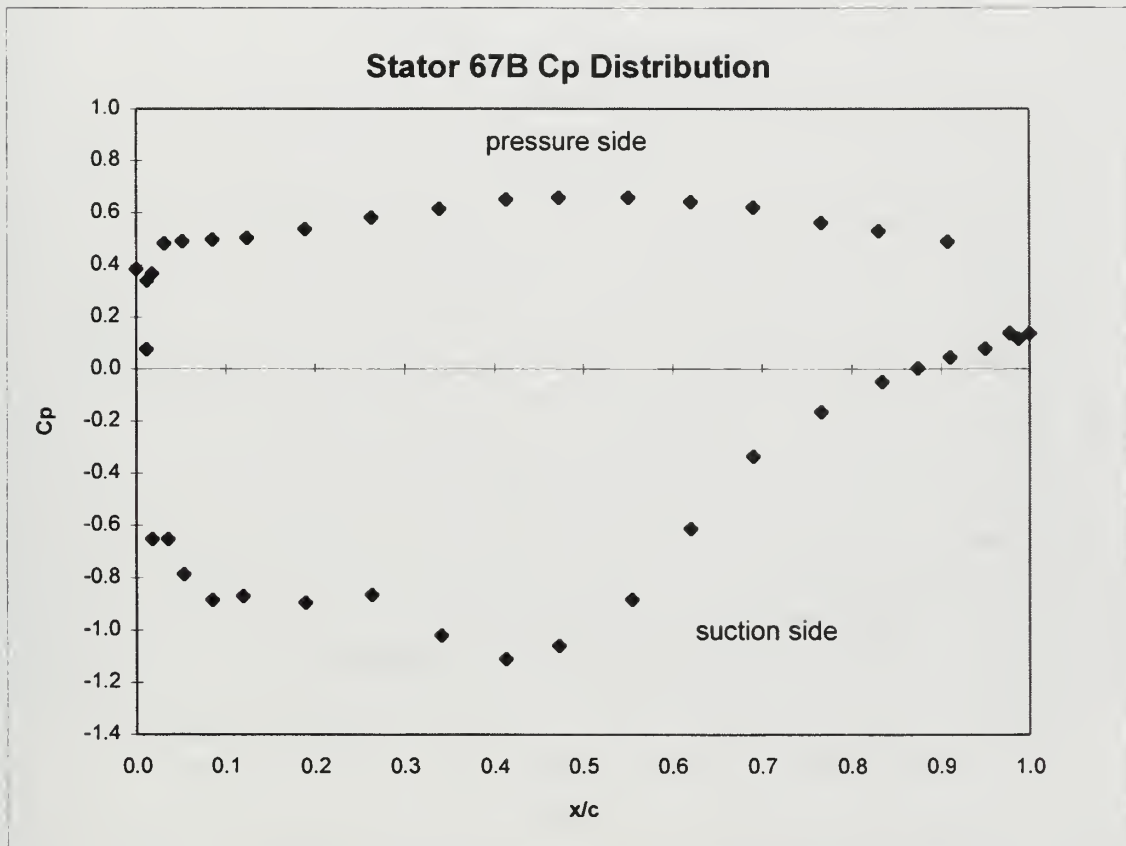


Figure 7. Experimental C_p Distribution at $Re=640,000$.

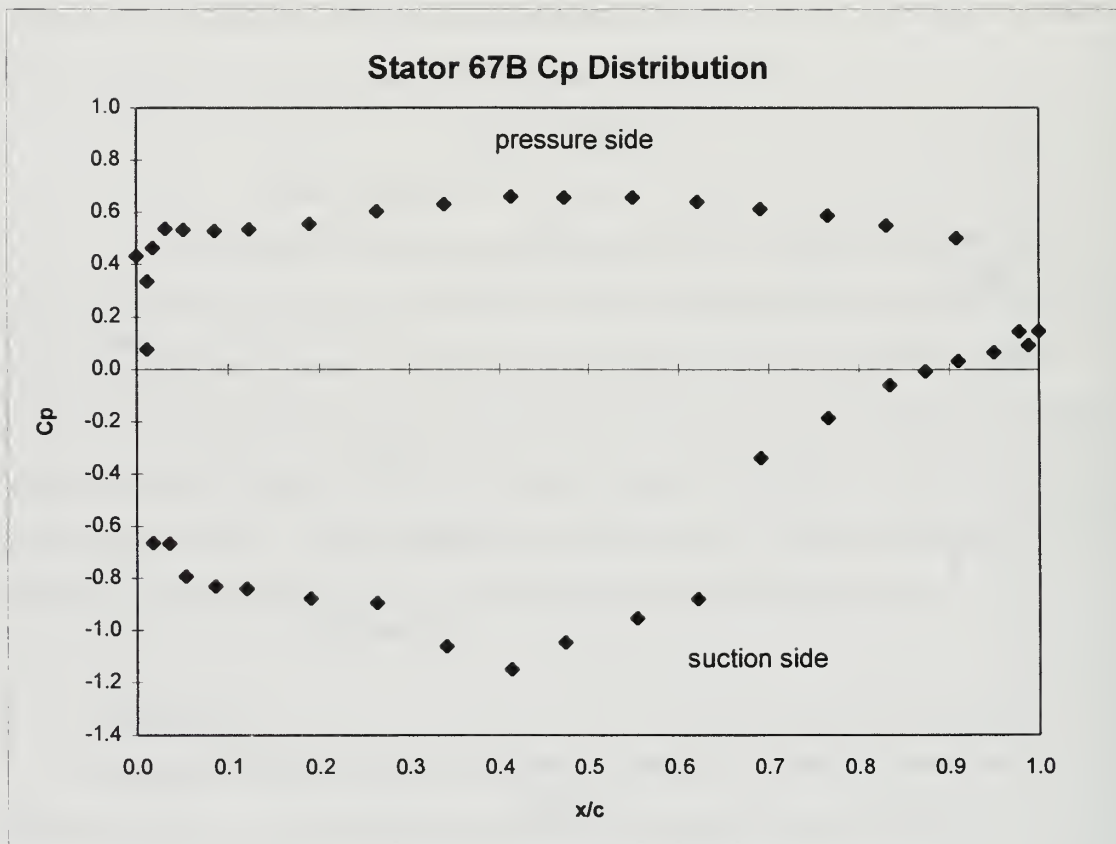


Figure 8. Experimental C_p Distribution at $Re=380,000$.

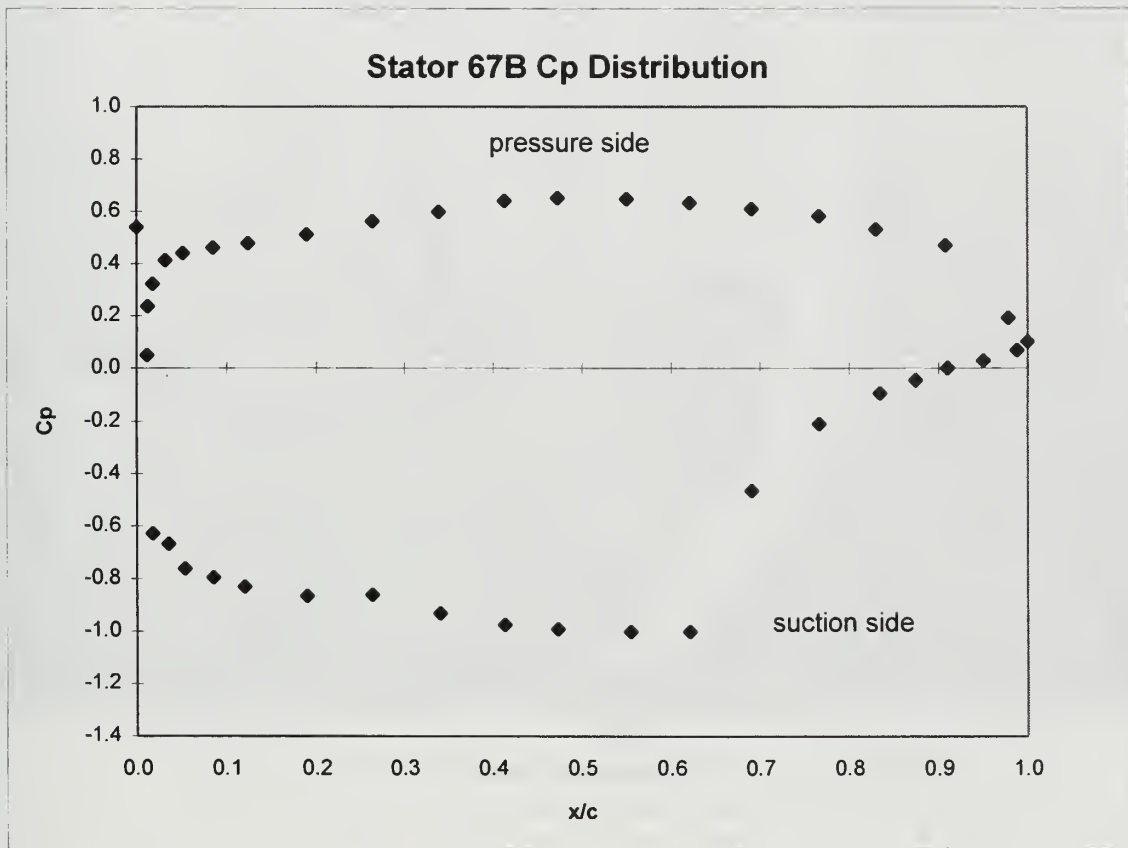


Figure 9. Experimental C_p Distribution at $Re=210,000$.

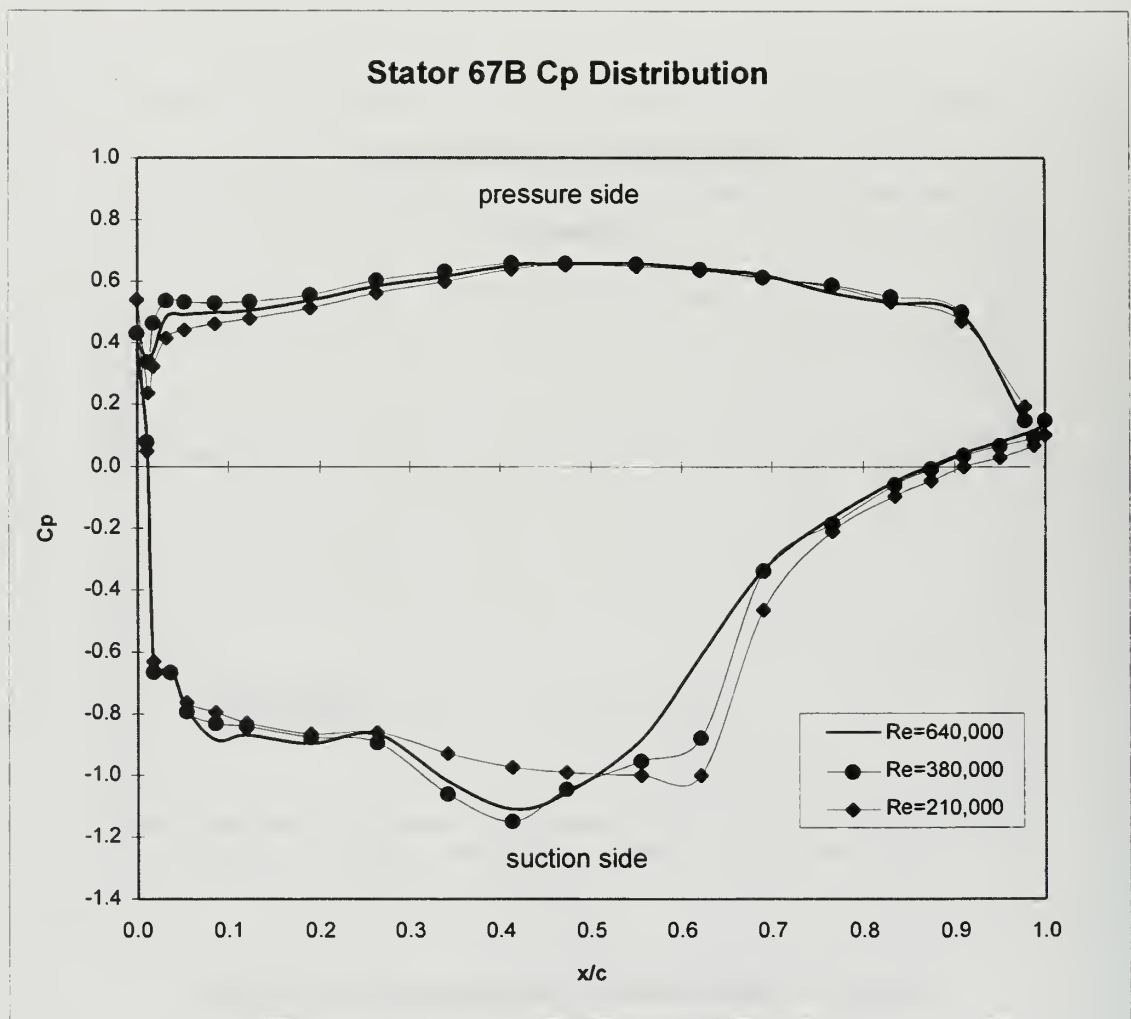


Figure 10. Experimental Cp Distributions.



Figure 11. Blade Surface Flow Visualization at $Re=640,000$.



Figure 12. Blade Surface Flow Visualization at $Re=380,000$.

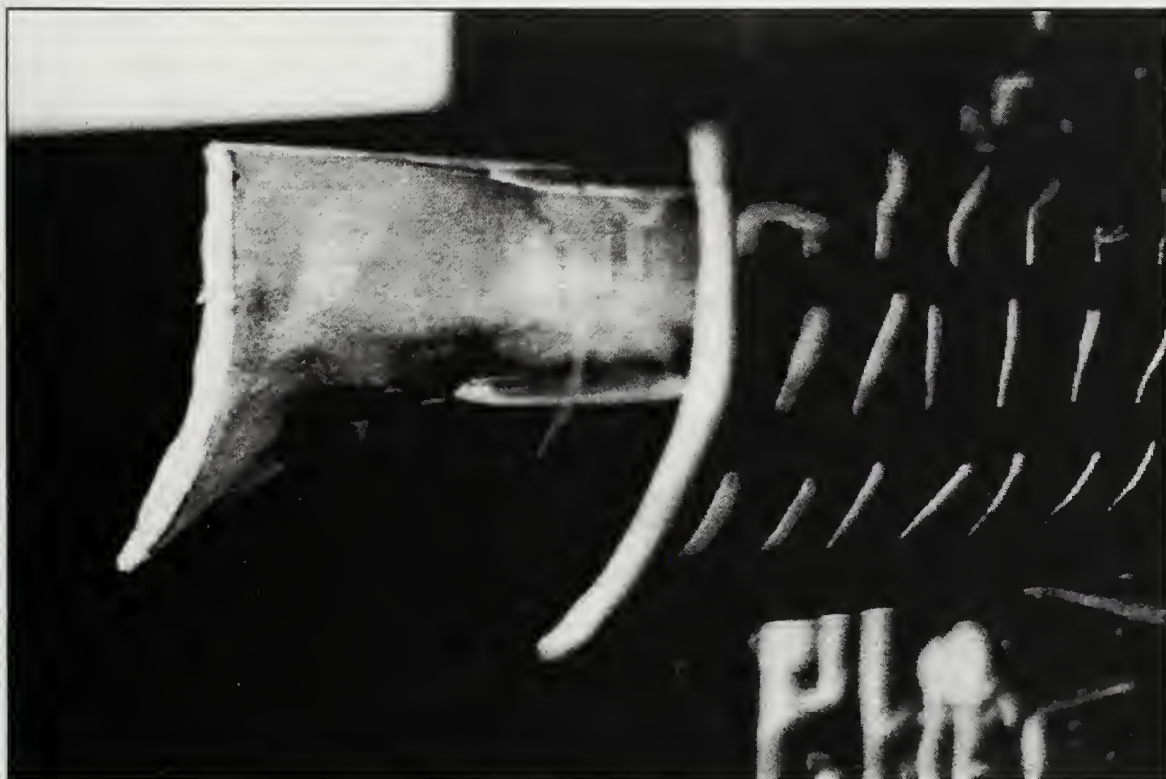


Figure 13. Blade Surface Flow Visualization at $Re=210,000$.

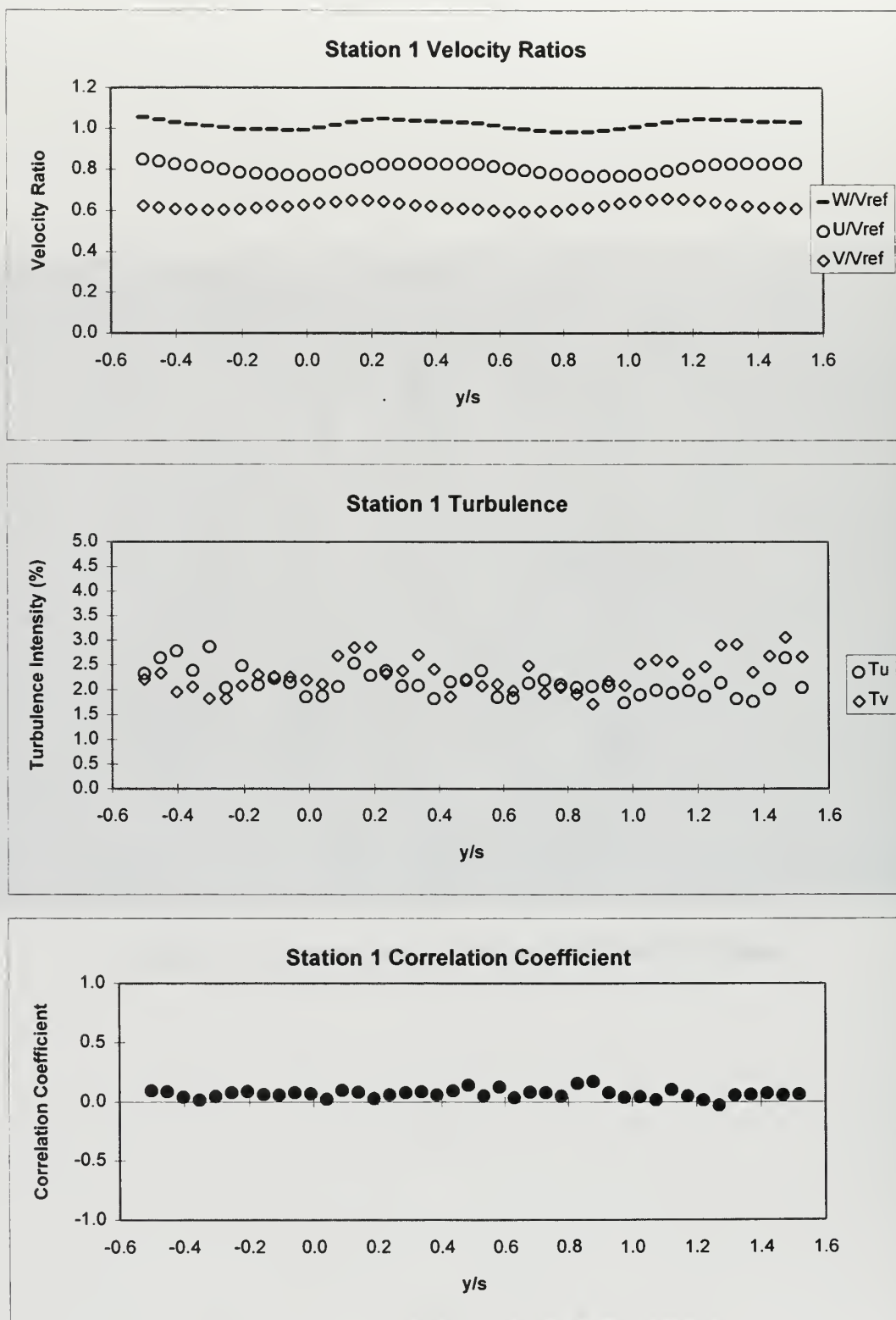


Figure 14. Station 1 Inlet Survey Results at $Re=640,000$.

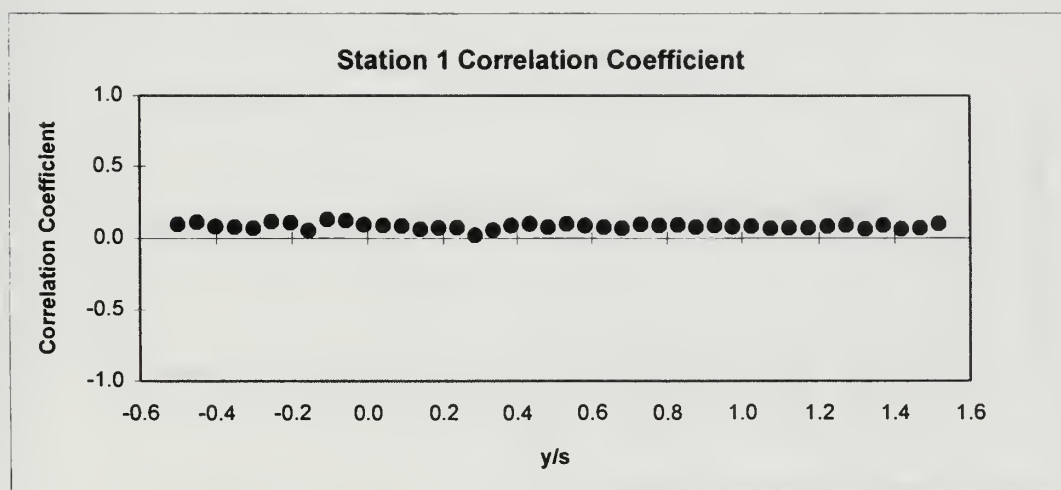
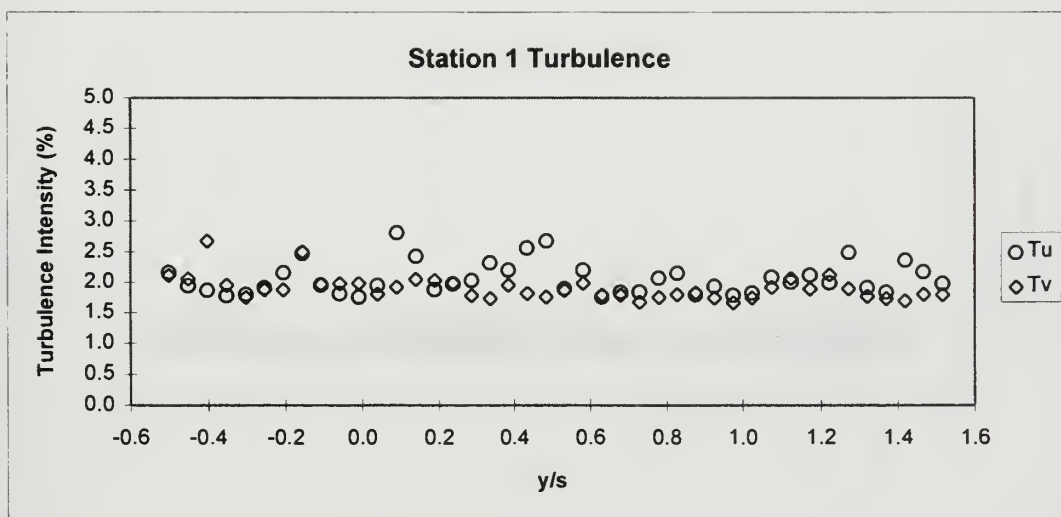
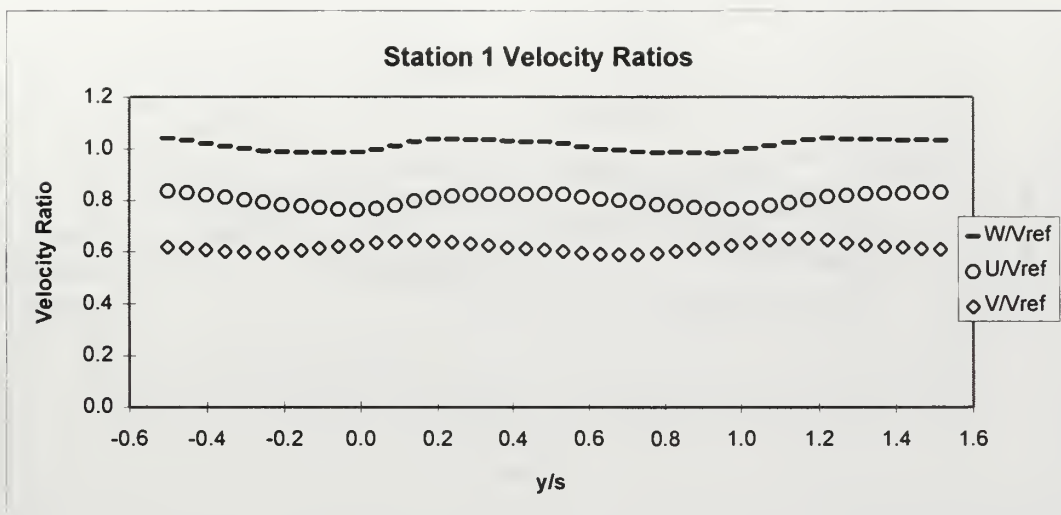


Figure 15. Station 1 Inlet Survey Results at 3000 Data Points.

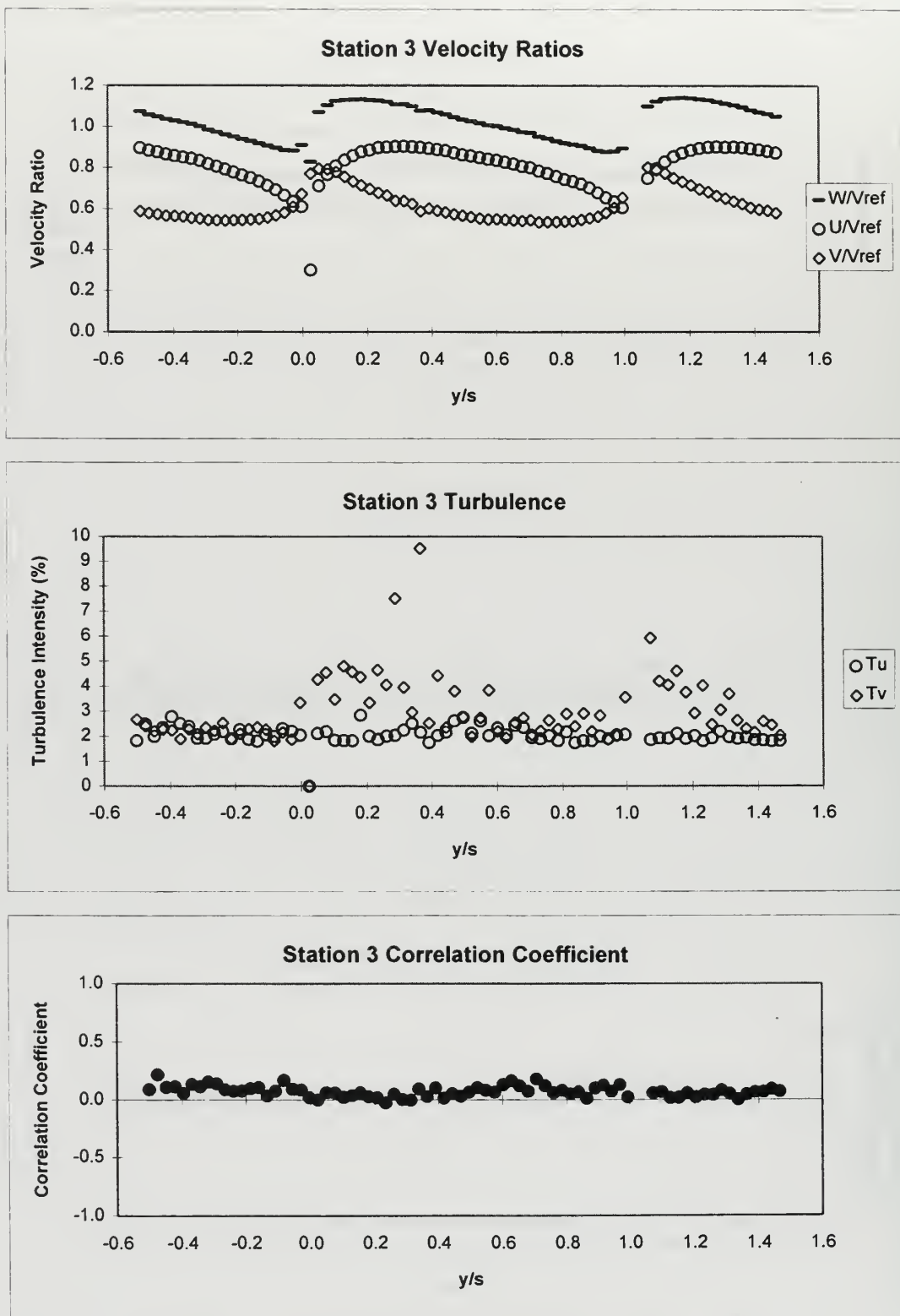


Figure 16. Station 3 Inlet Survey Results at $Re=640,000$.

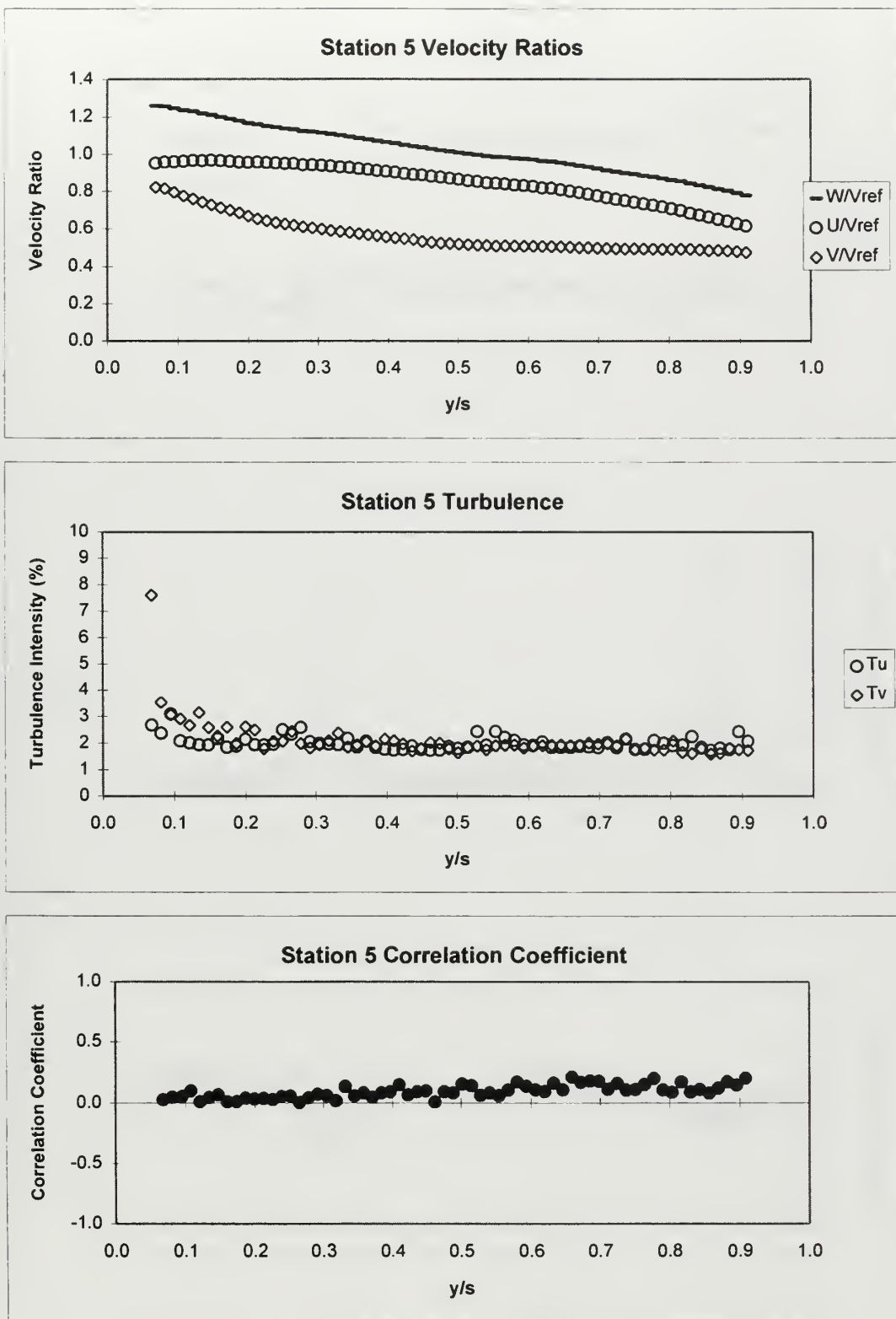


Figure 17. Station 5 Passage Survey Results at $Re=640,000$.

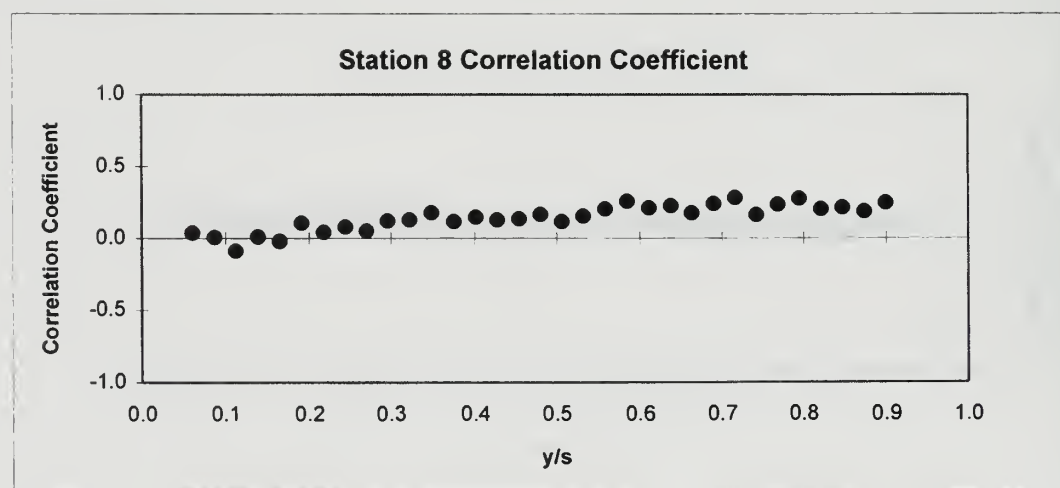
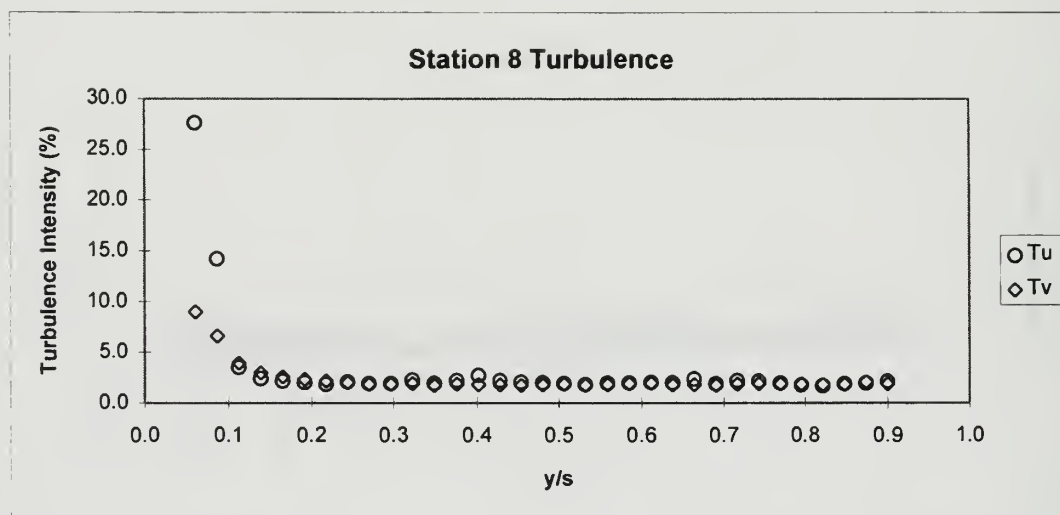
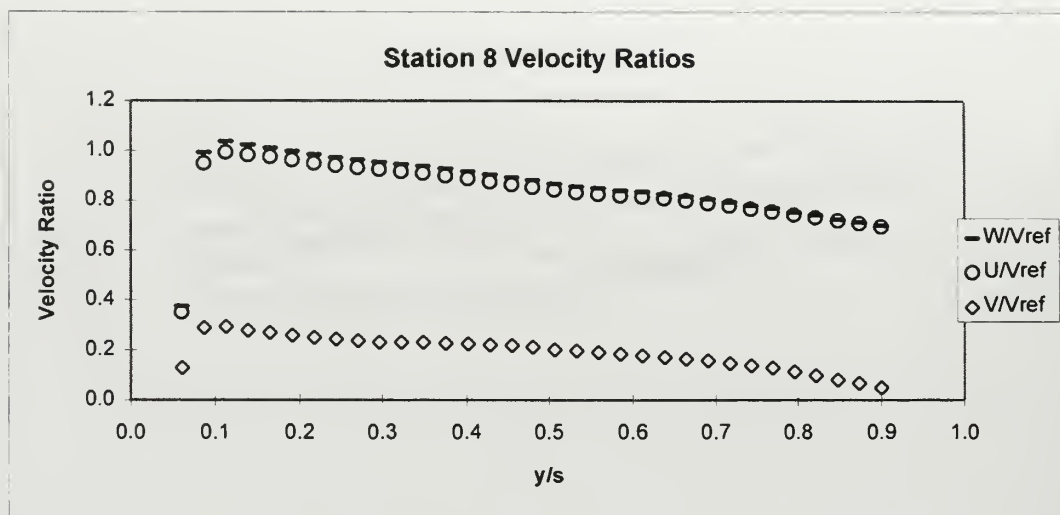


Figure 18. Station 8 Passage Survey Results at $Re=640,000$.

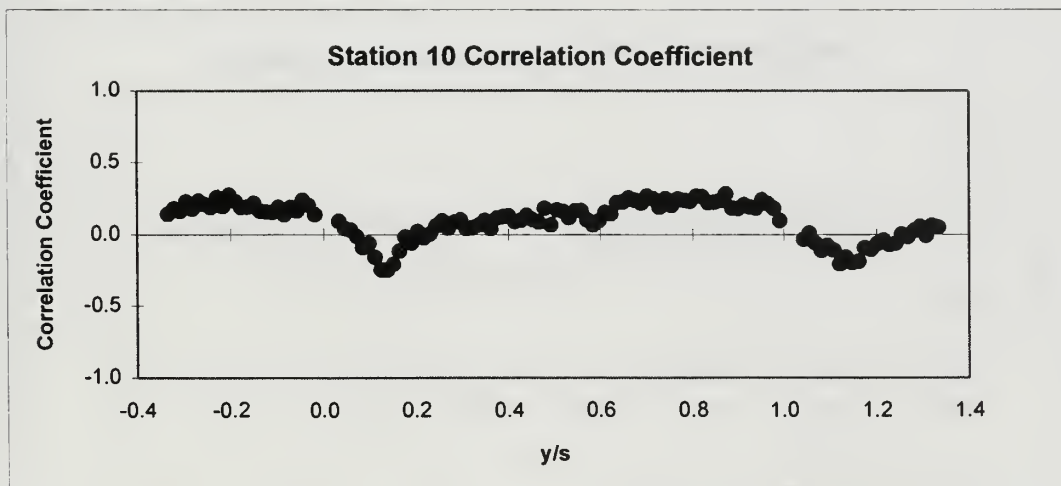
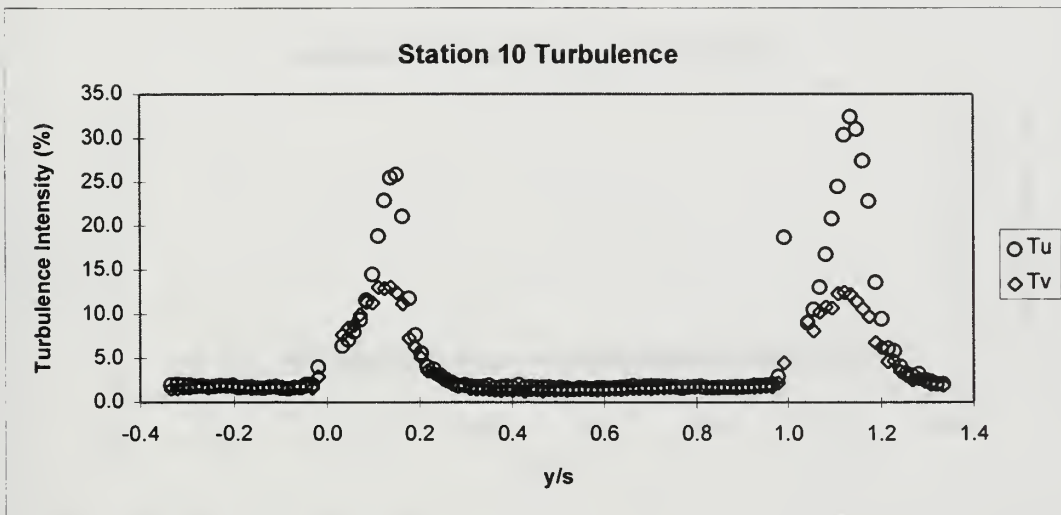
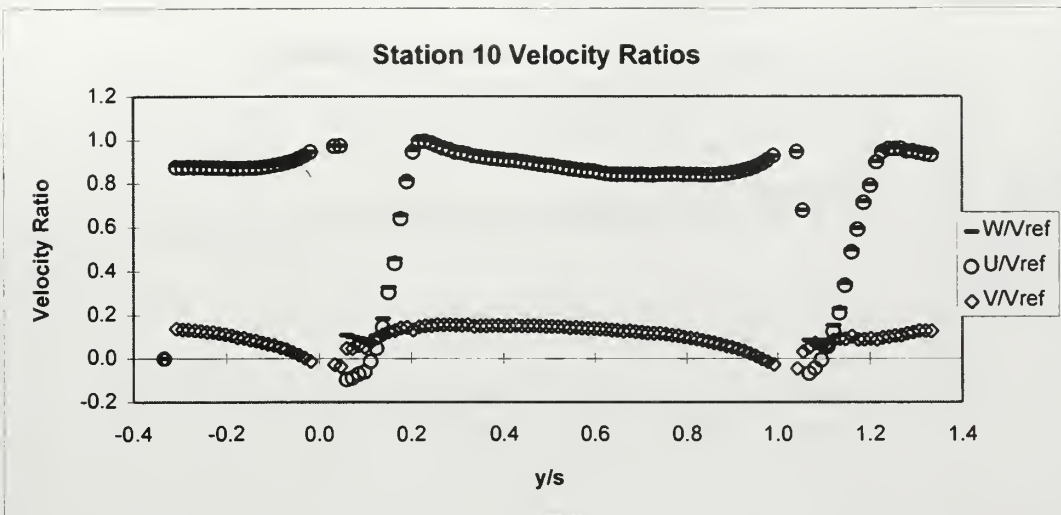


Figure 19. Station 10 Passage Survey Results at $Re=640,000$.

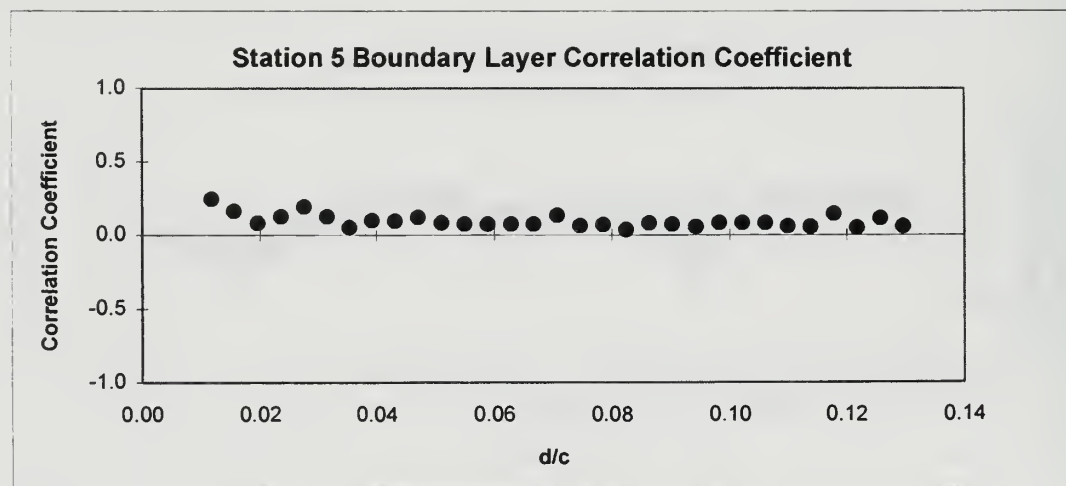
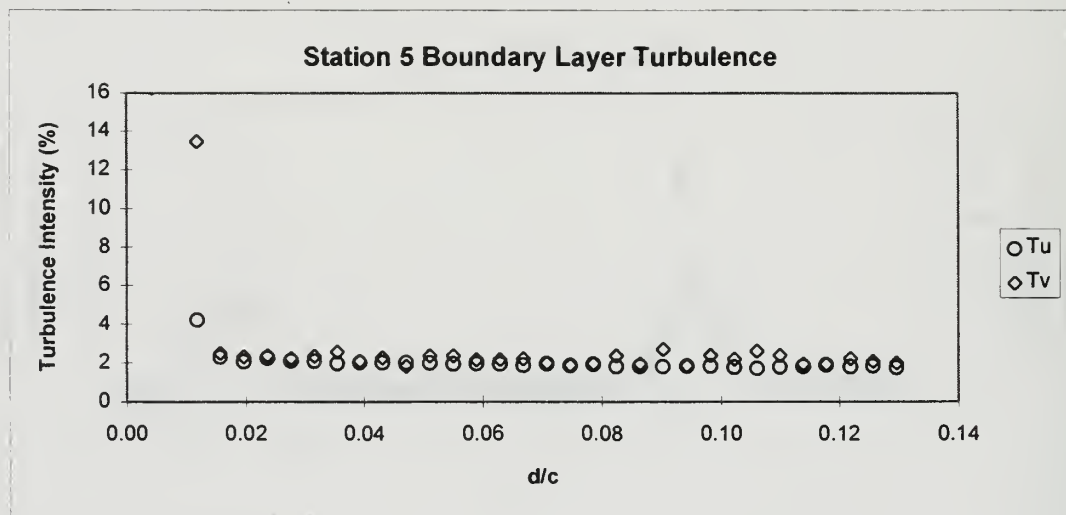
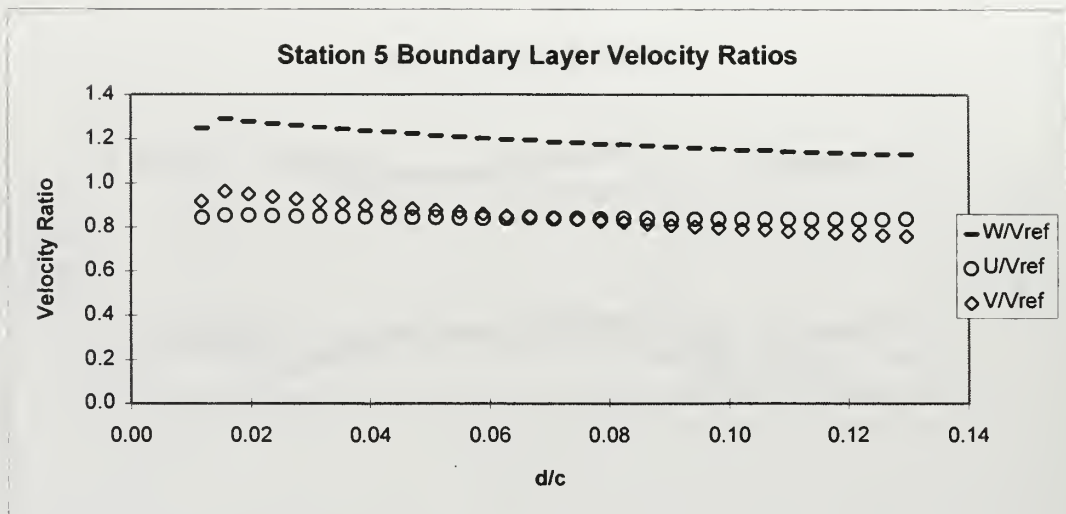


Figure 20. Station 5 Boundary Layer Survey Results at $Re=640,000$.

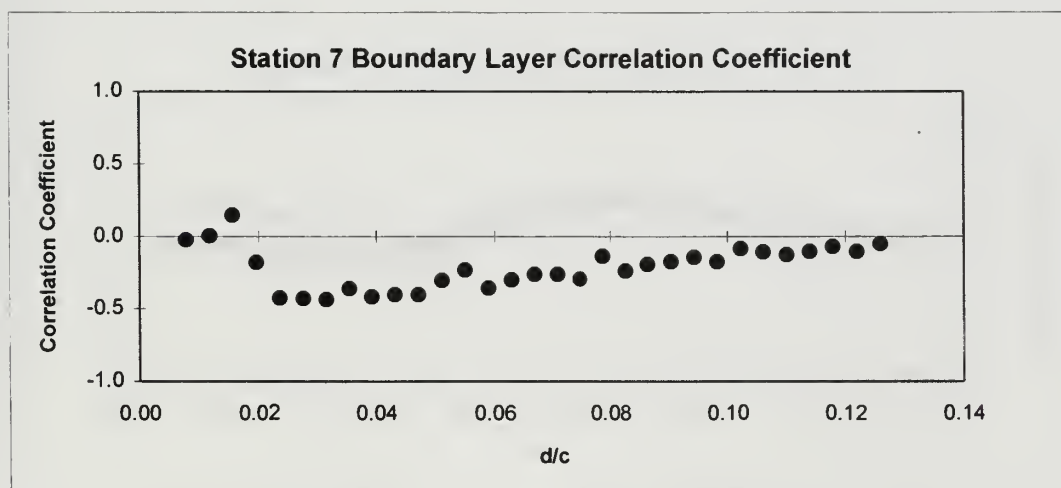
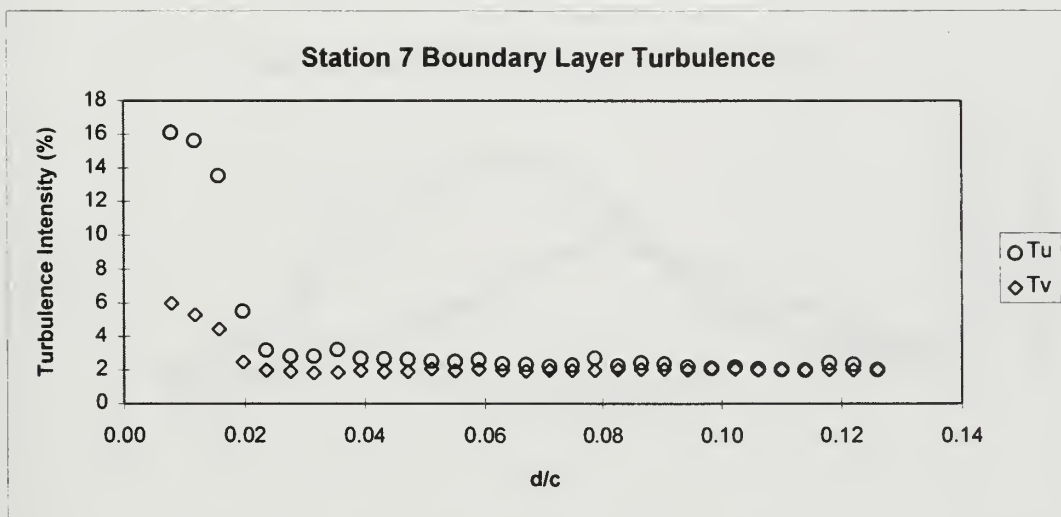
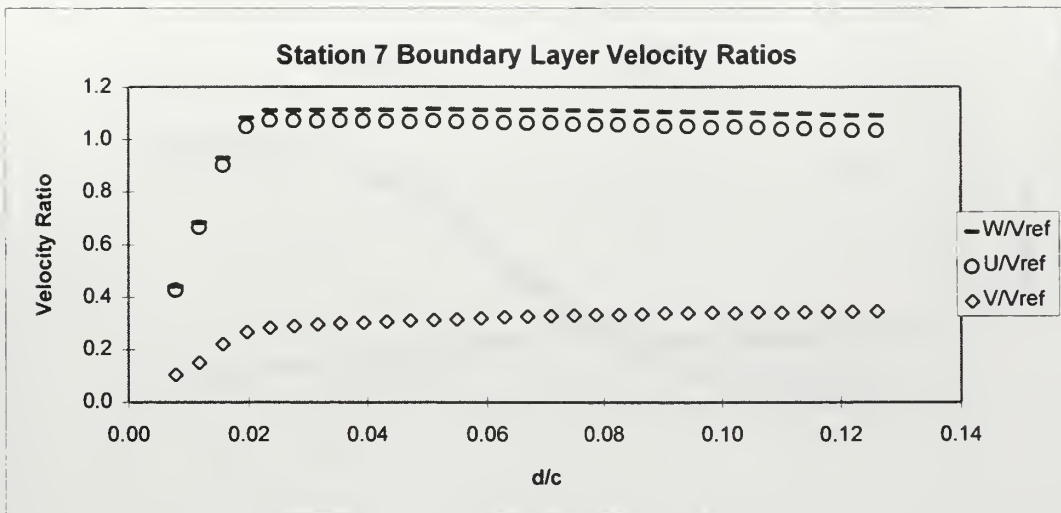


Figure 21. Station 7 Boundary Layer Survey Results at $Re=640,000$.

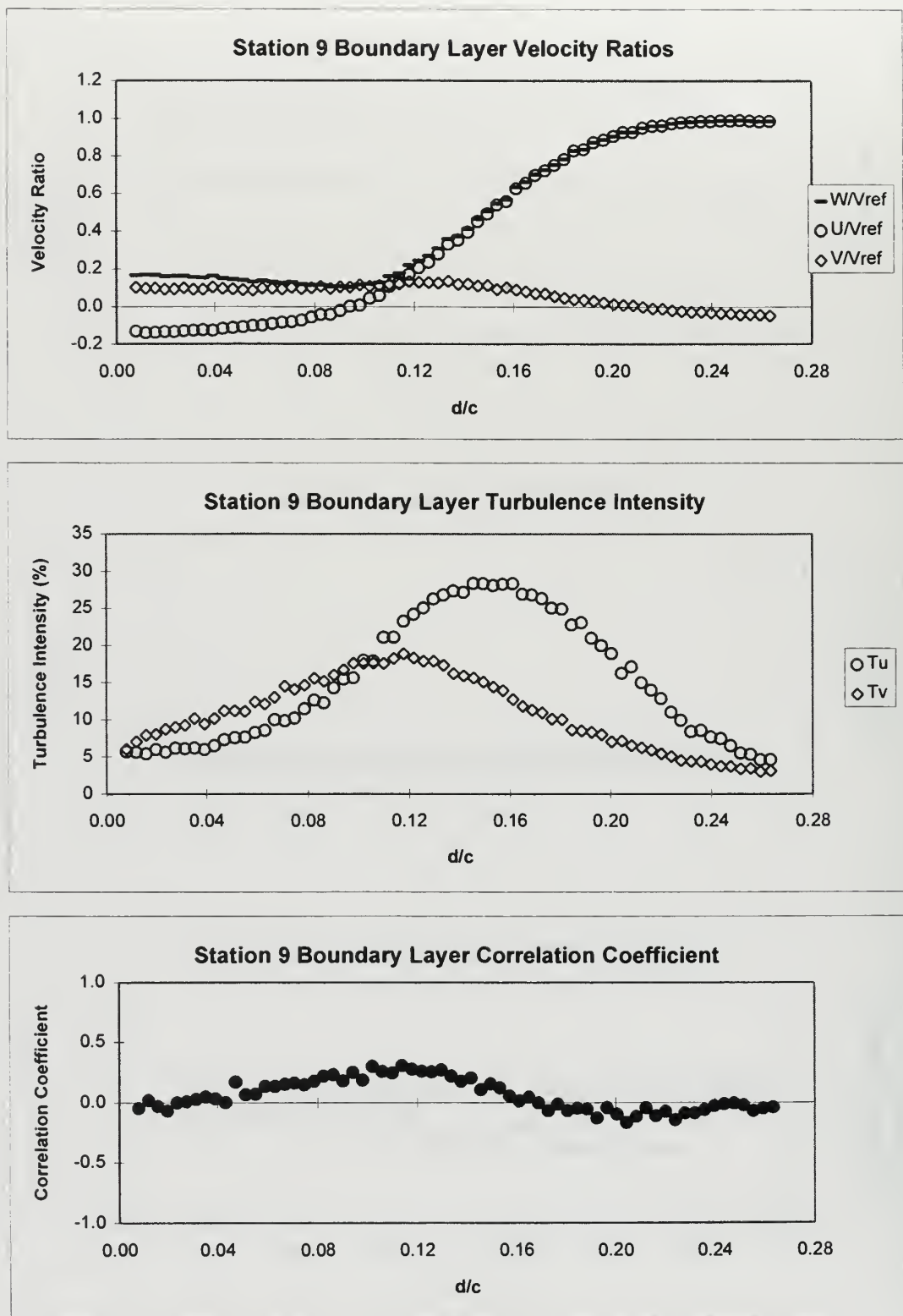


Figure 22. Station 9 Boundary Layer Survey Results at $Re=640,000$.

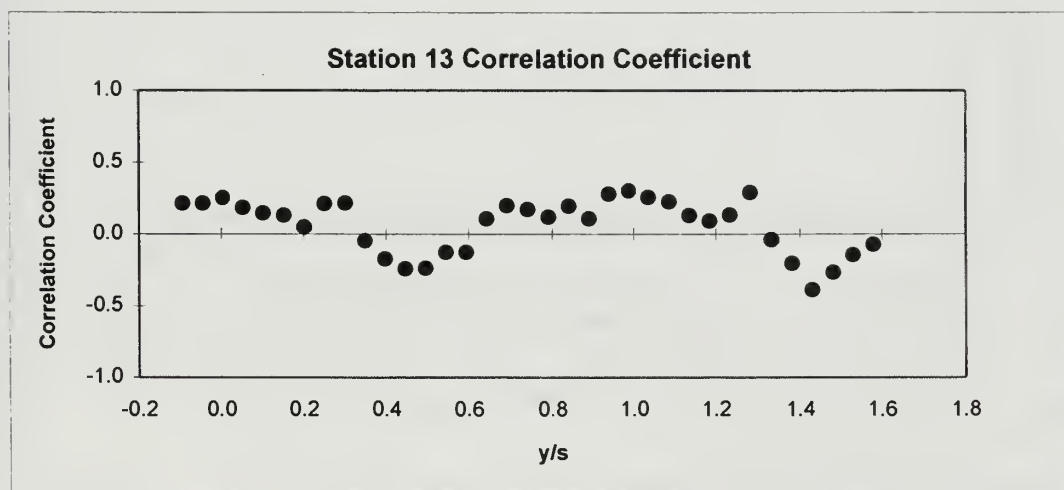
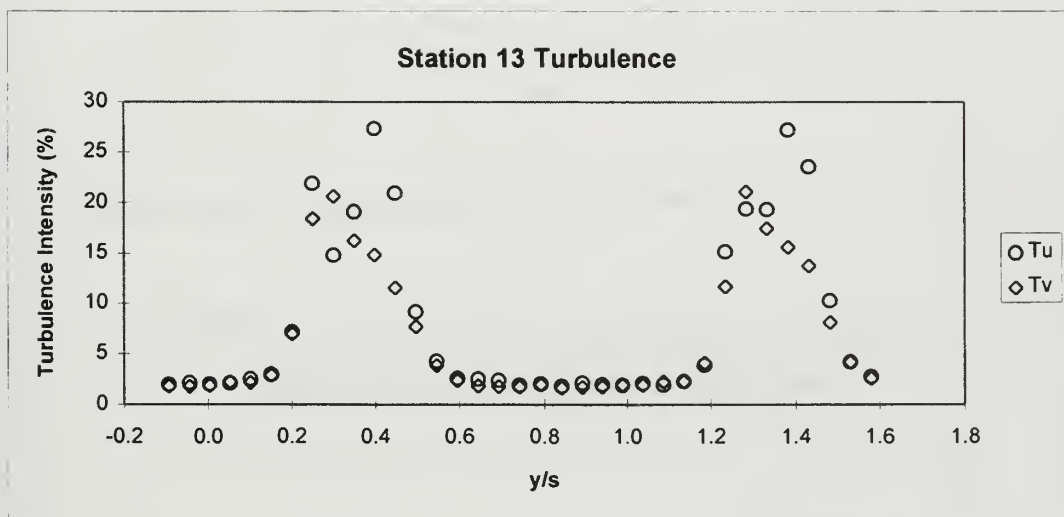
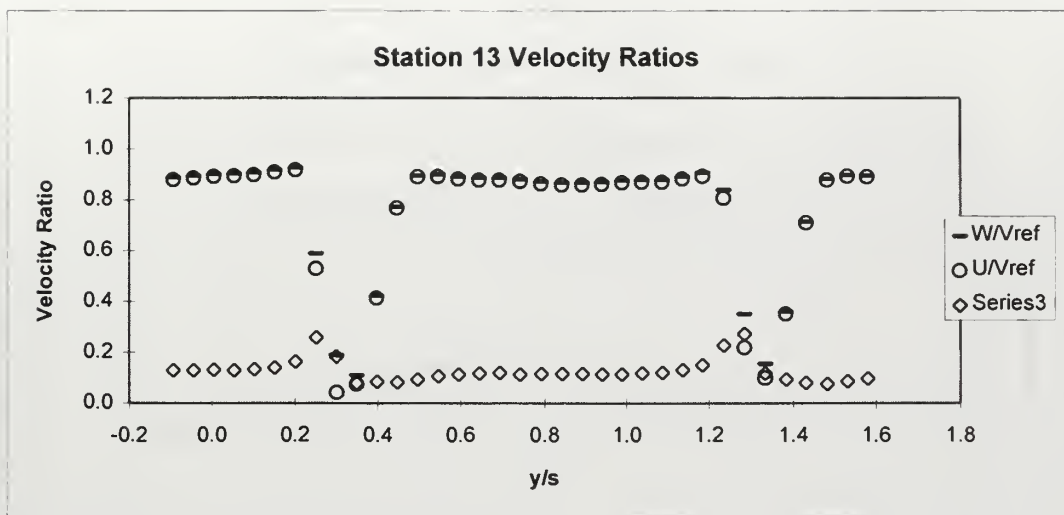


Figure 23. Station 13 Wake Survey Results at $Re=640,000$.

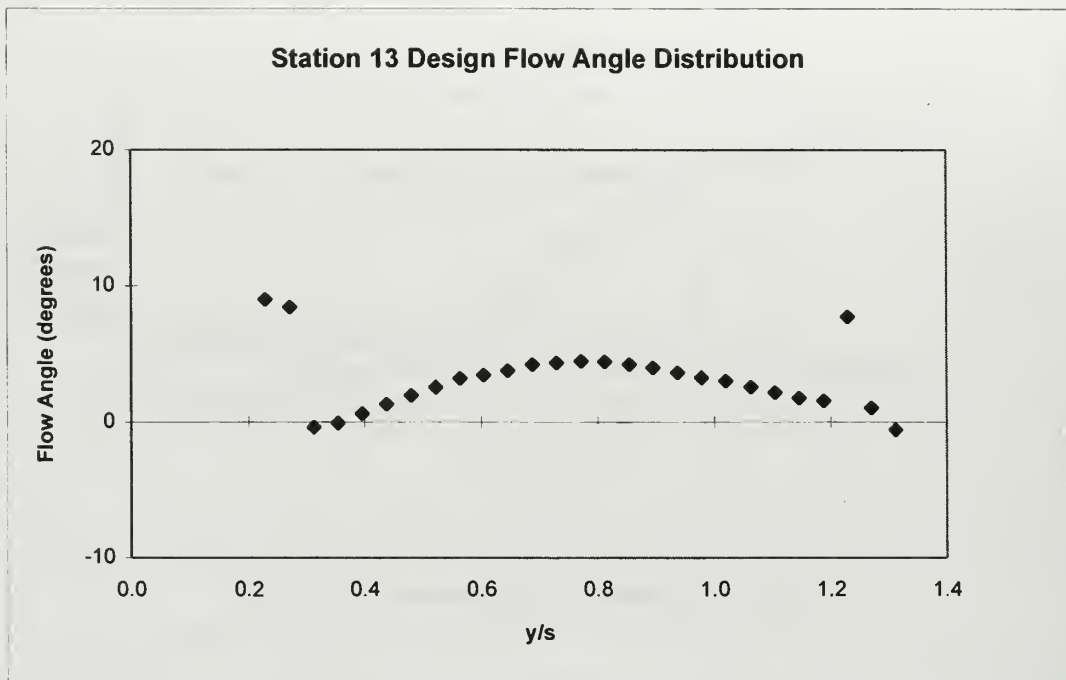


Figure 24a. Station 13 Wake Flow Angle Distribution at Design Incidence.

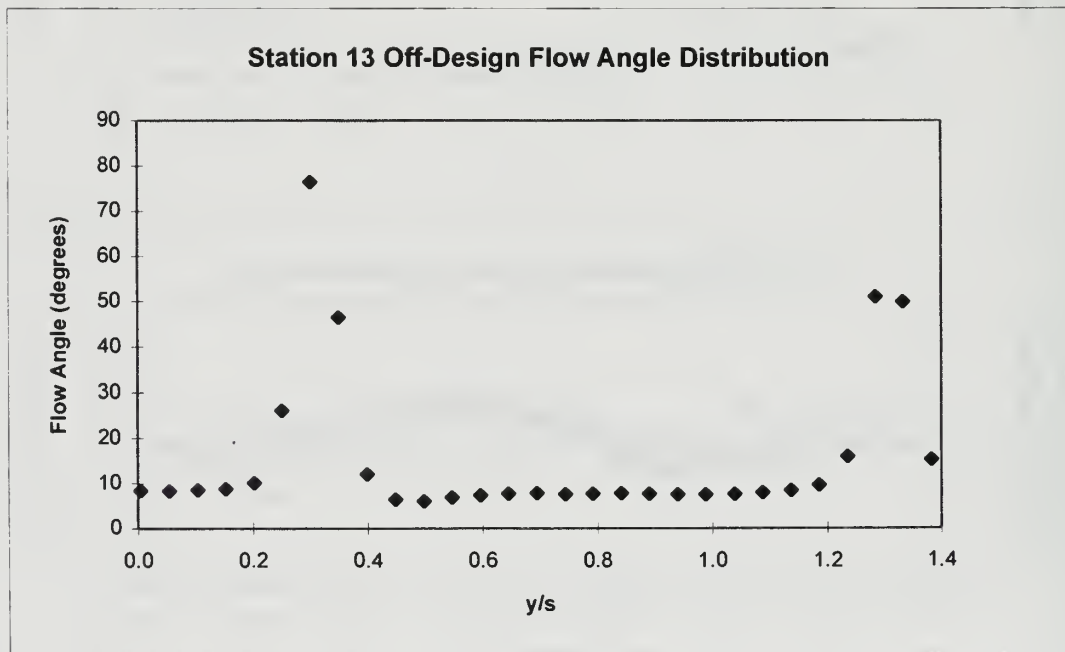


Figure 24b. Station 13 Wake Flow Angle Distribution at Off-Design Incidence.

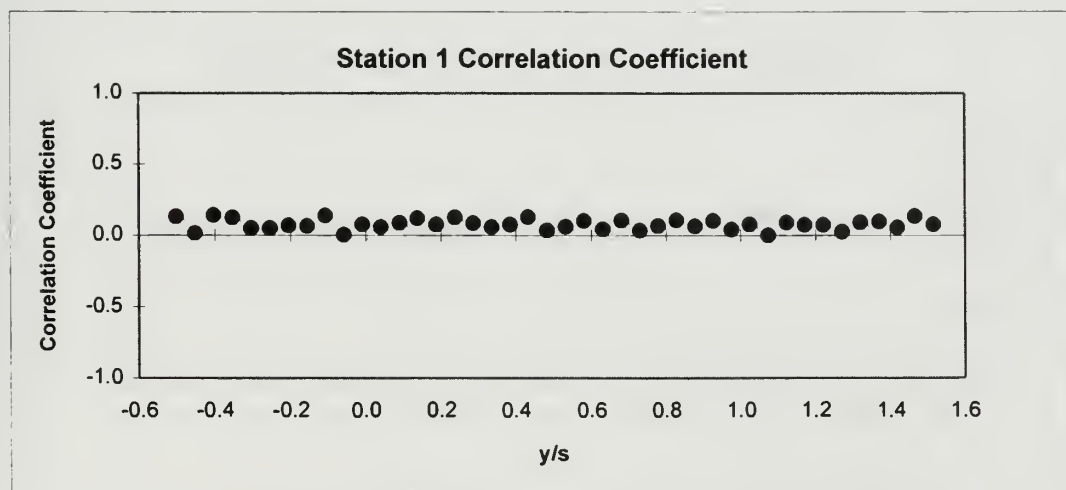
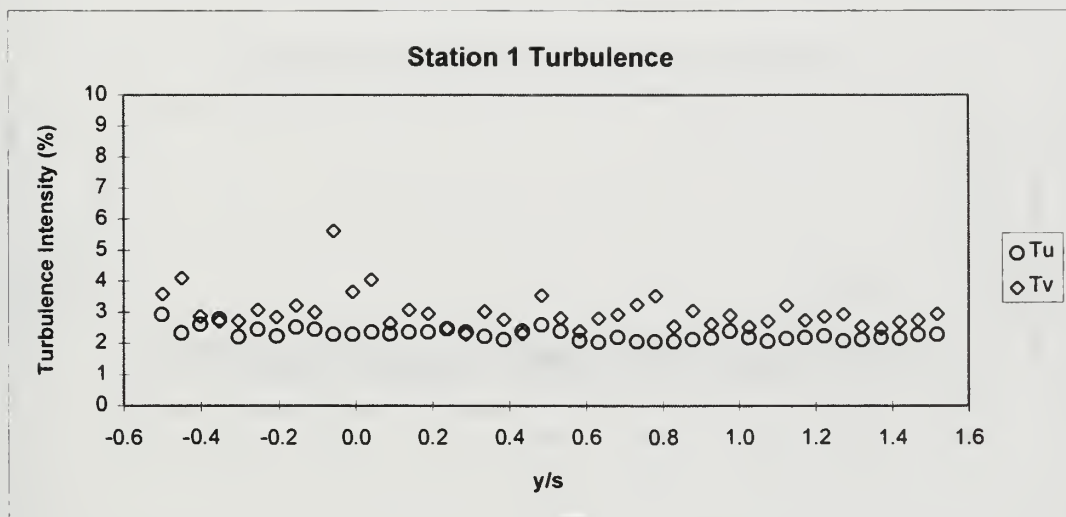
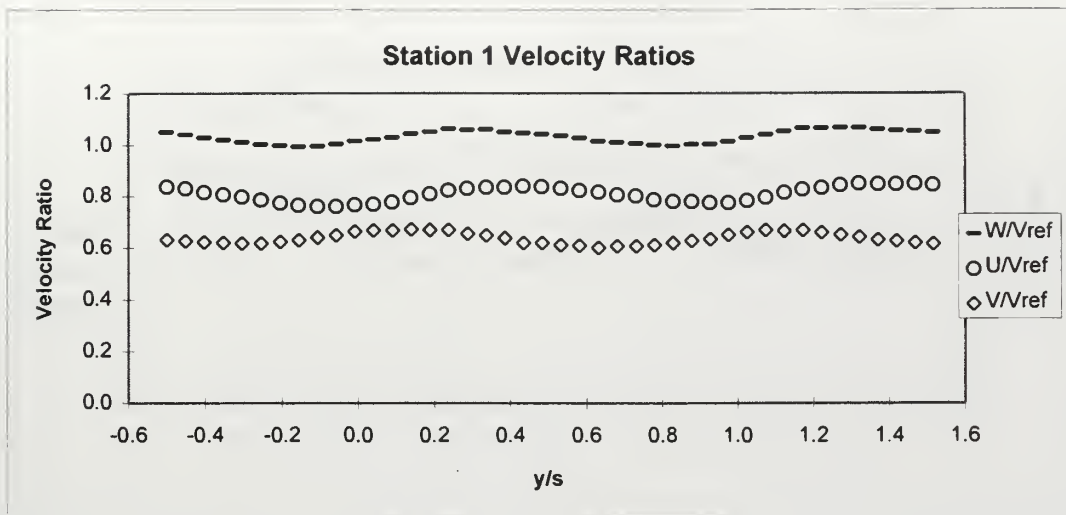


Figure 25. Station 1 Inlet Survey Results at $Re=210,000$.

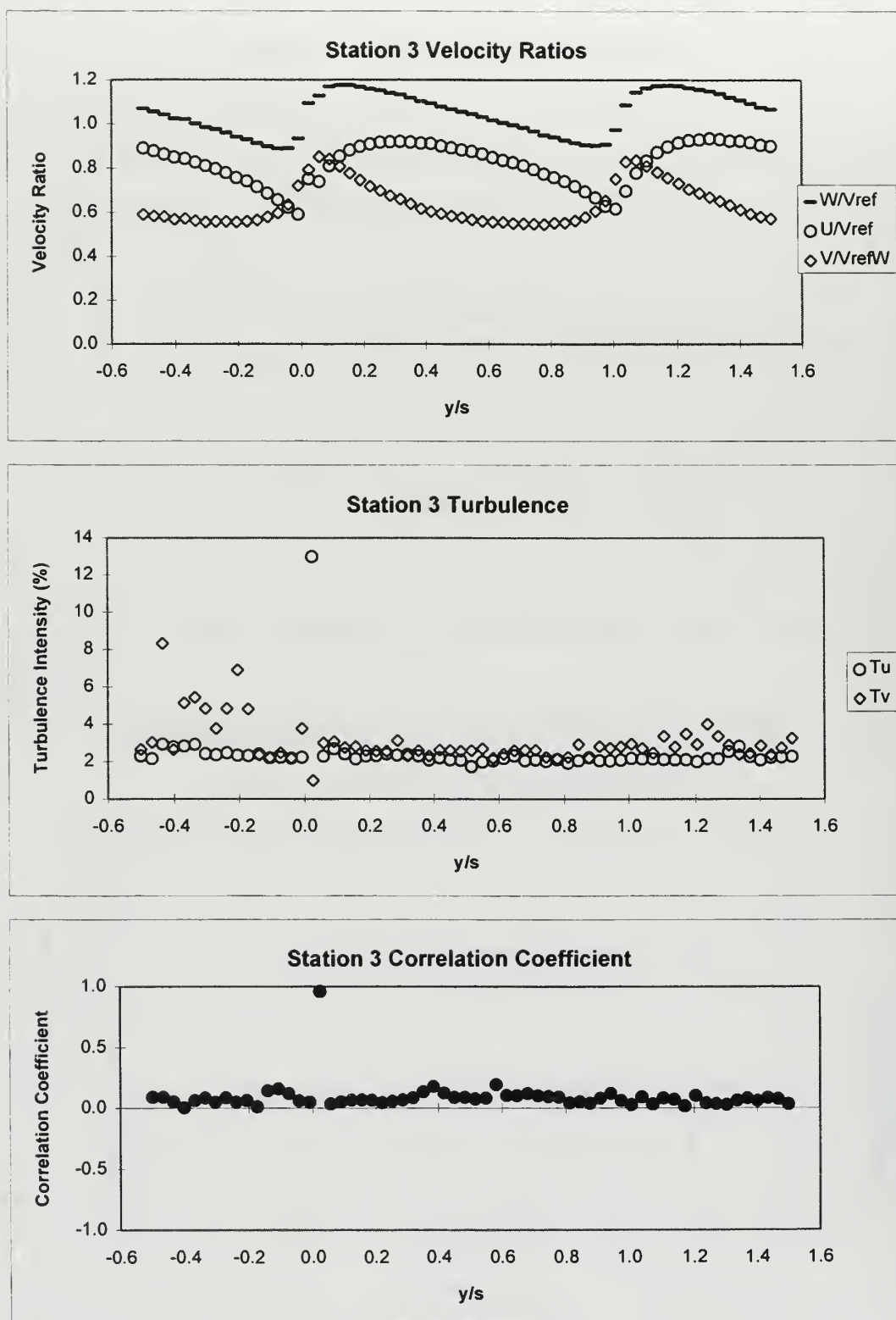


Figure 26. Station 3 Inlet Survey Results at $Re=210,000$.

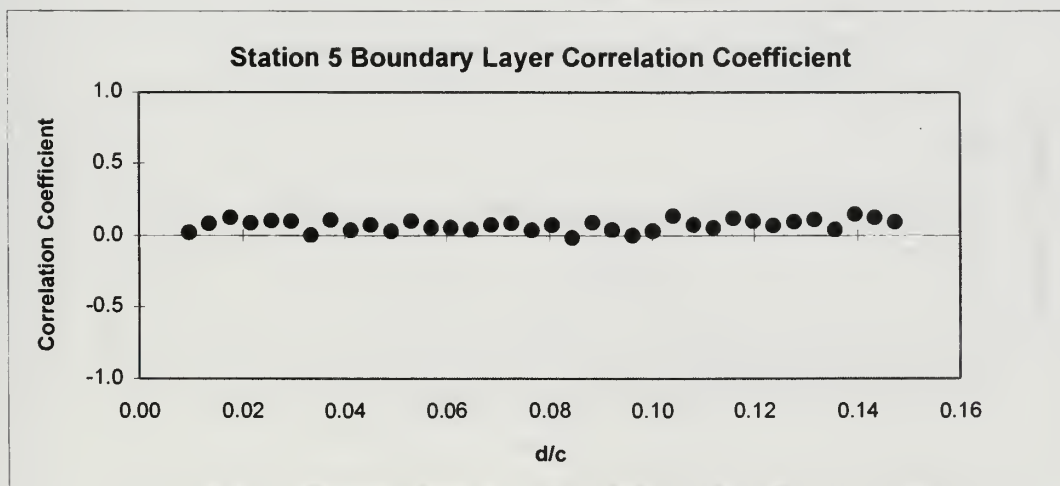
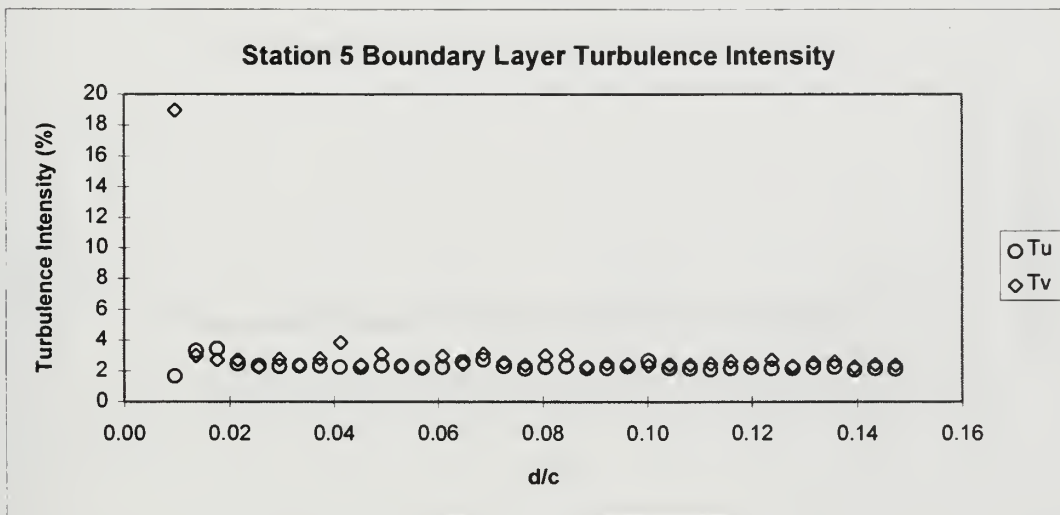
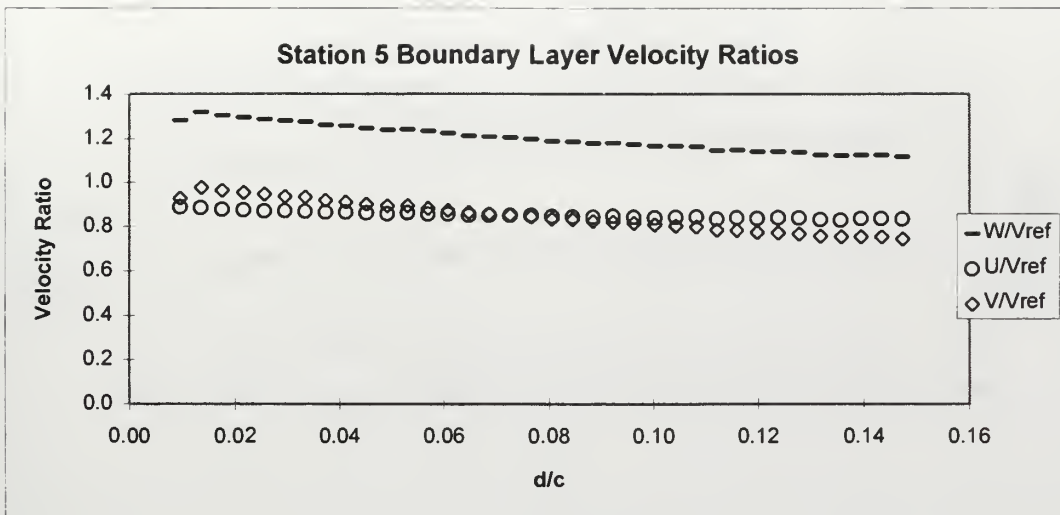


Figure 27. Station 5 Boundary Layer Survey Results at $Re=210,000$.

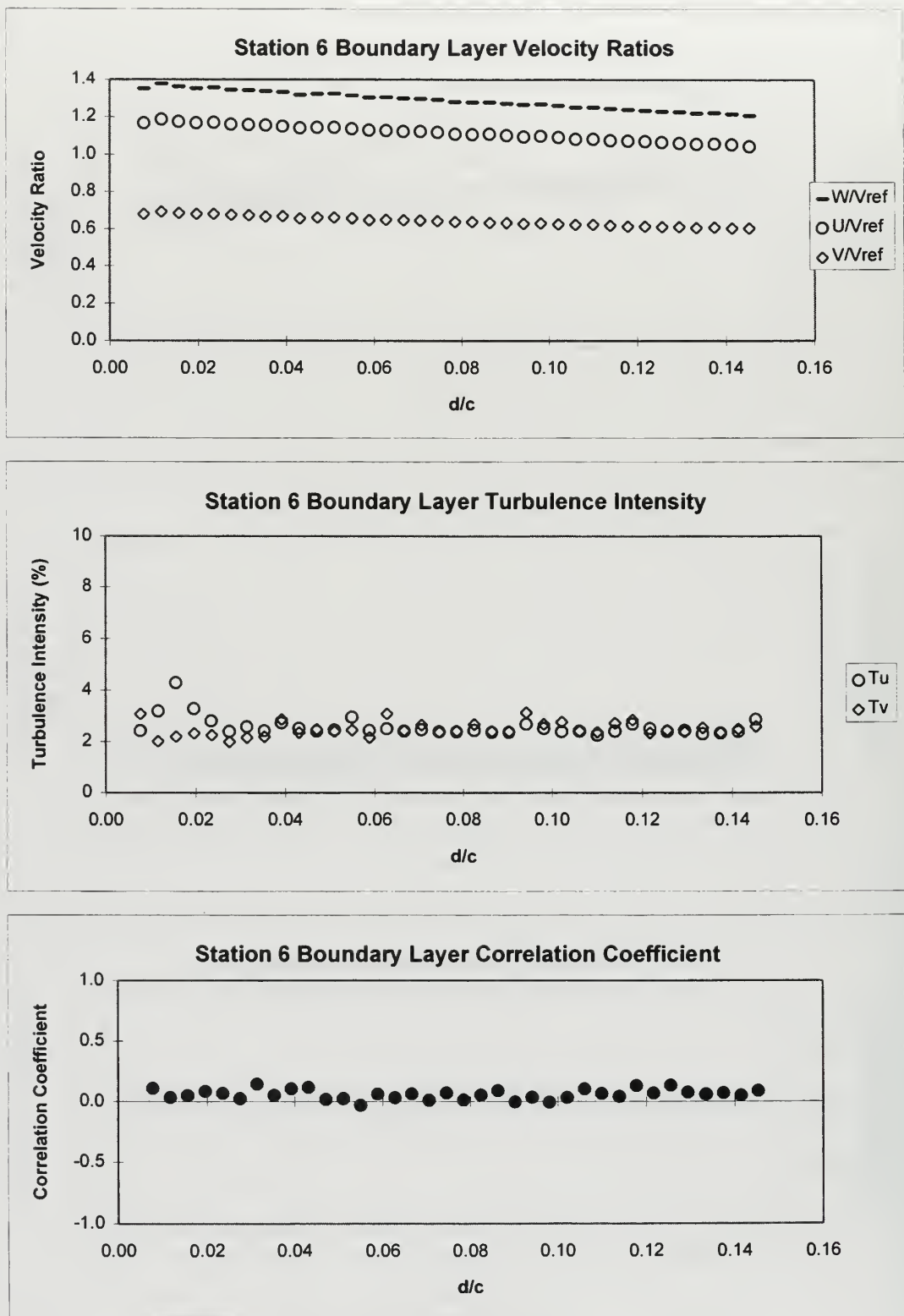


Figure 28. Station 6 Boundary Layer Survey Results at $Re=210,000$.

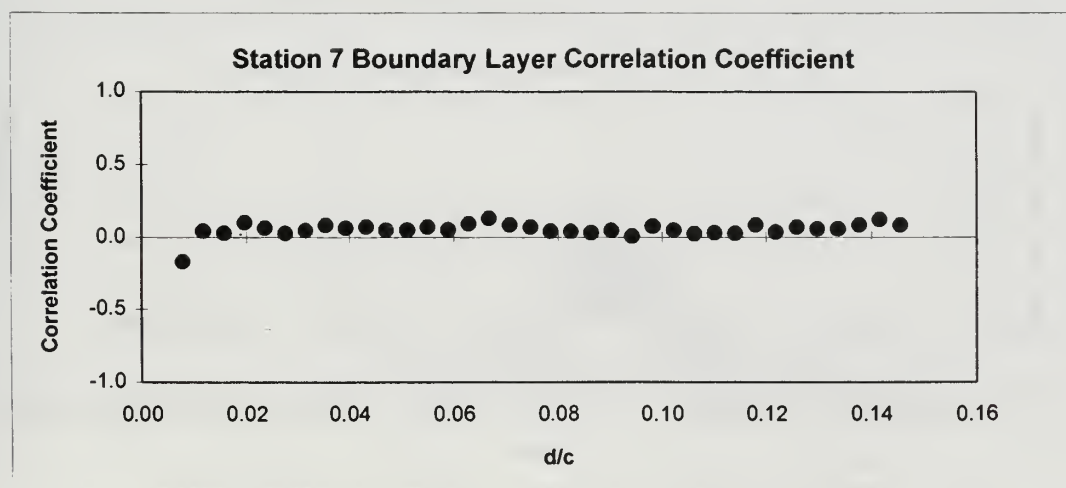
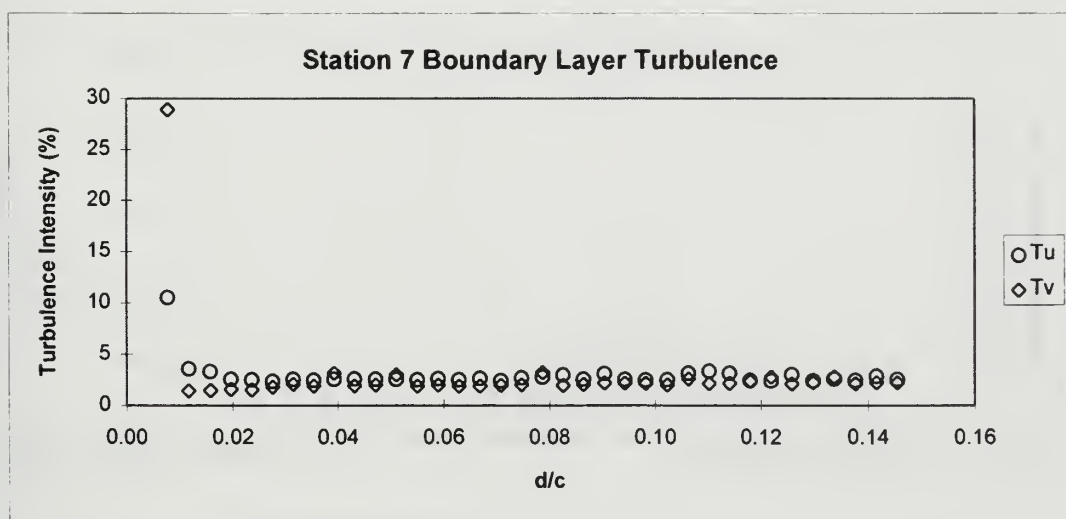
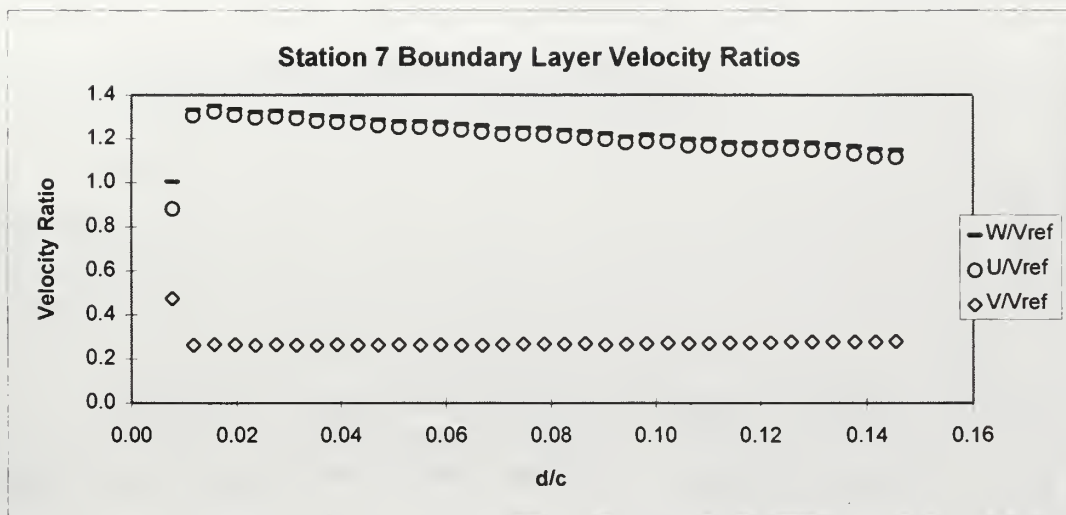


Figure 29a. Station 7 Boundary Layer Survey Results at $Re=210,000$.

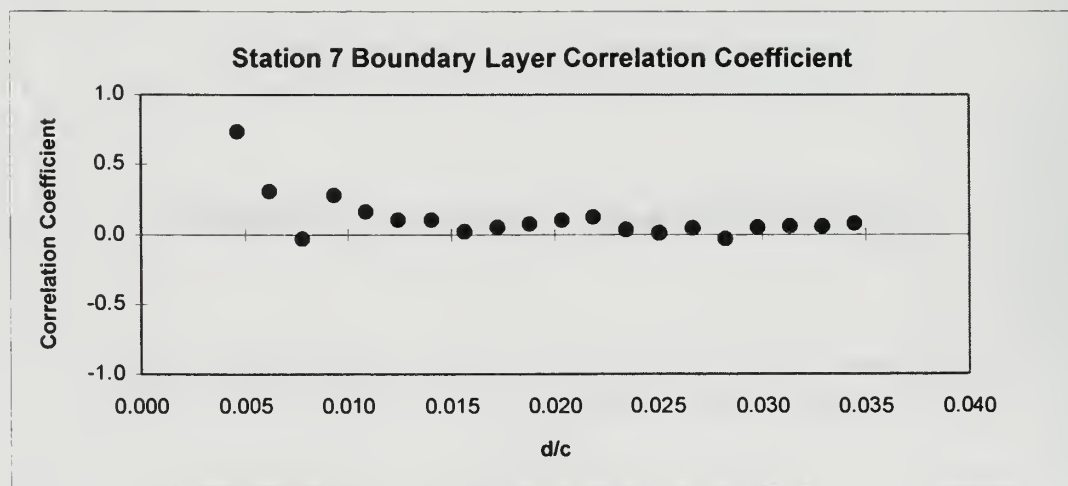
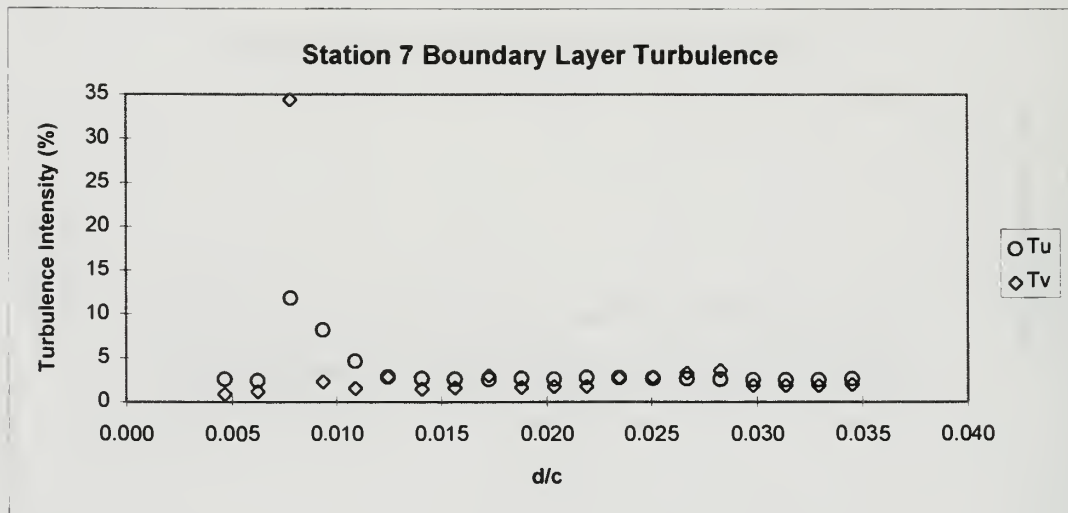
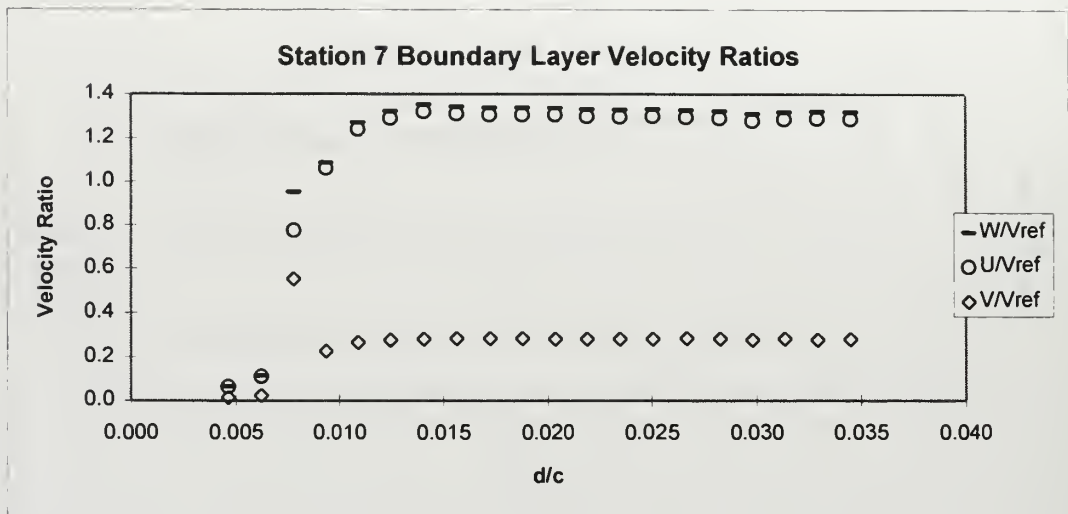


Figure 29b. Station 7 Boundary Layer Survey Results at $Re=210,000$.

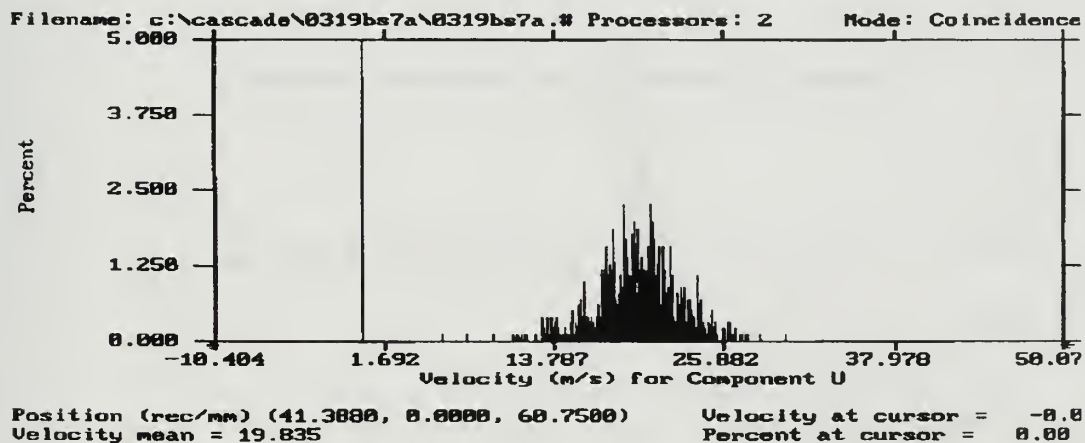
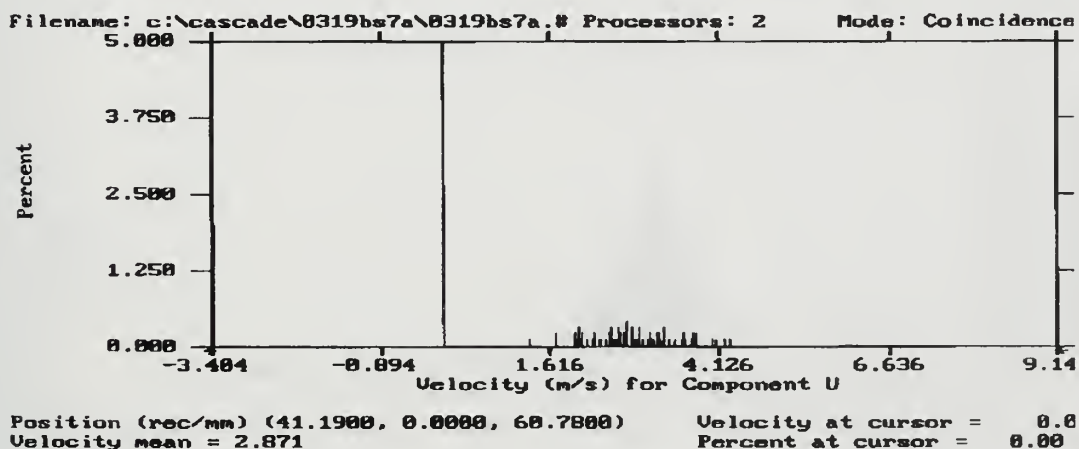
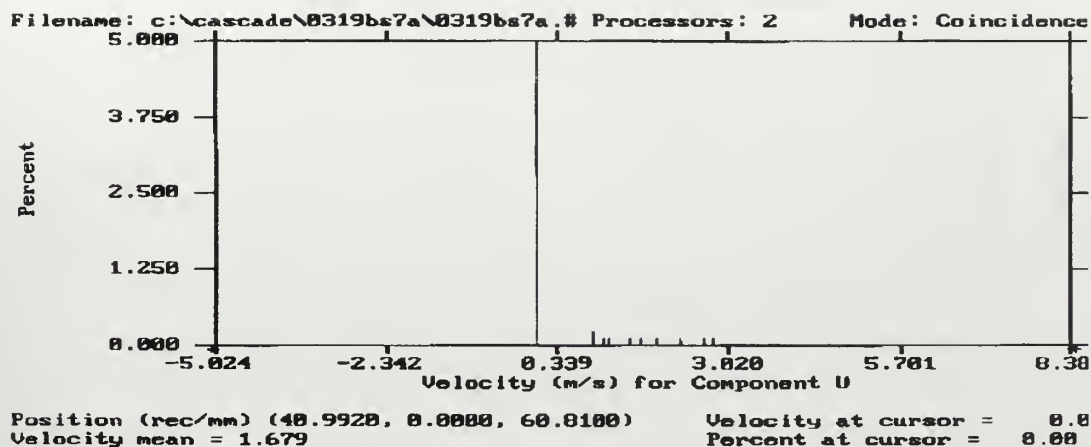


Figure 29c. Station 7 Axial Velocity Histograms.

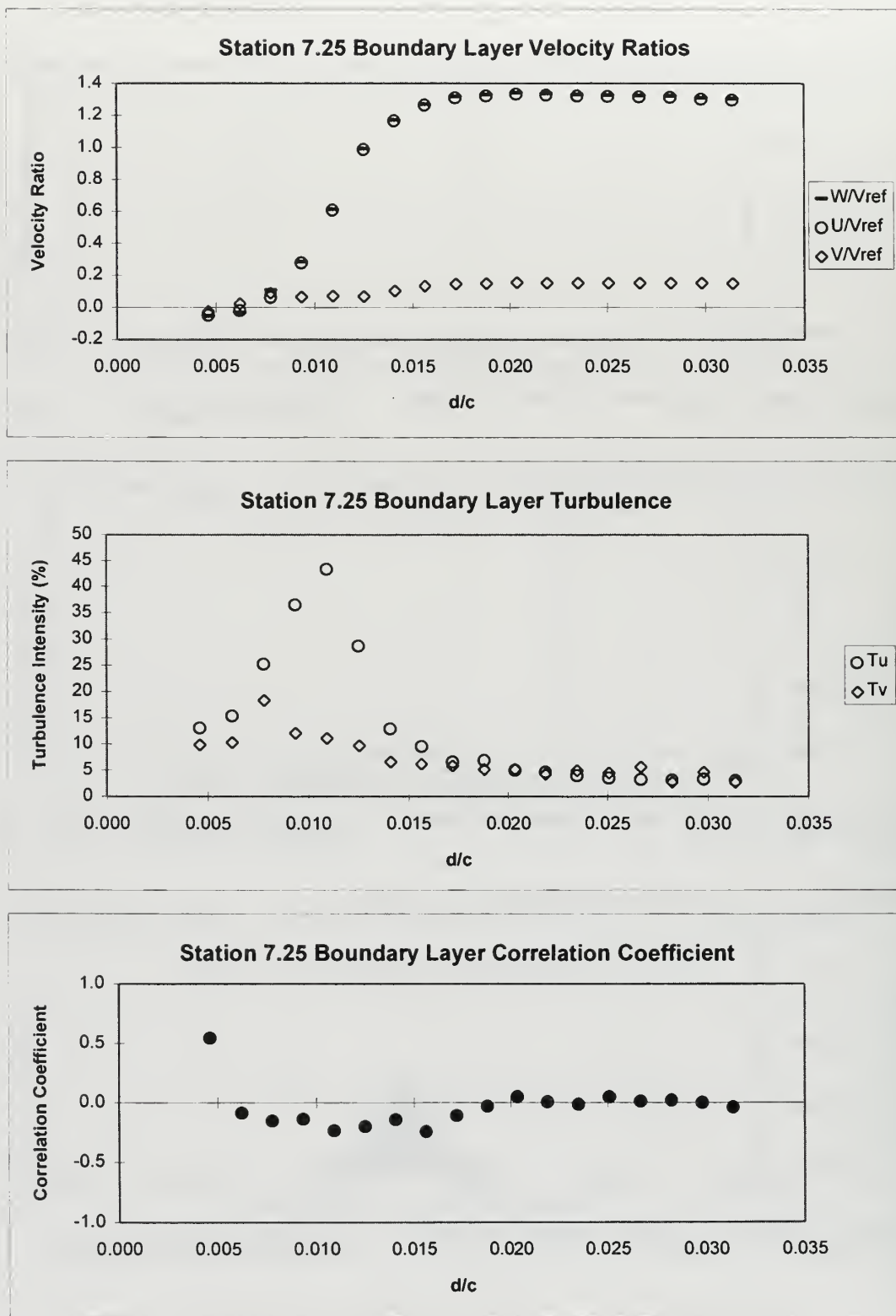


Figure 30a. Station 7.25 Boundary Layer Survey Results at $Re=210,000$.

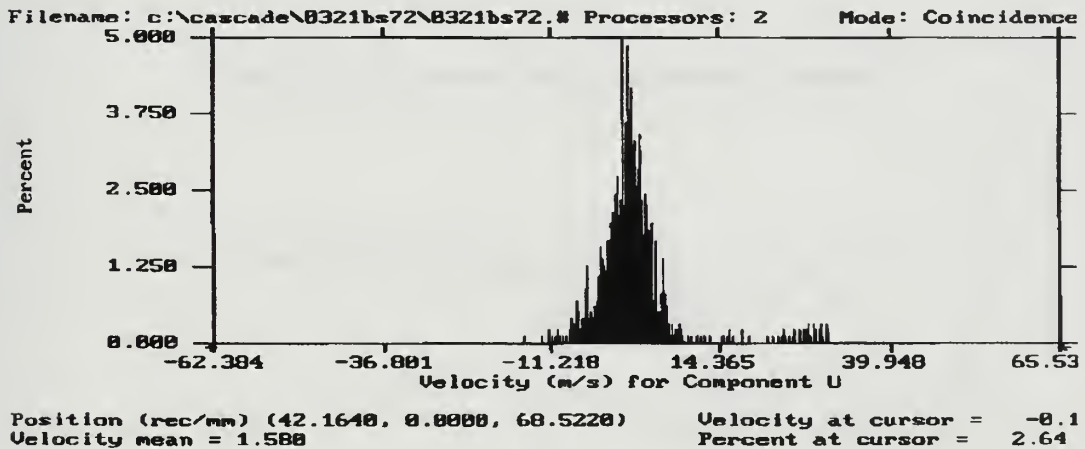
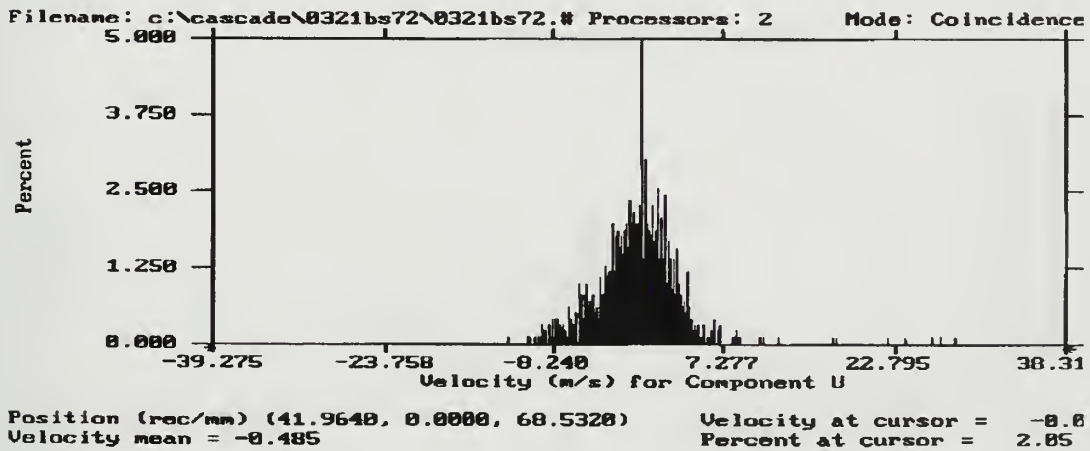
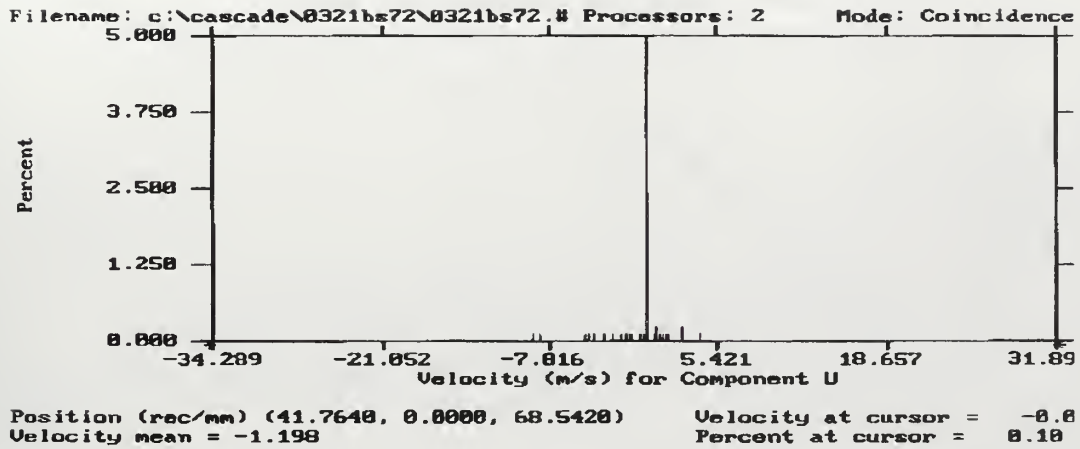


Figure 30b. Station 7.25 Axial Velocity Histograms.

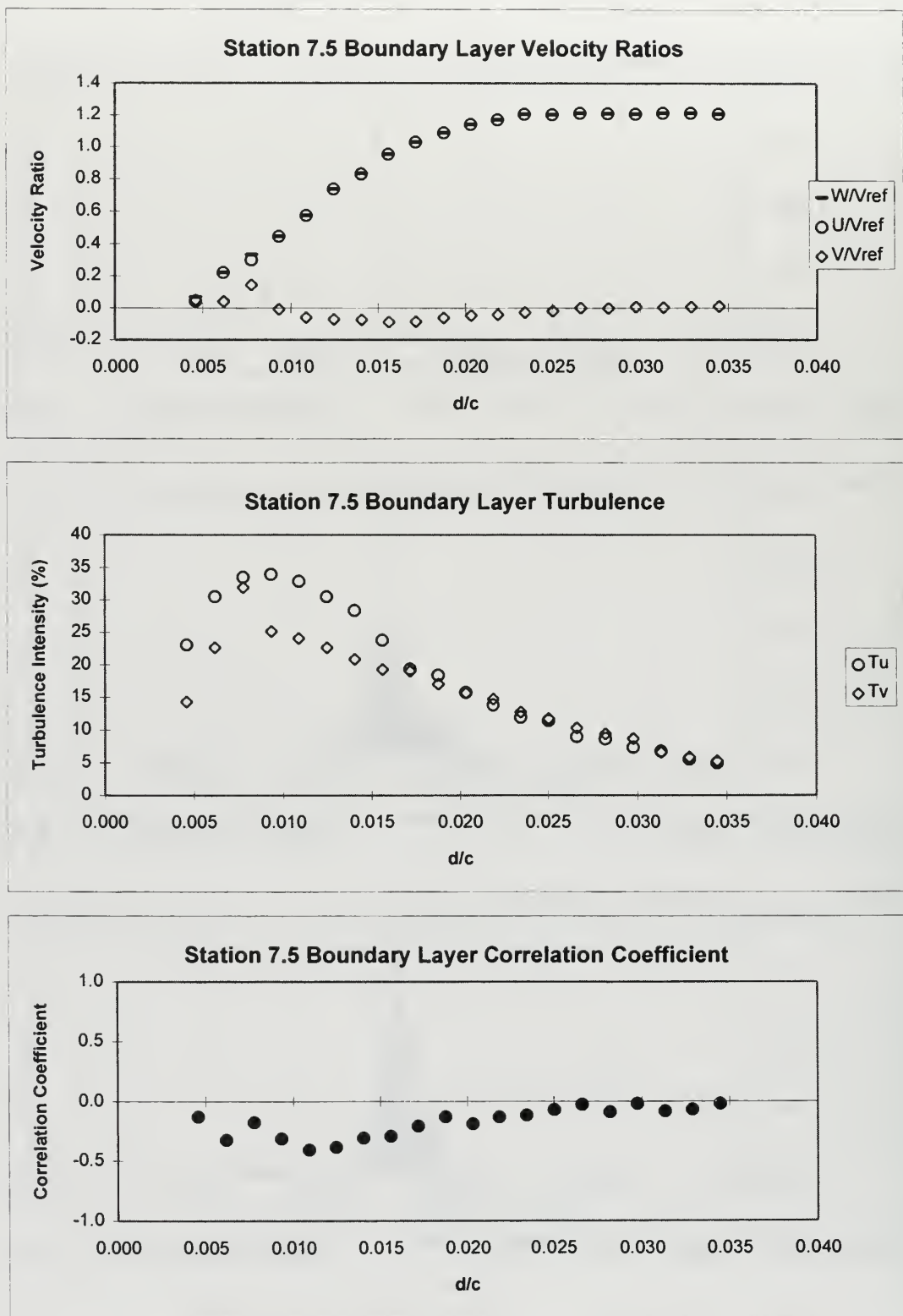


Figure 31a. Station 7.5 Boundary Layer Survey Results at $Re=210,000$.

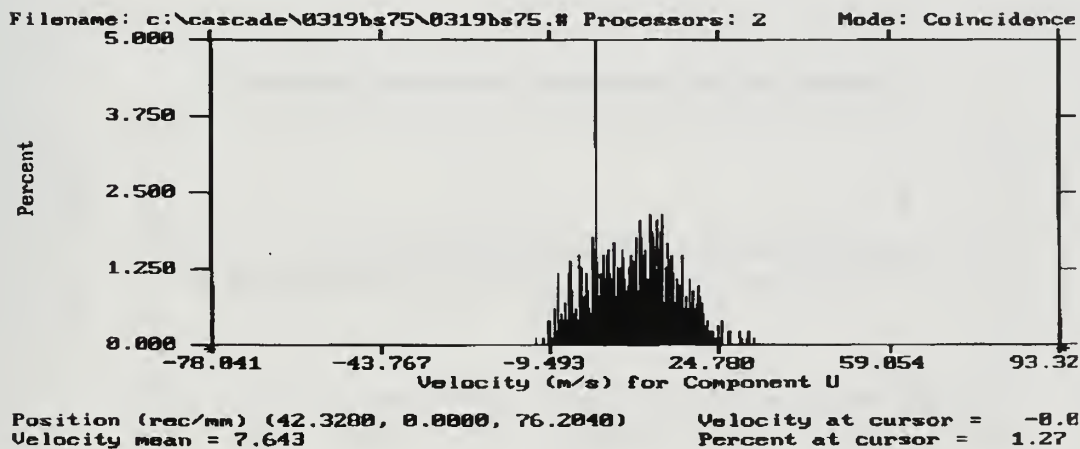
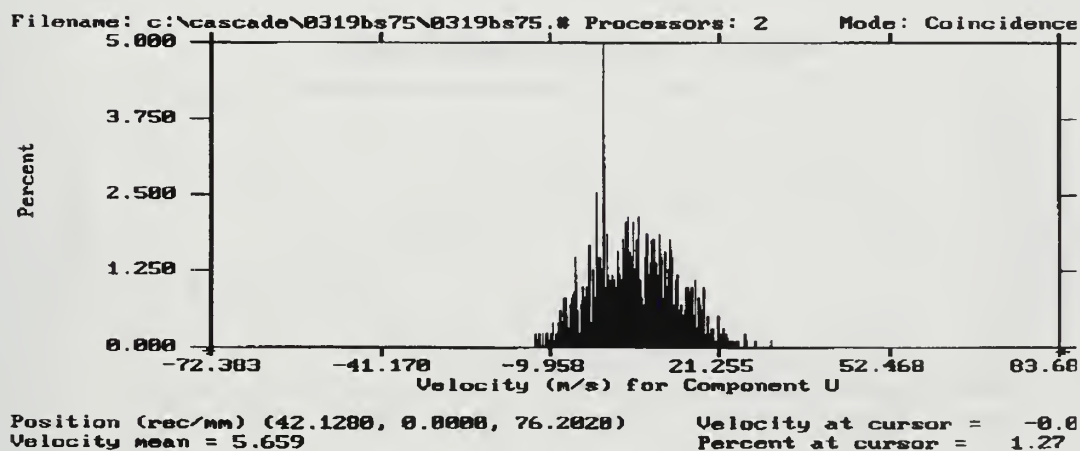
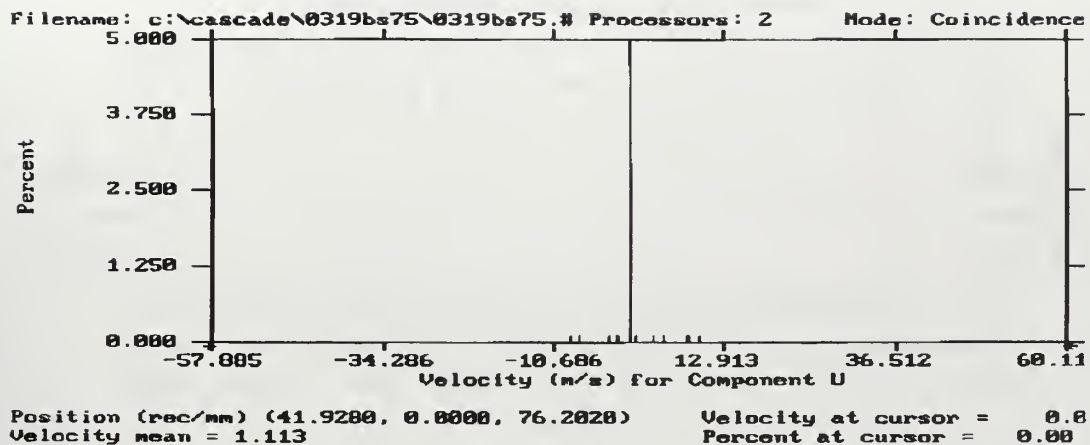


Figure 31b. Station 7.5 Axial Velocity Histograms.

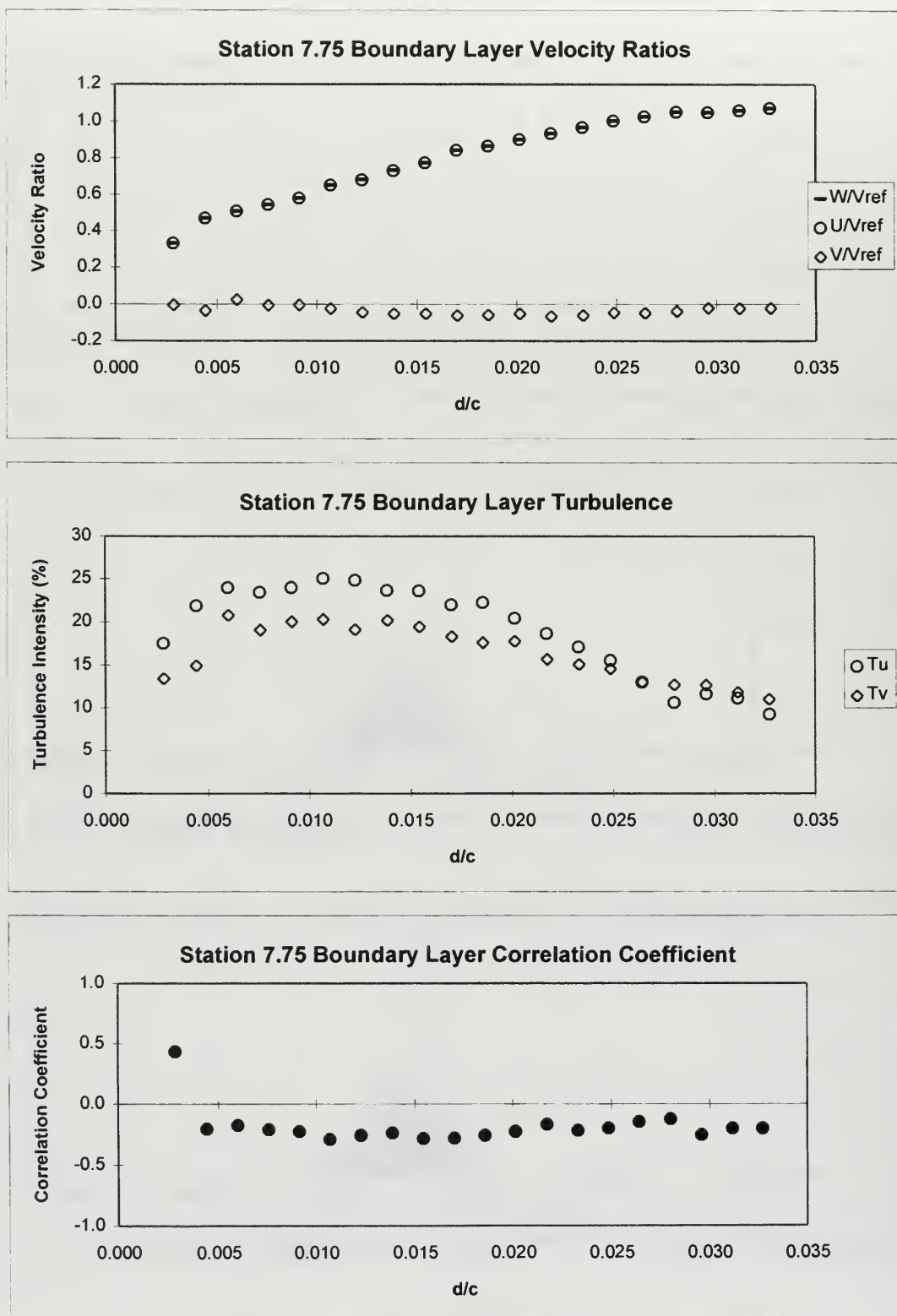


Figure 32. Station 7.75 Boundary Layer Survey Results at $Re=210,000$.

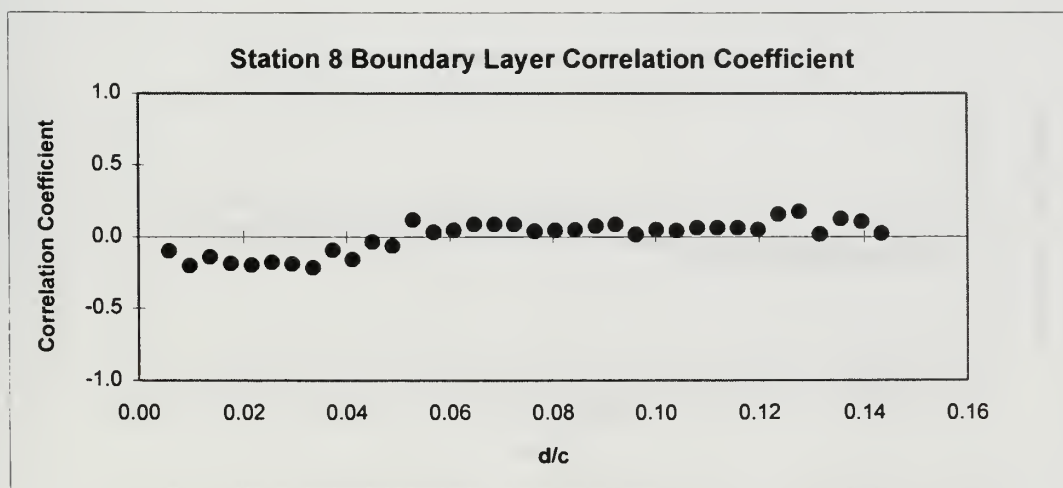
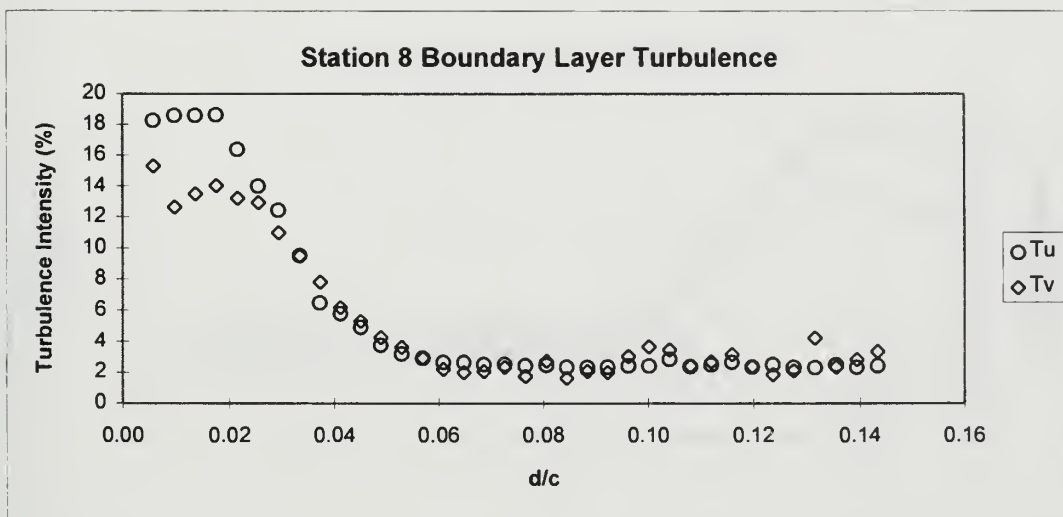
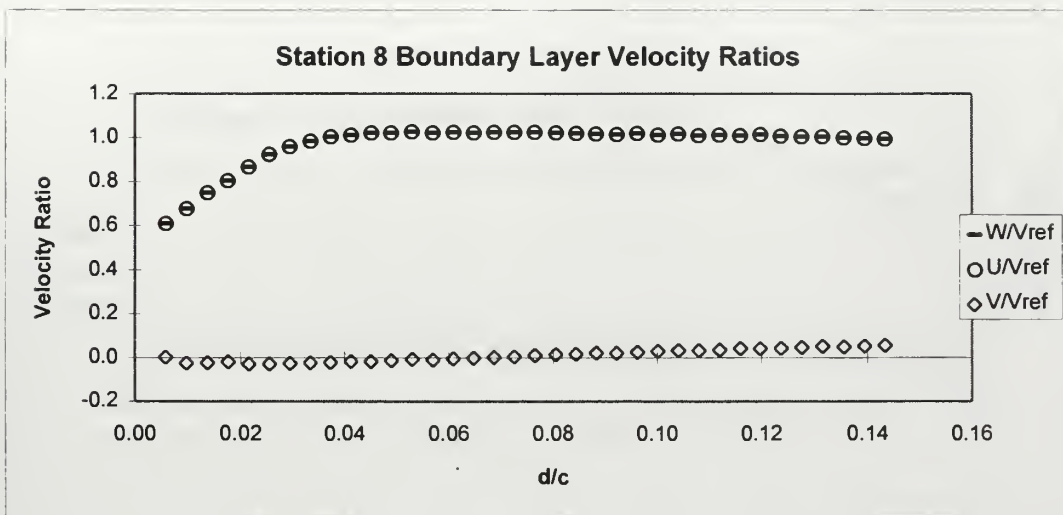


Figure 33. Station 8 Boundary Layer Survey Results at $Re=210,000$.

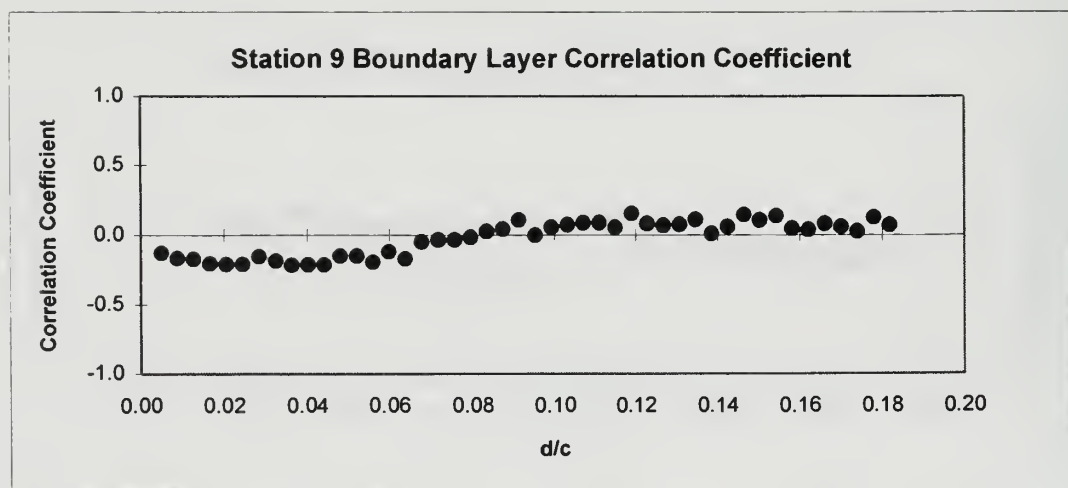
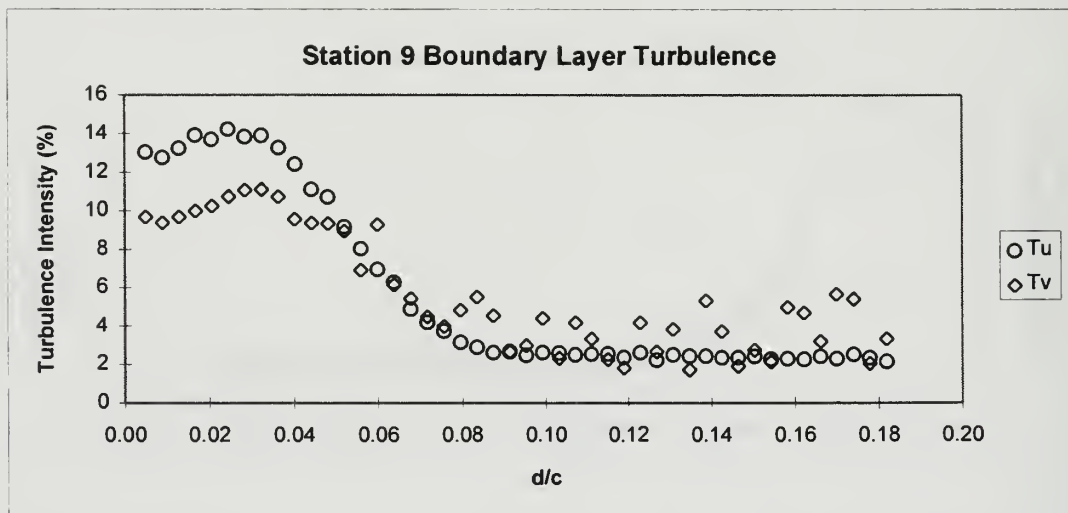
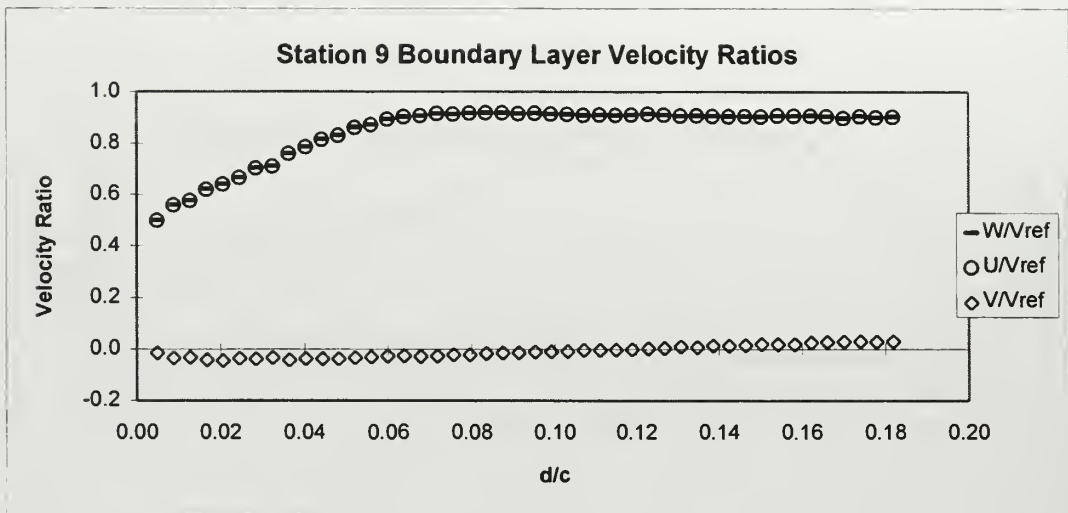


Figure 34. Station 9 Boundary Layer Survey Results at $Re=210,000$.

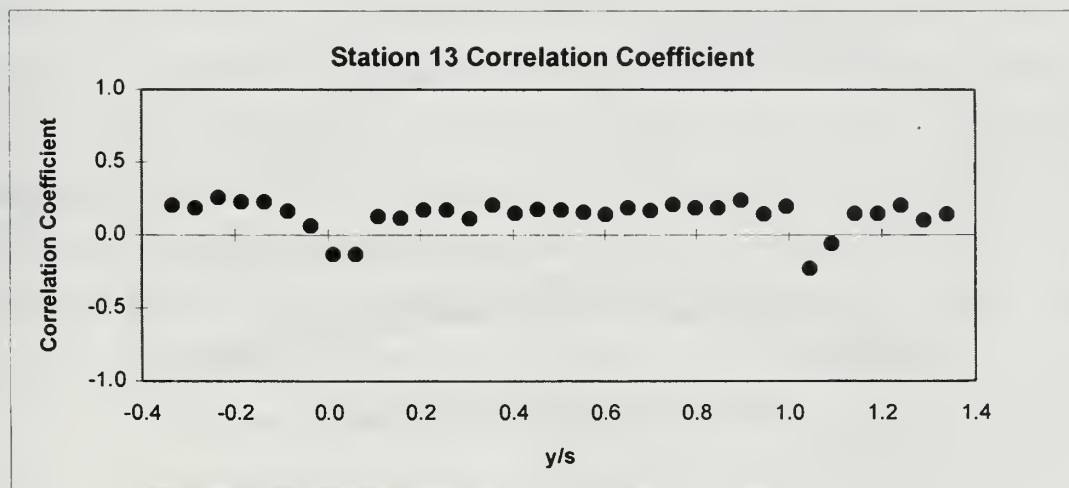
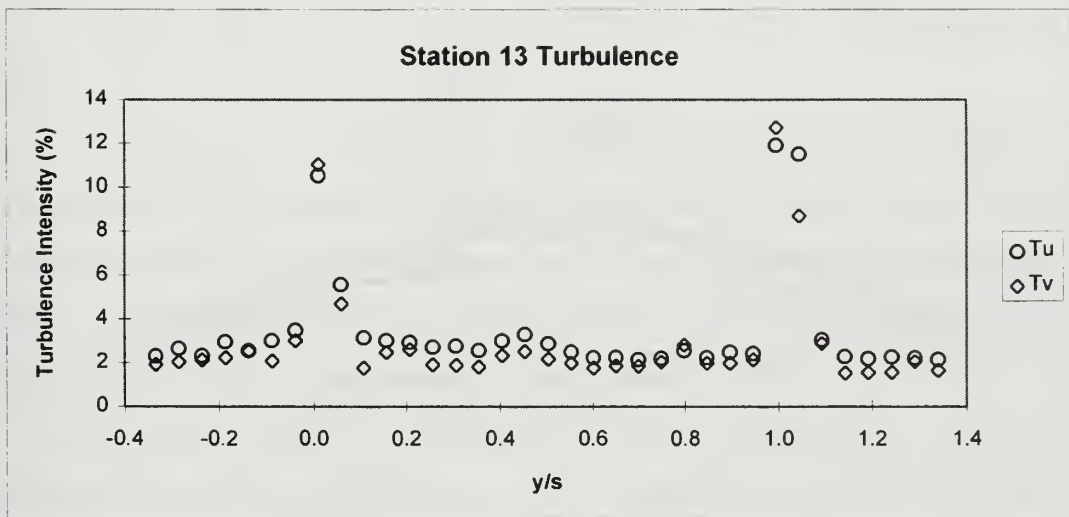
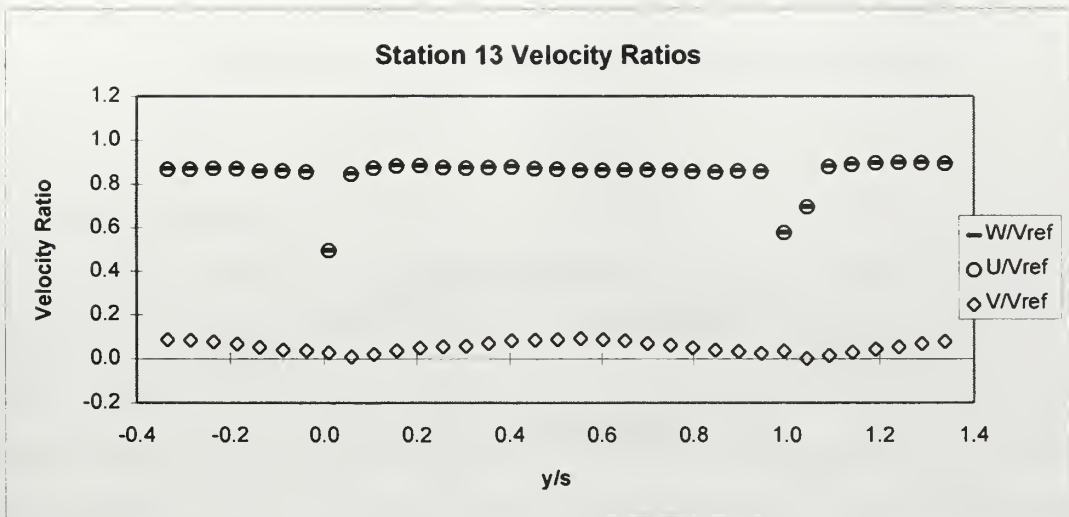
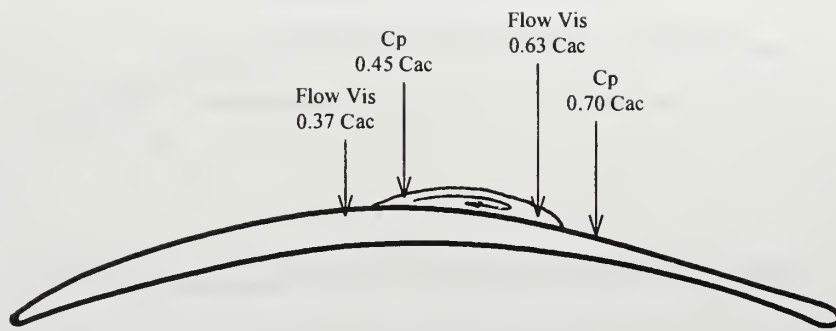
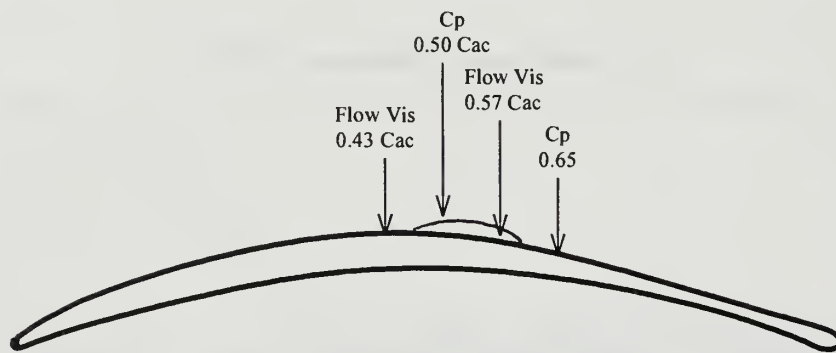


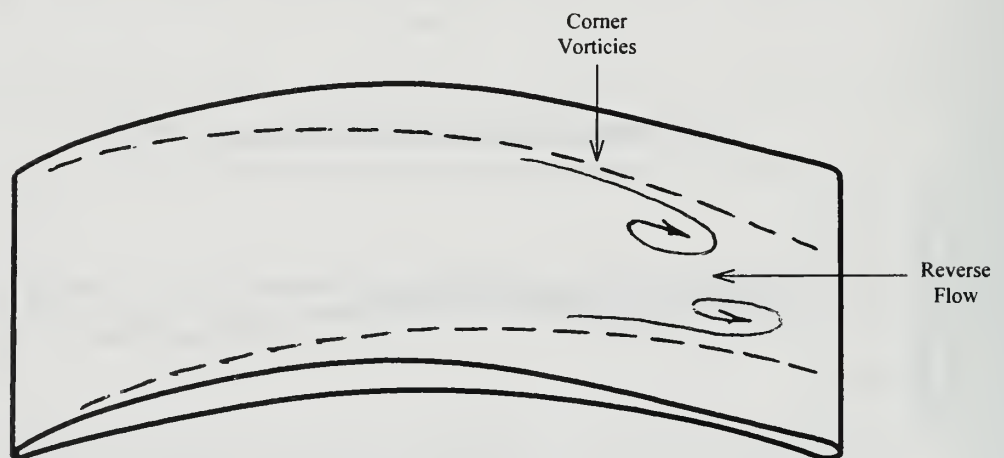
Figure 35. Station 13 Wake Survey Results at $Re=210,000$.



Flow Characteristics at $Re=210,000$.



Flow Characteristics at $Re=380,000$.



Flow Characteristics at $Re=640,000$.

Figure 36. Flow Structure Variation with Reynolds Number.

V. CONCLUSIONS AND RECOMMENDATIONS

A. CONCLUSIONS

Compressor Stator 67B cascade blading was experimentally tested at an off-design inlet-flow angle in a low speed cascade wind tunnel. Objectives of the tests included the characterization of the off-design flow field in general and investigation of the flow separation region in detail. Primarily, the effect of Reynolds number variation on flow separation was investigated. Experiments were conducted at an off-design inlet-flow angle of 38 degrees and Reynolds numbers based on chord of 640,000, 380,000 and 210,000.

Experimental blade surface pressure measurements were obtained at the three Reynolds numbers. No separation indications were noted at the high Reynolds number. A mid-chord separation bubble was apparent at the low and intermediate Reynolds numbers. The separation point moved forward and the separation region decreased in length as the Reynolds number increased.

Surface flow visualization utilizing a titanium oxide and kerosene mixture was performed at the three Reynolds numbers. Flow visualization revealed a highly three-dimensional flow field at the high Reynolds number with trailing edge reverse flow between two counter rotating vortices. Flow visualization at the low and intermediate Reynolds numbers indicated a predominately two-dimensional flow field with separation at mid-chord. The separation was laminar at the low Reynolds number and became transitional at the intermediate Reynolds number. The separation point moved downstream and the region decreased in length with increasing Reynolds number. Good periodicity was noted across the test section at all three Reynolds numbers.

LDV results were obtained to characterize the flow in the inlet, in the blade passage, in the blade boundary layers and at the exit of the test section at the three

Reynolds numbers. Detailed LDV boundary layer measurements at the low Reynolds number revealed the initiation of flow separation ahead of $0.55 C_{ac}$ with flow reattachment near $0.78 C_{ac}$. LDV results at the intermediate Reynolds number also indicated flow separation between $0.55 C_{ac}$ and $0.78 C_{ac}$; however, no reversed flow was measured. LDV results at the high Reynolds number showed trailing edge reverse flow; however, these measurements were taken in a region of highly three-dimensional flow.

B. RECOMMENDATIONS

Further LDV boundary layer surveys should be performed at the low and intermediate Reynolds to further characterize the separation region. Specifically, surveys should be conducted between approximately $0.35 C_{ac}$ and $0.55 C_{ac}$ at the low Reynolds number in an attempt to pinpoint the actual separation point.

Laser sheet flow visualization with fog should be performed to remove the gravity effect on the TiO_2 and kerosene mixture and attempt to visually observe flow particles inside the separation bubble.

APPENDIX A. LDV SUMMARY AND REDUCED DATA

Survey Number	Survey Name	Station	Date taken	Reynolds Number	Survey Points	Patm (psi)	Ppl (in H2o)	Tpl (F)	Vref (m/s)	Yaw-Pitch (deg)
1	0108s1a	1	8-Jan-96	640000	42	14.71	12	70	75.6446	
2	0120s1a	1	20-Jan-96	640000	42	14.78	11.95	70	75.3133	
3	0109s3a	3	9-Jan-96	640000	74	14.76	12	73	75.7328	
4	0115s5a	5	15-Jan-96	640000	65	14.81	11.9	71	75.1538	
5	0115s8a	8	15-Jan-96	640000	33	14.81	12	72	75.5354	
6	0114s10a	10	14-Jan-96	640000	122	14.8	11.95	68	75.1206	
7	0116bs5a	5 bl	16-Jan-96	640000	31	14.62	11.85	72	75.548	4 left
8	0116bs7a	7 bl	16-Jan-96	640000	31	14.64	12.1	73	76.3493	4 left
9	0120bs9a	9 bl	20-Jan-96	640000	66	14.84	12.1	69	75.5552	4 left
10	0110s13a	13	10-Jan-96	640000	35	14.8	11.95	74	75.5467	
11	0210s1a	1	10-Feb-96	210000	42	14.72	1.52	67	27.6885	
12	0210s3a	3	10-Feb-96	210000	62	14.72	1.52	67	27.6885	
13	0203bs5a	5 bl	3-Feb-96	210000	36	14.72	1.75	62	29.4427	4 left
14	0203bs6a	6 bl	3-Feb-96	210000	36	14.72	1.75	62	29.4427	4 left
15	0203bs7a	7 bl	3-Feb-96	210000	36	14.72	1.73	62	29.2853	4 left
16	0319bs7a	7 bl	19-Mar-96	210000	20	14.73	1.29	64	25.5721	4 left
17	0321bs72	7.25 bl	21-Mar-96	210000	18	14.7	1.25	65	25.2504	4 left
18	0319bs75	7.5 bl	19-Mar-96	210000	20	14.73	1.28	67	25.5531	4 left
19	0321bs77	7.75 bl	21-Mar-96	210000	20	14.7	1.25	65	25.4362	4 left
20	0203bs8a	8 bl	3-Feb-96	210000	36	14.72	1.73	62	29.2835	4 left
21	0203bs9a	9 bl	3-Feb-96	210000	46	14.72	1.49	62	27.3011	4 left
22	0210s13a	13	10-Feb-96	210000	35	14.72	1.52	67	27.6885	
23	1027bs7	7 bl	27-Oct-95	640000	30	14.64	12	80	76.5375	4 left-4 up
24	1102bs75	7.5 bl	2-Nov-95	640000	30	14.75	12	72	75.6865	4 left
25	1031bs6	6 bl	31-Oct-95	640000	30	14.66	11.8	72	75.2886	4 left
26	1031bs8	8 bl	31-Oct-95	640000	30	14.66	11.9	72	75.6024	4 left
27	0213s1a	1	13-Feb-96	380000	42	14.76	4	73	44.1855	
28	0213s3a	3	13-Feb-96	380000	61	14.76	4	77	44.3511	
29	0203bs5b	5 bl	3-Feb-96	380000	36	14.7	4	72	44.2316	4 left
30	0203bs6b	6 bl	3-Feb-96	380000	36	14.7	4	71	44.19	4 left
31	0203bs7b	7 bl	3-Feb-96	380000	36	14.7	4	70	44.1483	4 left
32	0203bs8b	8 bl	3-Feb-96	380000	36	14.7	4	68	44.0649	4 left
33	0203bs9b	9 bl	3-Feb-96	380000	46	14.7	4	66	43.9813	4 left
34	0213s13a	13	13-Feb-96	380000	52	14.76	3.96	80	44.2518	

Survey Number 1 (Station 1 inlet)									
x(mm)	y(mm)	y/s	W/Vref	U/Vref	V/Vref	Tu	Tv	Re stress	Cuv
-36.576	-76.200	-0.500	1.055	0.850	0.625	2.324	2.209	0.278	0.095
-36.576	-68.698	-0.451	1.043	0.842	0.617	2.642	2.335	0.309	0.088
-36.576	-61.200	-0.402	1.030	0.830	0.610	2.790	1.958	0.133	0.043
-36.576	-53.700	-0.352	1.020	0.820	0.606	2.393	2.061	0.049	0.017
-36.576	-46.200	-0.303	1.013	0.812	0.605	2.866	1.827	0.141	0.047
-36.574	-38.700	-0.254	1.006	0.804	0.605	2.038	1.825	0.170	0.080
-36.574	-31.200	-0.205	0.996	0.789	0.607	2.490	2.083	0.263	0.089
-36.576	-23.700	-0.156	0.995	0.783	0.614	2.097	2.305	0.176	0.064
-36.576	-16.200	-0.106	0.997	0.778	0.623	2.233	2.268	0.170	0.059
-36.576	-8.700	-0.057	0.992	0.774	0.620	2.140	2.261	0.221	0.080
-36.576	-1.200	-0.008	0.994	0.771	0.628	1.867	2.190	0.164	0.070
-36.576	6.300	0.041	1.005	0.777	0.637	1.882	2.115	0.056	0.025
-36.576	13.800	0.091	1.017	0.787	0.644	2.070	2.687	0.310	0.097
-36.576	21.300	0.140	1.032	0.800	0.651	2.531	2.854	0.333	0.081
-36.576	28.800	0.189	1.043	0.814	0.651	2.290	2.863	0.106	0.028
-36.576	36.300	0.238	1.048	0.825	0.647	2.385	2.323	0.195	0.061
-36.576	43.800	0.287	1.043	0.826	0.636	2.074	2.378	0.221	0.078
-36.576	51.300	0.337	1.040	0.829	0.628	2.086	2.709	0.294	0.091
-36.576	58.800	0.386	1.037	0.830	0.623	1.830	2.416	0.157	0.062
-36.576	66.302	0.435	1.031	0.829	0.614	2.167	1.869	0.224	0.097
-36.576	73.800	0.484	1.030	0.829	0.611	2.190	2.215	0.398	0.143
-36.576	81.302	0.533	1.026	0.826	0.608	2.397	2.081	0.151	0.053
-36.576	88.800	0.583	1.015	0.817	0.602	1.855	2.117	0.289	0.129
-36.576	96.300	0.632	1.002	0.806	0.596	1.840	1.984	0.076	0.036
-36.576	103.800	0.681	0.997	0.798	0.597	2.138	2.482	0.257	0.085
-36.576	111.300	0.730	0.990	0.788	0.599	2.197	1.940	0.198	0.081
-36.576	118.800	0.780	0.984	0.779	0.601	2.105	2.053	0.124	0.050
-36.576	126.300	0.829	0.984	0.773	0.608	2.049	1.916	0.355	0.158
-36.576	133.800	0.878	0.984	0.767	0.616	2.070	1.727	0.356	0.174
-36.576	141.300	0.927	0.991	0.769	0.625	2.078	2.176	0.200	0.077
-36.576	148.800	0.976	0.998	0.770	0.635	1.746	2.093	0.079	0.038
-36.576	156.300	1.026	1.008	0.773	0.646	1.903	2.522	0.114	0.042
-36.576	163.800	1.075	1.020	0.782	0.655	1.997	2.603	0.054	0.018
-36.576	171.300	1.124	1.032	0.794	0.658	1.938	2.579	0.304	0.106
-36.576	178.800	1.173	1.041	0.807	0.657	1.988	2.323	0.129	0.049
-36.578	186.300	1.222	1.047	0.821	0.650	1.872	2.467	0.041	0.015
-36.576	193.800	1.272	1.046	0.828	0.641	2.145	2.906	-0.100	-0.028
-36.578	201.300	1.321	1.042	0.829	0.631	1.829	2.917	0.171	0.056
-36.576	208.800	1.370	1.037	0.830	0.623	1.770	2.350	0.153	0.064
-36.576	216.300	1.419	1.033	0.829	0.617	2.027	2.685	0.223	0.072
-36.576	223.800	1.469	1.034	0.831	0.615	2.647	3.062	0.265	0.057
-36.576	231.300	1.518	1.032	0.831	0.612	2.048	2.660	0.204	0.066

Survey Number 2 (Station 1 inlet)									
x(mm)	y(mm)	y/s	W/Vref	U/Vref	V/Vref	Tu	Tv	Re stress	Cuv
-36.576	-76.200	-0.500	1.042	0.838	0.619	2.161	2.115	0.252	0.097
-36.576	-68.700	-0.451	1.035	0.833	0.615	1.939	2.055	0.257	0.114
-36.576	-61.200	-0.402	1.023	0.822	0.608	1.871	2.676	0.226	0.079
-36.576	-53.700	-0.352	1.012	0.812	0.603	1.779	1.953	0.152	0.077
-36.576	-46.200	-0.303	1.003	0.803	0.601	1.802	1.749	0.123	0.069
-36.576	-38.700	-0.254	0.993	0.795	0.596	1.907	1.881	0.236	0.116
-36.576	-31.200	-0.205	0.989	0.785	0.600	2.155	1.874	0.252	0.110
-36.576	-23.700	-0.156	0.987	0.779	0.606	2.472	2.496	0.186	0.053
-36.576	-16.200	-0.106	0.988	0.773	0.615	1.950	1.969	0.289	0.133
-36.576	-8.700	-0.057	0.987	0.767	0.620	1.808	1.979	0.251	0.124
-36.576	-1.200	-0.008	0.988	0.765	0.626	1.759	1.982	0.187	0.094
-36.576	6.300	0.041	0.998	0.769	0.635	1.942	1.806	0.178	0.089
-36.576	13.800	0.091	1.011	0.782	0.641	2.804	1.918	0.266	0.087
-36.576	21.300	0.140	1.029	0.799	0.647	2.430	2.046	0.174	0.062
-36.576	28.800	0.189	1.037	0.813	0.644	1.876	2.030	0.155	0.072
-36.576	36.300	0.238	1.039	0.819	0.639	1.965	1.978	0.160	0.073
-36.576	43.800	0.287	1.037	0.823	0.631	2.031	1.782	0.037	0.018
-36.576	51.300	0.337	1.036	0.825	0.626	2.322	1.737	0.124	0.054
-36.576	58.800	0.386	1.032	0.826	0.618	2.201	1.950	0.214	0.088
-36.576	66.300	0.435	1.028	0.825	0.614	2.563	1.814	0.260	0.099
-36.576	73.800	0.484	1.029	0.829	0.609	2.677	1.764	0.202	0.075
-36.576	81.300	0.533	1.023	0.826	0.604	1.892	1.870	0.197	0.098
-36.576	88.800	0.583	1.010	0.815	0.596	2.199	1.983	0.215	0.087
-36.576	96.300	0.632	1.000	0.805	0.593	1.747	1.786	0.140	0.079
-36.576	103.800	0.681	0.996	0.803	0.589	1.836	1.789	0.133	0.072
-36.576	111.300	0.730	0.990	0.794	0.591	1.842	1.672	0.172	0.098
-36.576	118.800	0.780	0.987	0.786	0.596	2.072	1.751	0.186	0.090
-36.576	126.300	0.829	0.987	0.781	0.604	2.147	1.796	0.200	0.092
-36.576	133.800	0.878	0.986	0.775	0.610	1.793	1.826	0.140	0.075
-36.576	141.300	0.927	0.985	0.769	0.615	1.932	1.743	0.168	0.088
-36.576	148.800	0.976	0.992	0.767	0.629	1.784	1.665	0.131	0.078
-36.576	156.300	1.026	1.003	0.773	0.638	1.819	1.742	0.147	0.082
-36.576	163.800	1.075	1.014	0.782	0.647	2.075	1.911	0.159	0.071
-36.576	171.300	1.124	1.027	0.793	0.652	1.998	2.064	0.168	0.072
-36.576	178.800	1.173	1.037	0.805	0.654	2.116	1.890	0.166	0.073
-36.576	186.300	1.222	1.044	0.818	0.648	1.986	2.120	0.202	0.084
-36.578	193.800	1.272	1.040	0.823	0.635	2.485	1.889	0.246	0.092
-36.578	201.300	1.321	1.039	0.828	0.628	1.907	1.766	0.124	0.065
-36.576	208.800	1.370	1.038	0.830	0.622	1.835	1.731	0.167	0.093
-36.576	216.300	1.419	1.034	0.829	0.618	2.363	1.695	0.141	0.062
-36.576	223.800	1.469	1.036	0.835	0.614	2.167	1.803	0.152	0.069
-36.576	231.300	1.518	1.034	0.833	0.612	1.978	1.794	0.203	0.101

Survey Number 3 (Station 3 inlet)									
x(mm)	y(mm)	y/s	W/Vref	U/Vref	V/Vref	Tu	Tv	Re stress	Cuv
-6.098	-76.200	-0.500	1.074	0.897	0.590	1.816	2.677	0.253	0.091
-6.096	-72.200	-0.474	1.058	0.885	0.580	2.491	2.424	0.749	0.216
-6.096	-68.200	-0.448	1.049	0.877	0.576	1.998	2.208	0.278	0.110
-6.096	-64.200	-0.421	1.036	0.867	0.567	2.356	2.274	0.346	0.113
-6.096	-60.200	-0.395	1.028	0.859	0.565	2.786	2.244	0.206	0.057
-6.096	-56.200	-0.369	1.021	0.852	0.563	2.512	1.896	0.370	0.135
-6.096	-52.200	-0.343	1.012	0.846	0.556	2.405	2.287	0.359	0.114
-6.096	-48.200	-0.316	1.001	0.834	0.552	1.916	2.099	0.360	0.156
-6.094	-44.200	-0.290	0.984	0.819	0.545	1.915	2.351	0.361	0.140
-6.096	-40.200	-0.264	0.974	0.807	0.545	2.086	2.225	0.231	0.087
-6.096	-36.200	-0.238	0.961	0.793	0.543	2.188	2.534	0.234	0.074
-6.096	-32.200	-0.211	0.951	0.779	0.545	1.899	1.903	0.158	0.076
-6.096	-28.200	-0.185	0.939	0.764	0.546	2.268	2.099	0.266	0.097
-6.096	-24.200	-0.159	0.930	0.751	0.549	1.877	2.293	0.260	0.105
-6.096	-20.200	-0.133	0.918	0.734	0.551	1.800	2.363	0.085	0.035
-6.096	-16.200	-0.106	0.907	0.715	0.559	2.059	2.278	0.204	0.076
-6.096	-12.200	-0.080	0.897	0.694	0.569	1.998	1.821	0.349	0.167
-6.096	-8.200	-0.054	0.886	0.667	0.583	2.315	2.161	0.263	0.092
-6.096	-4.200	-0.028	0.883	0.637	0.612	2.202	1.871	0.204	0.087
-6.096	-0.200	-0.001	0.911	0.612	0.674	2.051	3.361	0.078	0.020
-6.096	3.800	0.025	0.830	0.302	0.773	0.000	0.000	0.000	0.000
-6.096	7.800	0.051	1.069	0.713	0.797	2.112	4.274	0.323	0.062
-6.096	11.800	0.077	1.104	0.768	0.794	2.196	4.559	0.347	0.060
-6.094	15.800	0.104	1.125	0.810	0.780	1.841	3.481	0.079	0.022
-6.096	19.800	0.130	1.128	0.838	0.756	1.833	4.801	0.183	0.036
-6.096	23.800	0.156	1.130	0.858	0.735	1.826	4.573	0.292	0.061
-6.096	27.800	0.182	1.133	0.878	0.716	2.850	4.370	0.191	0.027
-6.096	31.800	0.209	1.129	0.887	0.698	2.005	3.351	0.065	0.017
-6.098	35.800	0.235	1.126	0.897	0.679	1.871	4.646	-0.133	-0.027
-6.096	39.800	0.261	1.121	0.901	0.667	2.003	4.064	0.221	0.047
-6.096	43.800	0.287	1.108	0.903	0.641	2.037	7.521	0.025	0.003
-6.096	47.800	0.314	1.108	0.905	0.639	2.242	3.959	-0.017	-0.003
-6.096	51.800	0.340	1.098	0.902	0.626	2.517	2.976	0.396	0.092
-6.098	55.800	0.366	1.075	0.899	0.590	2.161	9.528	0.311	0.026
-6.096	59.800	0.392	1.079	0.895	0.603	1.751	2.522	0.259	0.102
-6.096	63.800	0.419	1.068	0.888	0.592	2.026	4.418	0.072	0.014
-6.096	67.800	0.445	1.059	0.883	0.584	2.155	2.355	0.156	0.053
-6.096	71.800	0.471	1.046	0.873	0.575	2.617	3.822	0.171	0.030
-6.096	75.800	0.497	1.033	0.863	0.568	2.754	2.773	0.281	0.064
-6.096	79.800	0.524	1.026	0.858	0.562	2.124	1.984	0.254	0.105
-6.096	83.800	0.550	1.016	0.851	0.555	2.614	2.745	0.336	0.082
-6.096	87.800	0.576	1.006	0.843	0.550	2.029	3.854	0.290	0.065
-6.096	91.800	0.602	1.002	0.837	0.551	2.328	2.203	0.384	0.130
-6.096	95.800	0.629	0.994	0.828	0.549	2.065	1.946	0.374	0.162
-6.094	99.800	0.655	0.985	0.820	0.546	2.438	2.564	0.430	0.120
-6.096	103.800	0.681	0.974	0.809	0.543	2.364	2.758	0.274	0.073
-6.096	107.800	0.707	0.970	0.802	0.547	1.955	2.071	0.414	0.178
-6.096	111.800	0.734	0.953	0.787	0.537	1.914	2.224	0.297	0.121
-6.096	115.800	0.760	0.943	0.774	0.538	2.030	2.650	0.182	0.059
-6.096	119.800	0.786	0.930	0.759	0.538	1.835	2.297	0.193	0.080
-6.094	123.800	0.812	0.920	0.745	0.540	2.184	2.904	0.185	0.051
-6.096	127.800	0.839	0.914	0.736	0.542	1.749	2.408	0.161	0.067
-6.096	131.800	0.865	0.907	0.722	0.548	1.820	2.922	0.031	0.010
-6.096	135.800	0.891	0.897	0.704	0.556	1.824	2.203	0.230	0.100
-6.096	139.800	0.917	0.884	0.680	0.565	2.005	2.838	0.407	0.125
-6.096	143.800	0.944	0.878	0.657	0.583	1.905	1.877	0.145	0.071
-6.096	147.800	0.970	0.880	0.637	0.608	2.047	2.033	0.305	0.128
-6.096	151.800	0.996	0.895	0.608	0.657	2.071	3.571	0.093	0.022
-6.096	163.800	1.075	1.100	0.751	0.804	1.871	5.918	0.359	0.056
-6.096	167.800	1.101	1.124	0.798	0.791	1.926	4.207	0.314	0.068
-6.096	171.800	1.127	1.137	0.831	0.775	1.922	4.058	0.066	0.015
-6.096	175.800	1.154	1.139	0.856	0.752	2.107	4.622	0.096	0.017

-6.094	179.800	1.180	1.142	0.873	0.735	1.905	3.760	0.238	0.058
-6.096	183.800	1.206	1.140	0.886	0.717	2.012	2.929	0.073	0.022
-6.096	187.800	1.232	1.134	0.895	0.697	1.812	4.032	0.185	0.044
-6.096	191.800	1.259	1.131	0.900	0.684	1.933	2.475	0.111	0.040
-6.096	195.800	1.285	1.123	0.903	0.666	2.190	3.071	0.311	0.081
-6.096	199.800	1.311	1.112	0.901	0.652	1.969	3.699	0.210	0.050
-6.096	203.800	1.337	1.105	0.903	0.638	1.904	2.634	0.004	0.001
-6.096	207.800	1.364	1.096	0.899	0.626	1.951	2.308	0.119	0.046
-6.096	211.800	1.390	1.081	0.894	0.609	1.854	2.164	0.149	0.065
-6.096	215.800	1.416	1.071	0.888	0.598	1.845	2.607	0.187	0.068
-6.096	219.800	1.442	1.063	0.882	0.593	1.808	2.448	0.235	0.093
-6.096	223.800	1.469	1.050	0.874	0.582	1.823	2.039	0.152	0.071

Survey Number 4 (Station 5 passage)									
x(mm)	y(mm)	y/s	W/Vref	U/Vref	V/Vref	Tu	Tv	Re stress	Cuv
6.096	20.200	0.069	1.259	0.952	0.823	2.675	7.610	0.285	0.025
6.096	22.200	0.082	1.258	0.958	0.815	2.371	3.529	0.222	0.047
6.096	24.200	0.095	1.247	0.960	0.795	3.097	3.069	0.273	0.051
6.096	26.200	0.108	1.236	0.962	0.777	2.085	2.916	0.333	0.097
6.096	28.200	0.122	1.230	0.967	0.760	2.009	2.669	0.029	0.010
6.096	30.200	0.135	1.218	0.965	0.744	1.934	3.152	0.150	0.044
6.096	32.200	0.148	1.211	0.968	0.729	1.931	2.581	0.187	0.066
6.096	34.200	0.161	1.200	0.966	0.712	2.160	2.264	0.026	0.010
6.096	36.200	0.174	1.190	0.962	0.700	1.839	2.595	0.026	0.010
6.096	38.200	0.187	1.179	0.959	0.686	1.880	1.986	0.085	0.040
6.096	40.200	0.200	1.168	0.957	0.669	2.139	2.620	0.102	0.032
6.096	42.200	0.213	1.160	0.958	0.653	1.936	2.489	0.103	0.038
6.096	44.200	0.227	1.151	0.954	0.643	1.923	1.790	0.053	0.027
6.096	46.200	0.240	1.146	0.954	0.635	1.959	2.072	0.119	0.052
6.096	48.200	0.253	1.138	0.950	0.627	2.507	2.069	0.169	0.058
6.096	50.200	0.266	1.134	0.950	0.620	2.332	2.439	0.010	0.003
6.096	52.200	0.279	1.124	0.944	0.611	2.580	1.987	0.123	0.042
6.096	54.200	0.292	1.121	0.944	0.604	2.044	1.822	0.151	0.072
6.096	56.200	0.305	1.116	0.941	0.599	1.992	1.945	0.132	0.060
6.096	58.200	0.318	1.109	0.938	0.592	1.964	2.095	0.045	0.019
6.096	60.200	0.331	1.101	0.933	0.586	1.941	2.377	0.351	0.135
6.096	62.200	0.345	1.095	0.930	0.579	2.175	1.854	0.129	0.057
6.096	64.200	0.358	1.088	0.924	0.574	1.856	1.931	0.168	0.083
6.096	66.200	0.371	1.080	0.918	0.569	2.068	2.062	0.111	0.046
6.096	68.200	0.384	1.073	0.913	0.564	1.833	1.890	0.162	0.083
6.096	70.200	0.397	1.066	0.908	0.557	1.775	2.157	0.198	0.092
6.096	72.200	0.410	1.059	0.904	0.552	1.740	2.087	0.303	0.148
6.096	74.200	0.423	1.051	0.897	0.548	1.762	1.965	0.130	0.066
6.096	76.202	0.436	1.044	0.891	0.544	1.894	1.706	0.168	0.092
6.096	78.200	0.450	1.038	0.890	0.534	1.759	1.799	0.176	0.098
6.096	80.200	0.463	1.030	0.883	0.530	1.734	2.019	0.018	0.009
6.096	82.200	0.476	1.023	0.878	0.524	1.744	2.002	0.178	0.090
6.096	84.200	0.489	1.017	0.872	0.523	1.876	1.793	0.158	0.083
6.096	86.200	0.502	1.011	0.866	0.520	1.804	1.652	0.259	0.154
6.096	88.200	0.515	1.003	0.859	0.517	1.847	1.848	0.269	0.140
6.096	90.200	0.528	0.998	0.855	0.515	2.430	1.894	0.161	0.062
6.096	92.200	0.541	0.991	0.848	0.513	1.930	1.762	0.158	0.082
6.096	94.202	0.555	0.987	0.844	0.510	2.438	1.906	0.157	0.060
6.096	96.200	0.568	0.985	0.842	0.511	2.213	1.923	0.253	0.105
6.096	98.200	0.581	0.980	0.836	0.511	2.106	1.935	0.393	0.171
6.098	100.200	0.594	0.976	0.833	0.509	1.939	1.820	0.272	0.136
6.096	102.200	0.607	0.972	0.828	0.509	1.913	1.903	0.222	0.108
6.096	104.200	0.620	0.965	0.820	0.509	2.053	1.918	0.206	0.093
6.096	106.200	0.633	0.963	0.818	0.507	1.848	1.929	0.323	0.160
6.096	108.200	0.646	0.955	0.810	0.506	1.847	1.940	0.218	0.108
6.096	110.200	0.660	0.948	0.803	0.505	1.848	1.917	0.421	0.211
6.096	112.200	0.673	0.941	0.796	0.502	1.887	1.923	0.344	0.168
6.096	114.200	0.686	0.933	0.786	0.502	1.868	2.012	0.378	0.178
6.096	116.200	0.699	0.925	0.778	0.499	1.838	1.971	0.361	0.176
6.096	118.200	0.712	0.914	0.768	0.497	2.015	1.989	0.252	0.111
6.096	120.200	0.725	0.907	0.759	0.496	1.834	1.906	0.311	0.158
6.096	122.200	0.738	0.900	0.752	0.495	2.152	2.159	0.273	0.104
6.096	124.200	0.751	0.894	0.743	0.496	1.771	1.755	0.193	0.110
6.096	126.200	0.765	0.885	0.734	0.495	1.773	1.813	0.271	0.149
6.096	128.200	0.778	0.879	0.728	0.494	2.105	1.751	0.415	0.199
6.096	130.200	0.791	0.871	0.718	0.492	1.998	1.754	0.214	0.108
6.096	132.200	0.804	0.863	0.708	0.492	1.904	2.077	0.194	0.087
6.096	134.200	0.817	0.855	0.698	0.493	1.922	1.655	0.307	0.171
6.096	136.200	0.830	0.843	0.684	0.492	2.250	1.614	0.183	0.089
6.096	138.200	0.843	0.832	0.673	0.490	1.848	1.799	0.203	0.108
6.096	140.200	0.856	0.822	0.663	0.486	1.726	1.592	0.123	0.080
6.096	142.200	0.870	0.813	0.652	0.486	1.816	1.625	0.202	0.121
6.096	144.200	0.883	0.804	0.642	0.484	1.761	1.812	0.312	0.173
6.096	146.200	0.896	0.791	0.627	0.481	2.427	1.760	0.353	0.146
6.096	148.200	0.909	0.777	0.615	0.475	2.066	1.727	0.405	0.201

Survey Number 5 (Station 8 passage)									
x(mm)	y(mm)	y/s	W/Vref	U/Vref	V/Vref	Tu	Tv	Re stress	Cuv
91.440	50.000	0.061	0.375	0.352	0.131	27.648	9.028	5.134	0.036
91.440	54.000	0.087	0.993	0.950	0.289	14.233	6.637	0.320	0.006
91.440	58.000	0.113	1.035	0.993	0.293	3.494	3.952	-0.693	-0.088
91.440	62.000	0.139	1.023	0.984	0.279	2.411	2.965	0.039	0.010
91.440	66.000	0.166	1.013	0.976	0.270	2.150	2.559	-0.063	-0.020
91.440	70.000	0.192	0.998	0.963	0.260	2.035	2.346	0.290	0.106
91.440	74.000	0.218	0.984	0.951	0.253	1.843	2.169	0.096	0.042
91.440	78.000	0.244	0.972	0.941	0.244	2.125	2.019	0.194	0.079
91.440	82.000	0.271	0.963	0.933	0.239	1.923	1.857	0.103	0.051
91.440	86.000	0.297	0.954	0.926	0.233	1.965	1.868	0.254	0.121
91.440	90.000	0.323	0.946	0.918	0.232	2.222	1.892	0.308	0.128
91.440	94.000	0.349	0.939	0.911	0.231	1.952	1.781	0.353	0.178
91.440	98.000	0.376	0.929	0.901	0.228	2.217	1.875	0.280	0.118
91.440	102.000	0.402	0.917	0.889	0.225	2.709	1.838	0.419	0.147
91.440	106.000	0.428	0.905	0.877	0.222	2.208	1.814	0.293	0.128
91.440	110.000	0.454	0.892	0.865	0.218	2.040	1.726	0.273	0.136
91.440	114.000	0.481	0.881	0.855	0.212	2.004	1.821	0.345	0.166
91.440	118.000	0.507	0.868	0.845	0.203	1.936	1.857	0.239	0.116
91.440	122.000	0.533	0.857	0.834	0.196	1.797	1.801	0.281	0.152
91.440	126.000	0.559	0.850	0.827	0.193	1.971	1.839	0.424	0.205
91.440	130.000	0.586	0.841	0.820	0.185	1.990	1.926	0.569	0.260
91.440	134.000	0.612	0.835	0.816	0.179	2.052	1.946	0.482	0.212
91.440	138.000	0.638	0.828	0.810	0.172	1.992	1.814	0.469	0.228
91.440	142.000	0.664	0.818	0.801	0.166	2.358	1.843	0.440	0.178
91.440	146.000	0.691	0.807	0.791	0.159	1.912	1.778	0.469	0.242
91.440	150.000	0.717	0.795	0.781	0.149	2.161	1.856	0.649	0.283
91.440	154.000	0.743	0.781	0.768	0.139	2.143	1.890	0.372	0.161
91.438	158.000	0.769	0.768	0.757	0.131	1.938	1.912	0.501	0.237
91.438	162.000	0.796	0.754	0.745	0.115	1.771	1.877	0.530	0.279
91.440	166.000	0.822	0.740	0.733	0.101	1.718	1.787	0.359	0.205
91.440	170.002	0.848	0.728	0.723	0.084	1.892	1.828	0.423	0.214
91.440	174.000	0.874	0.713	0.710	0.069	1.949	2.078	0.430	0.186
91.440	178.000	0.901	0.699	0.697	0.051	2.111	1.846	0.550	0.247

Survey Number 6 (Station 10 passage)									
x(mm)	y(mm)	y/s	W/Vref	U/Vref	V/Vref	Tu	Tv	Re stress	Cuv
121.920	-14.220	-0.333	0.887	0.876	0.139	2.030	1.546	0.251	0.142
121.920	-12.220	-0.320	0.884	0.874	0.136	2.093	1.585	0.339	0.181
121.922	-10.220	-0.307	0.887	0.877	0.135	2.006	1.654	0.306	0.164
121.918	-8.220	-0.294	0.886	0.876	0.132	2.022	1.640	0.426	0.228
121.920	-6.220	-0.281	0.885	0.875	0.129	1.846	1.812	0.338	0.179
121.920	-4.220	-0.268	0.883	0.874	0.124	1.930	1.829	0.468	0.235
121.920	-2.220	-0.255	0.883	0.875	0.124	1.799	1.651	0.352	0.210
121.920	-0.218	-0.241	0.881	0.873	0.118	1.845	1.913	0.379	0.190
121.920	1.780	-0.228	0.880	0.872	0.114	1.942	1.898	0.539	0.259
121.920	3.780	-0.215	0.877	0.871	0.108	1.885	1.868	0.392	0.197
121.920	5.780	-0.202	0.877	0.871	0.100	1.992	1.840	0.571	0.276
121.920	7.780	-0.189	0.877	0.872	0.096	1.672	1.795	0.393	0.232
121.920	9.780	-0.176	0.877	0.872	0.088	1.758	1.771	0.332	0.189
121.920	11.780	-0.163	0.877	0.873	0.084	1.776	1.616	0.310	0.191
121.920	13.780	-0.150	0.879	0.876	0.076	1.662	1.690	0.348	0.220
121.920	15.780	-0.136	0.881	0.879	0.068	1.617	1.736	0.261	0.165
121.920	17.780	-0.123	0.886	0.884	0.062	1.766	1.731	0.278	0.161
121.920	19.780	-0.110	0.891	0.890	0.053	1.835	1.725	0.278	0.156
121.920	21.780	-0.097	0.898	0.897	0.045	1.618	1.784	0.309	0.190
121.920	23.780	-0.084	0.905	0.904	0.032	1.519	1.582	0.187	0.138
121.920	25.780	-0.071	0.916	0.916	0.019	1.688	1.831	0.330	0.189
121.920	27.780	-0.058	0.930	0.930	0.005	1.668	1.818	0.281	0.164
121.920	29.782	-0.045	0.947	0.946	-0.012	2.036	1.815	0.500	0.240
121.920	31.780	-0.031	0.974	0.973	-0.027	2.059	1.623	0.384	0.204
121.920	33.780	-0.018	0.975	0.975	-0.035	4.040	2.926	0.935	0.140
121.920	41.780	0.034	0.108	-0.095	0.050	6.385	7.696	2.616	0.094
121.920	43.780	0.047	0.101	-0.089	0.048	7.104	8.430	1.506	0.045
121.920	45.780	0.060	0.093	-0.071	0.060	8.002	8.723	1.290	0.033
121.922	47.780	0.073	0.080	-0.060	0.053	9.378	9.947	-0.688	-0.013
121.920	49.780	0.087	0.077	-0.013	0.076	11.564	11.323	-6.768	-0.092
121.918	51.780	0.100	0.107	0.048	0.096	14.467	11.277	-5.595	-0.061
121.918	53.780	0.113	0.182	0.145	0.111	18.852	13.029	-21.952	-0.158
121.918	55.780	0.126	0.326	0.302	0.123	22.931	12.927	-41.290	-0.247
121.920	57.780	0.139	0.455	0.436	0.130	25.536	13.058	-46.720	-0.248
121.920	59.780	0.152	0.656	0.641	0.142	25.899	12.422	-37.904	-0.209
121.920	61.780	0.165	0.823	0.810	0.145	21.118	11.193	-15.564	-0.117
121.920	63.780	0.178	0.955	0.946	0.133	11.782	7.332	-0.856	-0.018
121.920	65.780	0.192	1.003	0.992	0.147	7.648	6.239	-1.581	-0.059
121.920	67.780	0.205	1.007	0.996	0.151	5.584	5.092	0.351	0.022
121.920	69.780	0.218	1.000	0.988	0.153	4.064	3.568	-0.185	-0.023
121.920	71.780	0.231	0.988	0.976	0.157	3.773	3.378	0.024	0.003
121.920	73.780	0.244	0.977	0.964	0.156	3.094	2.959	0.308	0.060
121.920	75.780	0.257	0.970	0.957	0.157	2.603	2.498	0.349	0.095
121.920	77.780	0.270	0.957	0.945	0.155	2.280	2.073	0.123	0.046
121.920	79.780	0.283	0.954	0.942	0.153	1.899	1.823	0.167	0.086
121.920	81.780	0.297	0.949	0.936	0.156	2.019	1.896	0.219	0.101
121.920	83.780	0.310	0.940	0.928	0.149	1.810	1.591	0.068	0.042
121.920	85.780	0.323	0.936	0.924	0.151	1.786	1.501	0.073	0.049
121.920	87.780	0.336	0.932	0.920	0.151	1.779	1.482	0.099	0.067
121.920	89.780	0.349	0.929	0.916	0.153	1.943	1.470	0.159	0.099
121.920	91.780	0.362	0.927	0.914	0.153	1.699	1.354	0.054	0.042
121.920	93.780	0.375	0.923	0.911	0.151	1.762	1.300	0.150	0.116
121.920	95.780	0.388	0.921	0.909	0.151	1.846	1.480	0.192	0.125
121.922	97.780	0.402	0.919	0.907	0.153	1.757	1.367	0.179	0.132
121.920	99.780	0.415	0.915	0.902	0.151	2.012	1.460	0.151	0.091
121.920	101.780	0.428	0.910	0.898	0.151	1.678	1.256	0.120	0.101
121.920	103.782	0.441	0.907	0.894	0.152	1.788	1.422	0.190	0.133
121.920	105.780	0.454	0.903	0.890	0.150	1.733	1.420	0.145	0.105
121.920	107.780	0.467	0.898	0.886	0.150	1.727	1.286	0.111	0.089
121.920	109.780	0.480	0.897	0.885	0.150	1.768	1.430	0.261	0.183
121.920	111.780	0.493	0.891	0.879	0.148	1.639	1.405	0.090	0.070
121.920	113.780	0.507	0.887	0.875	0.147	1.711	1.432	0.237	0.171

121.920	115.780	0.520	0.882	0.870	0.144	1.618	1.356	0.201	0.162
121.920	117.780	0.533	0.878	0.866	0.144	1.474	1.420	0.139	0.118
121.920	119.780	0.546	0.874	0.863	0.142	1.638	1.423	0.218	0.166
121.920	121.780	0.559	0.870	0.859	0.140	1.621	1.487	0.227	0.167
121.920	123.780	0.572	0.869	0.858	0.139	1.520	1.424	0.127	0.104
121.920	125.780	0.585	0.863	0.852	0.138	1.661	1.403	0.091	0.069
121.920	127.780	0.598	0.859	0.848	0.136	1.695	1.441	0.135	0.098
121.920	129.780	0.612	0.856	0.845	0.133	1.600	1.472	0.205	0.154
121.920	131.780	0.625	0.854	0.844	0.131	1.667	1.505	0.205	0.145
121.920	133.780	0.638	0.853	0.843	0.128	1.740	1.461	0.320	0.223
121.920	135.780	0.651	0.852	0.843	0.128	1.747	1.526	0.344	0.229
121.920	137.780	0.664	0.851	0.842	0.126	1.913	1.577	0.435	0.255
121.918	139.780	0.677	0.852	0.843	0.123	1.758	1.574	0.373	0.239
121.918	141.780	0.690	0.851	0.842	0.120	1.870	1.641	0.382	0.221
121.920	143.780	0.703	0.848	0.840	0.118	1.909	1.588	0.459	0.268
121.920	145.780	0.717	0.851	0.843	0.118	1.866	1.639	0.434	0.251
121.920	147.780	0.730	0.852	0.845	0.113	1.876	1.689	0.344	0.192
121.920	149.780	0.743	0.851	0.844	0.109	1.811	1.711	0.439	0.251
121.920	151.780	0.756	0.852	0.845	0.106	1.778	1.710	0.348	0.203
121.920	153.780	0.769	0.848	0.842	0.100	1.613	1.784	0.404	0.249
121.920	155.780	0.782	0.847	0.841	0.096	1.772	1.752	0.421	0.240
121.920	157.780	0.795	0.847	0.842	0.091	1.788	1.738	0.410	0.234
121.920	159.780	0.808	0.845	0.841	0.087	1.847	1.770	0.491	0.266
121.920	161.780	0.822	0.844	0.840	0.081	1.691	1.840	0.463	0.264
121.920	163.780	0.835	0.844	0.841	0.074	1.685	1.747	0.371	0.223
121.920	165.780	0.848	0.846	0.843	0.068	1.737	1.696	0.374	0.225
121.920	167.780	0.861	0.847	0.845	0.060	1.734	1.717	0.397	0.236
121.920	169.780	0.874	0.851	0.849	0.053	1.731	1.727	0.478	0.283
121.920	171.780	0.887	0.855	0.853	0.044	1.780	1.635	0.303	0.185
121.920	173.780	0.900	0.862	0.861	0.036	1.755	1.683	0.300	0.180
121.920	175.780	0.913	0.869	0.868	0.026	1.785	1.713	0.359	0.208
121.920	177.780	0.927	0.880	0.879	0.013	1.922	1.719	0.358	0.192
121.922	179.780	0.940	0.892	0.892	-0.001	1.884	1.779	0.350	0.185
121.918	181.780	0.953	0.909	0.909	-0.013	1.939	1.837	0.487	0.242
121.920	183.780	0.966	0.929	0.929	-0.025	2.067	1.798	0.454	0.217
121.920	185.780	0.979	0.949	0.948	-0.043	2.936	2.225	0.672	0.182
121.918	187.780	0.992	0.680	0.679	0.033	18.711	4.481	4.630	0.098
121.918	195.780	1.045	0.085	-0.067	0.052	9.034	9.205	-1.497	-0.032
121.920	197.780	1.058	0.085	-0.044	0.073	10.548	8.124	0.480	0.010
121.920	199.780	1.071	0.061	-0.006	0.061	13.036	10.235	-4.236	-0.056
121.920	201.780	1.084	0.086	0.054	0.066	16.796	10.837	-11.336	-0.110
121.918	203.780	1.097	0.152	0.126	0.086	20.806	10.715	-9.373	-0.075
121.920	205.780	1.110	0.229	0.210	0.093	24.554	12.317	-18.629	-0.109
121.920	207.780	1.123	0.348	0.335	0.092	30.405	12.468	-43.901	-0.205
121.920	209.780	1.136	0.499	0.488	0.103	32.425	12.220	-35.687	-0.160
121.920	211.780	1.150	0.599	0.592	0.090	31.057	11.488	-39.556	-0.196
121.920	213.780	1.163	0.718	0.713	0.091	27.480	10.613	-30.954	-0.188
121.920	215.780	1.176	0.798	0.793	0.094	22.848	9.742	-11.769	-0.094
121.920	217.780	1.189	0.905	0.900	0.089	13.597	6.811	-5.511	-0.105
121.920	219.780	1.202	0.952	0.947	0.098	9.465	6.255	-2.108	-0.063
121.922	221.780	1.215	0.965	0.960	0.100	6.151	4.653	-0.644	-0.040
121.922	223.780	1.228	0.965	0.959	0.106	5.848	4.700	-1.091	-0.070
121.920	225.780	1.241	0.969	0.963	0.108	4.090	3.537	-0.505	-0.062
121.920	227.780	1.255	0.956	0.949	0.117	3.333	3.063	0.017	0.003
121.920	229.780	1.268	0.957	0.949	0.122	3.046	2.548	-0.077	-0.018
121.920	231.780	1.281	0.951	0.942	0.129	3.238	2.689	0.124	0.025
121.920	233.780	1.294	0.945	0.936	0.128	2.613	2.360	0.193	0.055
121.920	235.780	1.307	0.940	0.931	0.128	2.418	2.066	-0.021	-0.007
121.920	237.780	1.320	0.935	0.925	0.133	2.126	2.040	0.159	0.065
121.920	239.780	1.333	0.935	0.925	0.135	2.104	1.956	0.119	0.051

Survey Number 7 (Station 5 boundary layer)									
x(mm)	y(mm)	d/c	W/Vref	U/Vref	V/Vref	Tu	Tv	Re stress	Cuv
4.970	10.674	0.012	1.249	0.845	0.920	4.211	13.473	7.940	0.245
4.598	11.004	0.016	1.290	0.856	0.965	2.299	2.492	0.530	0.162
4.220	11.336	0.020	1.280	0.855	0.952	2.063	2.312	0.217	0.080
3.844	11.666	0.024	1.269	0.853	0.939	2.240	2.372	0.386	0.127
3.472	11.998	0.028	1.261	0.852	0.930	2.077	2.218	0.510	0.194
3.096	12.328	0.031	1.253	0.851	0.920	2.082	2.346	0.344	0.123
2.722	12.660	0.035	1.245	0.850	0.910	1.960	2.566	0.152	0.053
2.344	12.990	0.039	1.236	0.848	0.900	2.017	2.097	0.247	0.102
1.972	13.322	0.043	1.231	0.847	0.893	2.005	2.285	0.256	0.098
1.596	13.654	0.047	1.224	0.846	0.884	2.017	1.822	0.250	0.119
1.220	13.986	0.051	1.215	0.843	0.876	2.000	2.361	0.221	0.082
0.846	14.314	0.055	1.211	0.843	0.870	1.941	2.355	0.197	0.075
0.472	14.646	0.059	1.204	0.841	0.861	1.969	2.167	0.181	0.074
0.096	14.976	0.063	1.197	0.840	0.853	1.940	2.142	0.181	0.076
-0.278	15.308	0.067	1.194	0.843	0.846	1.883	2.205	0.180	0.076
-0.656	15.640	0.071	1.188	0.840	0.840	1.957	1.961	0.296	0.135
-1.030	15.970	0.075	1.184	0.840	0.835	1.870	1.879	0.127	0.063
-1.402	16.302	0.079	1.178	0.838	0.827	1.924	1.959	0.154	0.071
-1.778	16.632	0.083	1.176	0.841	0.822	1.805	2.358	0.092	0.038
-2.152	16.962	0.086	1.171	0.840	0.816	1.822	1.939	0.169	0.084
-2.530	17.294	0.090	1.164	0.838	0.808	1.836	2.700	0.218	0.077
-2.904	17.626	0.094	1.160	0.838	0.803	1.826	1.886	0.111	0.056
-3.280	17.956	0.098	1.157	0.838	0.797	1.840	2.383	0.211	0.084
-3.654	18.288	0.102	1.151	0.836	0.791	1.782	2.161	0.187	0.085
-4.028	18.618	0.106	1.150	0.837	0.789	1.738	2.600	0.211	0.082
-4.404	18.950	0.110	1.144	0.836	0.781	1.775	2.383	0.147	0.061
-4.780	19.280	0.114	1.140	0.835	0.776	1.796	1.901	0.111	0.057
-5.154	19.610	0.118	1.140	0.837	0.774	1.873	1.937	0.298	0.144
-5.528	19.942	0.122	1.133	0.835	0.767	1.803	2.218	0.114	0.050
-5.904	20.274	0.126	1.131	0.835	0.763	1.830	2.058	0.243	0.113
-6.278	20.604	0.130	1.131	0.837	0.761	1.741	1.985	0.117	0.059

Survey Number 8 (Station 7 boundary layer)									
x(mm)	y(mm)	d/c	W/Vref	U/Vref	V/Vref	Tu	Tv	Re stress	Cuv
60.810	41.410	0.008	0.441	0.428	0.106	16.115	6.022	-1.318	-0.023
60.734	41.904	0.012	0.684	0.667	0.151	15.632	5.324	0.293	0.006
60.660	42.400	0.016	0.929	0.902	0.223	13.538	4.472	5.186	0.147
60.584	42.896	0.020	1.083	1.049	0.268	5.533	2.514	-1.451	-0.179
60.510	43.390	0.024	1.111	1.074	0.285	3.180	2.013	-1.579	-0.423
60.436	43.886	0.028	1.111	1.072	0.291	2.824	1.935	-1.358	-0.426
60.360	44.380	0.031	1.111	1.071	0.297	2.827	1.869	-1.332	-0.433
60.284	44.874	0.035	1.114	1.073	0.302	3.258	1.910	-1.302	-0.359
60.210	45.370	0.039	1.114	1.071	0.305	2.718	1.984	-1.307	-0.416
60.134	45.866	0.043	1.113	1.070	0.308	2.679	1.917	-1.201	-0.401
60.060	46.360	0.047	1.114	1.069	0.313	2.599	1.909	-1.155	-0.400
59.986	46.858	0.051	1.116	1.071	0.315	2.542	2.089	-0.943	-0.304
59.910	47.350	0.055	1.115	1.069	0.318	2.521	1.973	-0.668	-0.230
59.834	47.844	0.059	1.114	1.066	0.322	2.609	2.046	-1.107	-0.356
59.760	48.340	0.063	1.113	1.065	0.325	2.382	2.011	-0.843	-0.302
59.686	48.836	0.067	1.113	1.063	0.327	2.353	1.950	-0.694	-0.259
59.610	49.330	0.071	1.115	1.065	0.330	2.229	1.997	-0.674	-0.260
59.536	49.824	0.075	1.110	1.060	0.332	2.310	1.989	-0.782	-0.292
59.460	50.320	0.079	1.110	1.058	0.335	2.726	1.991	-0.429	-0.135
59.386	50.814	0.083	1.110	1.058	0.334	2.232	2.031	-0.621	-0.235
59.310	51.310	0.087	1.108	1.055	0.339	2.450	2.064	-0.564	-0.191
59.234	51.804	0.090	1.106	1.052	0.340	2.409	2.082	-0.505	-0.173
59.160	52.300	0.094	1.106	1.052	0.341	2.211	2.026	-0.371	-0.142
59.086	52.794	0.098	1.103	1.049	0.343	2.128	2.117	-0.451	-0.172
59.010	53.290	0.102	1.103	1.049	0.343	2.188	2.077	-0.219	-0.083
58.936	53.784	0.106	1.102	1.047	0.344	2.079	2.032	-0.268	-0.109
58.858	54.280	0.110	1.098	1.042	0.344	2.030	2.016	-0.293	-0.123
58.788	54.776	0.114	1.099	1.044	0.345	2.011	2.011	-0.238	-0.101
58.710	55.270	0.118	1.096	1.040	0.346	2.435	2.049	-0.195	-0.067
58.634	55.764	0.122	1.093	1.037	0.346	2.349	2.033	-0.290	-0.104
58.560	56.260	0.126	1.092	1.036	0.347	2.038	2.030	-0.122	-0.050

Survey Number 9 (Station 9 boundary layer)									
x(mm)	y(mm)	d/c	W/Vref	U/Vref	V/Vref	Tu	Tv	Re stress	Cuv
115.900	40.080	0.008	0.167	-0.130	0.104	5.697	6.060	-0.931	-0.047
115.940	40.582	0.012	0.169	-0.139	0.097	5.634	7.051	0.416	0.018
115.978	41.078	0.016	0.169	-0.136	0.099	5.425	7.942	-0.772	-0.031
116.016	41.578	0.020	0.162	-0.132	0.093	6.004	8.030	-1.869	-0.068
116.058	42.076	0.024	0.163	-0.133	0.095	5.622	8.751	-0.014	0.000
116.096	42.576	0.028	0.163	-0.129	0.101	6.169	9.002	0.236	0.007
116.134	43.074	0.031	0.156	-0.125	0.094	6.108	9.250	0.892	0.028
116.174	43.574	0.035	0.154	-0.122	0.094	6.202	10.168	1.721	0.048
116.212	44.072	0.039	0.163	-0.125	0.105	5.981	9.441	1.020	0.032
116.250	44.572	0.043	0.151	-0.115	0.098	6.526	10.152	0.083	0.002
116.288	45.070	0.047	0.145	-0.110	0.094	7.301	11.173	7.958	0.171
116.330	45.570	0.051	0.140	-0.107	0.091	7.558	11.177	3.239	0.067
116.368	46.070	0.055	0.133	-0.099	0.088	7.627	11.126	3.414	0.070
116.408	46.568	0.059	0.139	-0.098	0.099	8.247	12.411	7.822	0.134
116.446	47.066	0.063	0.133	-0.090	0.098	8.556	12.095	7.987	0.135
116.486	47.566	0.067	0.126	-0.083	0.094	9.966	13.016	11.257	0.152
116.524	48.064	0.071	0.131	-0.080	0.103	9.849	14.507	13.368	0.164
116.564	48.564	0.075	0.120	-0.071	0.096	10.214	14.093	12.118	0.147
116.602	49.064	0.079	0.114	-0.055	0.100	11.438	14.623	16.932	0.177
116.640	49.562	0.083	0.116	-0.040	0.109	12.603	15.589	24.669	0.220
116.682	50.060	0.087	0.106	-0.041	0.098	12.248	15.164	24.529	0.231
116.720	50.560	0.090	0.108	-0.020	0.106	14.276	16.011	23.581	0.181
116.758	51.060	0.094	0.105	0.003	0.105	15.421	16.706	36.565	0.249
116.796	51.558	0.098	0.117	0.009	0.116	15.627	17.599	29.101	0.185
116.836	52.058	0.102	0.119	0.047	0.110	17.982	17.603	54.056	0.299
116.874	52.556	0.106	0.129	0.060	0.114	17.909	17.622	46.572	0.259
116.914	53.054	0.110	0.162	0.109	0.120	21.116	17.606	52.272	0.246
116.954	53.554	0.114	0.177	0.129	0.120	21.099	18.257	67.292	0.306
116.994	54.054	0.118	0.220	0.173	0.136	23.246	18.889	69.122	0.276
117.030	54.552	0.122	0.245	0.207	0.132	24.214	18.319	66.012	0.261
117.072	55.050	0.126	0.269	0.236	0.130	25.061	17.902	65.280	0.255
117.108	55.550	0.130	0.307	0.280	0.126	26.254	17.884	72.227	0.269
117.148	56.050	0.134	0.359	0.332	0.136	26.817	17.327	58.502	0.221
117.186	56.550	0.138	0.374	0.354	0.121	27.340	16.201	44.618	0.176
117.228	57.048	0.142	0.413	0.395	0.122	27.191	15.926	50.614	0.205
117.266	57.546	0.146	0.465	0.451	0.113	28.388	15.604	27.431	0.108
117.304	58.044	0.149	0.505	0.492	0.115	28.362	15.075	37.714	0.155
117.344	58.544	0.153	0.547	0.539	0.094	28.078	14.393	28.266	0.123
117.382	59.044	0.157	0.568	0.558	0.104	28.263	13.945	12.636	0.056
117.422	59.544	0.161	0.633	0.626	0.090	28.338	12.720	2.830	0.014
117.460	60.042	0.165	0.661	0.656	0.082	26.909	11.808	8.590	0.047
117.498	60.540	0.169	0.702	0.698	0.072	26.840	11.301	-0.085	0.000
117.538	61.040	0.173	0.725	0.722	0.071	26.324	10.933	-10.833	-0.066
117.578	61.538	0.177	0.753	0.751	0.057	25.036	10.078	-1.923	-0.013
117.616	62.038	0.181	0.784	0.782	0.048	24.894	10.006	-9.474	-0.067
117.656	62.536	0.185	0.829	0.828	0.039	22.790	8.642	-5.203	-0.046
117.696	63.034	0.189	0.836	0.835	0.038	23.064	8.537	-6.053	-0.054
117.734	63.534	0.193	0.873	0.873	0.032	20.981	8.346	-12.854	-0.129
117.772	64.034	0.197	0.887	0.887	0.022	19.962	8.026	-3.964	-0.043
117.812	64.532	0.201	0.907	0.907	0.015	18.919	7.068	-7.349	-0.096
117.850	65.032	0.205	0.928	0.928	0.011	16.235	7.160	-11.082	-0.167
117.890	65.530	0.208	0.928	0.928	0.009	17.131	6.561	-7.471	-0.116
117.926	66.028	0.212	0.951	0.951	0.000	14.949	6.271	-2.358	-0.044
117.968	66.528	0.216	0.961	0.961	-0.009	13.957	5.922	-5.177	-0.110
118.006	67.028	0.220	0.963	0.963	-0.010	12.847	5.437	-2.930	-0.073
118.046	67.526	0.224	0.974	0.974	-0.019	11.017	5.088	-4.590	-0.143
118.082	68.024	0.228	0.980	0.980	-0.022	9.908	4.521	-2.196	-0.086
118.124	68.524	0.232	0.983	0.982	-0.027	8.408	4.424	-1.840	-0.087
118.162	69.024	0.236	0.985	0.985	-0.025	8.569	4.379	-1.293	-0.060
118.202	69.522	0.240	0.986	0.985	-0.030	7.677	4.026	-0.488	-0.028
118.242	70.020	0.244	0.990	0.990	-0.034	7.460	3.781	-0.206	-0.013
118.280	70.520	0.248	0.989	0.988	-0.036	6.503	3.714	-0.078	-0.006
118.316	71.018	0.252	0.992	0.991	-0.041	5.540	3.406	-0.223	-0.021
118.358	71.518	0.256	0.989	0.988	-0.040	5.347	3.486	-0.737	-0.069
118.396	72.018	0.260	0.986	0.985	-0.042	4.623	3.053	-0.389	-0.048
118.434	72.516	0.264	0.988	0.987	-0.046	4.649	3.137	-0.328	-0.039

Survey Number 10 (Station 13 wake)									
x(mm)	y(mm)	y/s	W/Vref	U/Vref	V/Vref	Tu	Tv	Re stress	Cuv
146.302	-14.220	-0.093	0.892	0.882	0.131	1.979	1.804	0.434	0.213
146.302	-6.720	-0.044	0.897	0.887	0.130	2.133	1.745	0.459	0.216
146.304	0.780	0.005	0.904	0.894	0.133	2.016	1.892	0.550	0.253
146.304	8.280	0.054	0.906	0.897	0.131	2.105	2.247	0.505	0.187
146.304	15.780	0.104	0.910	0.900	0.136	2.534	2.168	0.459	0.146
146.304	23.280	0.153	0.922	0.911	0.142	2.950	2.888	0.647	0.133
146.302	30.780	0.202	0.934	0.919	0.166	7.183	6.993	1.403	0.049
146.304	38.280	0.251	0.589	0.529	0.260	21.898	18.384	49.002	0.213
146.304	45.780	0.300	0.190	0.044	0.185	14.805	20.653	37.501	0.215
146.304	53.280	0.350	0.110	0.075	0.080	19.089	16.294	-8.036	-0.045
146.304	60.780	0.399	0.423	0.413	0.088	27.367	14.902	-39.762	-0.171
146.304	68.280	0.448	0.774	0.769	0.087	20.957	11.560	-32.895	-0.238
146.302	75.780	0.497	0.899	0.893	0.096	9.176	7.700	-9.476	-0.235
146.302	83.280	0.546	0.901	0.894	0.109	4.287	3.869	-1.172	-0.124
146.304	90.780	0.596	0.892	0.885	0.115	2.588	2.381	-0.434	-0.123
146.304	98.280	0.645	0.889	0.881	0.119	2.511	1.861	0.288	0.108
146.302	105.780	0.694	0.890	0.881	0.122	2.385	1.789	0.483	0.198
146.304	113.280	0.743	0.882	0.875	0.117	1.870	1.776	0.326	0.172
146.302	120.780	0.793	0.875	0.867	0.118	2.026	1.979	0.271	0.118
146.302	128.280	0.842	0.870	0.862	0.119	1.718	1.650	0.316	0.195
146.302	135.780	0.891	0.869	0.861	0.118	2.096	1.706	0.223	0.109
146.302	143.280	0.940	0.872	0.864	0.116	1.985	1.764	0.562	0.281
146.302	150.780	0.989	0.879	0.871	0.116	1.911	1.960	0.648	0.303
146.302	158.280	1.039	0.880	0.872	0.118	2.089	1.958	0.601	0.258
146.302	165.780	1.088	0.882	0.874	0.122	1.949	2.276	0.574	0.227
146.304	173.282	1.137	0.895	0.886	0.133	2.248	2.313	0.384	0.129
146.304	180.780	1.186	0.908	0.895	0.153	3.893	4.105	0.864	0.095
146.304	188.280	1.235	0.841	0.809	0.231	15.190	11.713	13.438	0.132
146.302	195.780	1.285	0.351	0.220	0.273	19.405	21.113	67.682	0.289
146.302	203.280	1.334	0.156	0.100	0.119	19.362	17.512	-7.261	-0.038
146.304	210.780	1.383	0.364	0.351	0.096	27.180	15.657	-49.308	-0.203
146.304	218.280	1.432	0.717	0.712	0.082	23.578	13.807	-71.932	-0.387
146.304	225.780	1.481	0.883	0.880	0.077	10.344	8.135	-12.633	-0.263
146.302	233.280	1.531	0.901	0.896	0.087	4.219	4.199	-1.440	-0.142
146.300	240.780	1.580	0.899	0.893	0.099	2.740	2.601	-0.281	-0.069

Survey Number 11 (Station 1 inlet)									
x (mm)	z (mm)	y/s	W/Vref	U/Vref	V/Vref	Tu	Tv	Re stress	Cuv
-36.576	-76.200	-0.500	1.050	0.839	0.632	2.933	3.593	0.106	0.131
-36.576	-68.700	-0.451	1.041	0.831	0.627	2.334	4.115	0.011	0.015
-36.576	-61.200	-0.402	1.029	0.817	0.625	2.612	2.866	0.082	0.144
-36.576	-53.700	-0.352	1.021	0.809	0.623	2.787	2.717	0.073	0.125
-36.576	-46.200	-0.303	1.011	0.799	0.620	2.220	2.715	0.023	0.049
-36.576	-38.700	-0.254	1.002	0.787	0.620	2.454	3.085	0.029	0.050
-36.576	-31.200	-0.205	0.997	0.775	0.627	2.236	2.849	0.034	0.071
-36.576	-23.700	-0.156	0.993	0.766	0.632	2.526	3.232	0.041	0.066
-36.576	-16.200	-0.106	0.996	0.762	0.642	2.444	3.007	0.079	0.141
-36.576	-8.700	-0.057	1.003	0.764	0.650	2.303	5.641	0.005	0.006
-36.576	-1.200	-0.008	1.016	0.768	0.665	2.315	3.677	0.050	0.077
-36.576	6.300	0.041	1.021	0.772	0.669	2.372	4.066	0.043	0.058
-36.576	13.800	0.091	1.029	0.780	0.671	2.297	2.627	0.041	0.088
-36.576	21.300	0.140	1.044	0.797	0.674	2.359	3.093	0.069	0.123
-36.576	28.800	0.189	1.052	0.811	0.671	2.378	2.979	0.042	0.078
-36.576	36.300	0.238	1.063	0.824	0.671	2.465	2.480	0.059	0.126
-36.576	43.800	0.287	1.059	0.831	0.656	2.367	2.297	0.036	0.085
-36.576	51.300	0.337	1.061	0.838	0.651	2.223	3.023	0.030	0.059
-36.576	58.800	0.386	1.052	0.837	0.638	2.133	2.780	0.034	0.076
-36.576	66.300	0.435	1.047	0.843	0.621	2.394	2.313	0.055	0.130
-36.576	73.800	0.484	1.043	0.838	0.621	2.614	3.564	0.026	0.037
-36.576	81.300	0.533	1.036	0.834	0.614	2.394	2.804	0.032	0.061
-36.576	88.800	0.583	1.028	0.826	0.611	2.093	2.397	0.040	0.104
-36.576	96.300	0.632	1.016	0.817	0.604	2.051	2.815	0.020	0.045
-36.576	103.800	0.681	1.011	0.808	0.608	2.194	2.947	0.053	0.107
-36.576	111.300	0.730	1.007	0.802	0.609	2.070	3.256	0.019	0.036
-36.576	118.800	0.780	1.000	0.789	0.614	2.068	3.549	0.038	0.068
-36.576	126.300	0.829	0.997	0.780	0.620	2.065	2.546	0.044	0.110
-36.576	133.800	0.878	1.004	0.781	0.630	2.130	3.057	0.033	0.066
-36.576	141.300	0.927	1.004	0.778	0.636	2.176	2.627	0.046	0.104
-36.576	148.800	0.976	1.013	0.776	0.652	2.394	2.898	0.023	0.043
-36.576	156.300	1.026	1.028	0.785	0.663	2.185	2.530	0.034	0.080
-36.576	163.800	1.075	1.041	0.796	0.670	2.068	2.718	0.001	0.003
-36.576	171.300	1.124	1.054	0.817	0.666	2.166	3.232	0.049	0.091
-36.576	178.800	1.173	1.066	0.829	0.669	2.185	2.758	0.034	0.074
-36.576	186.300	1.222	1.065	0.835	0.662	2.252	2.865	0.037	0.074
-36.576	193.800	1.272	1.068	0.845	0.654	2.090	2.955	0.013	0.027
-36.576	201.300	1.321	1.067	0.851	0.643	2.112	2.525	0.038	0.093
-36.576	208.800	1.370	1.060	0.850	0.634	2.181	2.478	0.042	0.100
-36.576	216.300	1.419	1.057	0.849	0.629	2.169	2.683	0.026	0.057
-36.576	223.800	1.469	1.053	0.850	0.622	2.276	2.745	0.066	0.138
-36.576	231.300	1.518	1.049	0.847	0.619	2.290	2.961	0.041	0.078

Survey Number 12 (Station 3 inlet)									
x (mm)	z (mm)	y/s	W/Vref	U/Vref	V/VrefW	Tu	Tv	Re stress	Cuv
-6.096	-76.200	-0.500	1.069	0.891	0.592	2.299	2.651	0.043	0.091
-6.096	-71.200	-0.467	1.055	0.878	0.584	2.161	3.025	0.046	0.091
-6.096	-66.200	-0.434	1.042	0.864	0.582	2.929	8.317	0.099	0.053
-6.096	-61.200	-0.402	1.023	0.850	0.569	2.785	2.638	0.003	0.005
-6.096	-56.200	-0.369	1.020	0.844	0.573	2.831	5.147	0.070	0.063
-6.096	-51.200	-0.336	1.001	0.828	0.563	2.916	5.433	0.103	0.085
-6.096	-46.200	-0.303	0.984	0.811	0.557	2.412	4.857	0.043	0.048
-6.096	-41.200	-0.270	0.974	0.798	0.559	2.364	3.769	0.058	0.086
-6.096	-36.200	-0.238	0.959	0.779	0.559	2.463	4.852	0.045	0.049
-6.096	-31.200	-0.205	0.940	0.758	0.557	2.335	6.907	0.076	0.062
-6.096	-26.200	-0.172	0.929	0.742	0.560	2.317	4.826	0.009	0.010
-6.096	-21.200	-0.139	0.912	0.716	0.566	2.404	2.364	0.063	0.144
-6.096	-16.200	-0.106	0.899	0.687	0.580	2.198	2.216	0.059	0.159
-6.096	-11.200	-0.073	0.888	0.657	0.598	2.233	2.474	0.052	0.122
-6.096	-6.200	-0.041	0.890	0.623	0.636	2.188	2.192	0.022	0.059
-6.096	-1.200	-0.008	0.933	0.592	0.721	2.224	3.786	0.032	0.049
-6.096	3.800	0.025	1.094	0.752	0.795	12.995	0.991	0.948	0.960
-6.096	8.800	0.058	1.129	0.739	0.853	2.282	3.006	0.019	0.036
-6.096	13.800	0.091	1.170	0.812	0.843	2.685	3.074	0.033	0.052
-6.096	18.800	0.123	1.177	0.855	0.808	2.401	2.750	0.033	0.065
-6.096	23.800	0.156	1.177	0.882	0.778	2.137	2.808	0.030	0.066
-6.096	28.800	0.189	1.169	0.898	0.748	2.291	2.594	0.030	0.065
-6.096	33.800	0.222	1.160	0.910	0.719	2.312	2.559	0.021	0.046
-6.096	38.800	0.255	1.153	0.917	0.699	2.403	2.570	0.027	0.057
-6.096	43.800	0.287	1.141	0.919	0.676	2.349	3.116	0.038	0.067
-6.096	48.800	0.320	1.133	0.921	0.661	2.381	2.310	0.036	0.085
-6.096	53.800	0.353	1.119	0.918	0.639	2.295	2.597	0.062	0.135
-6.096	58.800	0.386	1.102	0.913	0.618	2.087	2.296	0.066	0.180
-6.096	63.800	0.419	1.094	0.912	0.605	2.200	2.618	0.055	0.125
-6.096	68.800	0.451	1.079	0.900	0.595	2.100	2.614	0.038	0.089
-6.096	73.800	0.484	1.068	0.893	0.585	2.068	2.558	0.036	0.088
-6.096	78.800	0.517	1.056	0.883	0.578	1.729	2.595	0.026	0.075
-6.096	83.800	0.550	1.045	0.877	0.568	1.989	2.696	0.034	0.082
-6.096	88.800	0.583	1.032	0.866	0.562	2.040	2.189	0.067	0.195
-6.096	93.800	0.615	1.017	0.850	0.559	2.167	2.407	0.042	0.106
-6.094	98.800	0.648	1.005	0.837	0.557	2.323	2.598	0.048	0.104
-6.096	103.800	0.681	0.995	0.828	0.552	2.051	2.623	0.050	0.121
-6.096	108.800	0.714	0.983	0.814	0.551	2.093	2.620	0.043	0.103
-6.096	113.800	0.747	0.967	0.796	0.549	2.012	2.247	0.033	0.096
-6.096	118.800	0.780	0.949	0.775	0.547	2.106	2.159	0.032	0.091
-6.096	123.800	0.812	0.940	0.760	0.553	1.922	2.247	0.014	0.044
-6.096	128.800	0.845	0.927	0.743	0.554	2.048	2.922	0.024	0.053
-6.096	133.800	0.878	0.915	0.720	0.564	2.214	2.204	0.015	0.041
-6.096	138.802	0.911	0.906	0.695	0.580	2.047	2.812	0.036	0.081
-6.096	143.800	0.944	0.903	0.668	0.608	2.046	2.719	0.052	0.121
-6.096	148.800	0.976	0.908	0.629	0.654	2.081	2.794	0.028	0.063
-6.096	153.800	1.009	0.974	0.618	0.753	2.169	2.949	0.014	0.029
-6.096	158.800	1.042	1.086	0.699	0.831	2.144	2.703	0.041	0.092
-6.096	163.800	1.075	1.145	0.781	0.837	2.145	2.462	0.014	0.034
-6.096	168.800	1.108	1.164	0.835	0.811	2.108	3.363	0.045	0.083
-6.096	173.800	1.140	1.175	0.874	0.785	2.103	2.777	0.032	0.072
-6.096	178.800	1.173	1.176	0.898	0.759	2.094	3.495	0.010	0.017
-6.096	183.800	1.206	1.174	0.916	0.734	2.000	2.934	0.046	0.102
-6.096	188.800	1.239	1.166	0.927	0.707	2.153	4.006	0.029	0.043
-6.096	193.800	1.272	1.158	0.930	0.690	2.140	3.361	0.019	0.035
-6.096	198.800	1.304	1.151	0.935	0.671	2.539	2.880	0.017	0.030
-6.096	203.800	1.337	1.138	0.931	0.653	2.810	2.394	0.032	0.062
-6.096	208.800	1.370	1.121	0.925	0.635	2.262	2.452	0.036	0.084
-6.096	213.800	1.403	1.109	0.924	0.614	2.083	2.834	0.027	0.060
-6.096	218.800	1.436	1.094	0.918	0.595	2.213	2.368	0.034	0.085
-6.096	223.800	1.469	1.076	0.906	0.581	2.249	2.736	0.035	0.075
-6.096	228.800	1.501	1.068	0.901	0.573	2.278	3.249	0.019	0.034

Survey Number 13 (Station 5 boundary layer)									
x(mm)	y(mm)	d/c	W/Vref	U/Vref	V/Vref	Tu	Tv	Re stress	Cuv
5.160	10.508	0.010	1.283	0.887	0.926	1.699	18.983	0.059	0.021
4.784	10.838	0.014	1.319	0.885	0.978	3.287	2.990	0.072	0.084
4.408	11.170	0.018	1.304	0.879	0.963	3.462	2.723	0.103	0.126
4.034	11.500	0.022	1.296	0.876	0.955	2.443	2.678	0.049	0.087
3.658	11.832	0.026	1.286	0.871	0.947	2.345	2.270	0.048	0.103
3.284	12.164	0.029	1.279	0.871	0.937	2.330	2.778	0.057	0.101
2.910	12.494	0.033	1.274	0.868	0.933	2.323	2.328	0.002	0.004
2.534	12.826	0.037	1.262	0.865	0.918	2.342	2.802	0.062	0.109
2.160	13.156	0.041	1.257	0.865	0.912	2.291	3.849	0.028	0.036
1.784	13.486	0.045	1.247	0.861	0.902	2.263	2.440	0.036	0.075
1.408	13.818	0.049	1.239	0.858	0.894	2.363	3.133	0.019	0.030
1.034	14.148	0.053	1.241	0.862	0.893	2.352	2.343	0.048	0.100
0.660	14.480	0.057	1.233	0.858	0.885	2.232	2.253	0.024	0.055
0.284	14.810	0.061	1.224	0.857	0.874	2.272	2.991	0.032	0.054
-0.092	15.142	0.065	1.213	0.851	0.864	2.598	2.450	0.023	0.041
-0.466	15.472	0.069	1.208	0.851	0.858	2.746	3.129	0.056	0.075
-0.840	15.804	0.073	1.204	0.851	0.852	2.336	2.581	0.045	0.087
-1.216	16.134	0.077	1.198	0.849	0.845	2.155	2.404	0.017	0.038
-1.590	16.466	0.081	1.188	0.846	0.835	2.262	3.009	0.043	0.072
-1.966	16.796	0.084	1.187	0.844	0.834	2.282	3.009	-0.008	-0.014
-2.342	17.128	0.088	1.179	0.843	0.824	2.207	2.282	0.040	0.091
-2.716	17.458	0.092	1.180	0.847	0.821	2.205	2.503	0.019	0.040
-3.092	17.790	0.096	1.174	0.845	0.815	2.307	2.462	0.001	0.001
-3.466	18.124	0.100	1.167	0.840	0.810	2.678	2.367	0.017	0.032
-3.842	18.452	0.104	1.165	0.844	0.804	2.194	2.432	0.063	0.137
-4.216	18.786	0.108	1.163	0.845	0.799	2.136	2.401	0.034	0.076
-4.592	19.114	0.112	1.146	0.835	0.785	2.088	2.470	0.024	0.053
-4.966	19.444	0.116	1.149	0.840	0.783	2.179	2.632	0.060	0.121
-5.342	19.776	0.120	1.141	0.837	0.775	2.246	2.521	0.050	0.101
-5.716	20.108	0.124	1.141	0.840	0.772	2.174	2.706	0.036	0.071
-6.092	20.438	0.128	1.138	0.841	0.767	2.170	2.347	0.043	0.098
-6.466	20.768	0.132	1.126	0.833	0.758	2.238	2.541	0.055	0.112
-6.840	21.100	0.136	1.123	0.831	0.755	2.255	2.599	0.021	0.041
-7.216	21.430	0.140	1.127	0.837	0.755	2.072	2.286	0.061	0.149
-7.590	21.762	0.143	1.125	0.836	0.753	2.140	2.399	0.056	0.125
-7.966	22.092	0.147	1.117	0.833	0.745	2.130	2.421	0.042	0.094

Survey Number 14 (Station 6 boundary layer)									
x(mm)	y(mm)	d/c	W/Vref	U/Vref	V/Vref	Tu	Tv	Re stress	Cuv
29.966	29.730	0.008	1.352	1.167	0.682	2.432	3.100	0.072	0.110
29.708	30.160	0.012	1.376	1.188	0.695	3.198	2.026	0.018	0.032
29.452	30.588	0.016	1.362	1.176	0.687	4.298	2.203	0.039	0.048
29.196	31.018	0.020	1.354	1.169	0.682	3.279	2.335	0.055	0.083
28.938	31.446	0.024	1.358	1.173	0.684	2.807	2.272	0.036	0.066
28.682	31.874	0.027	1.344	1.162	0.676	2.398	1.999	0.010	0.024
28.424	32.304	0.031	1.342	1.160	0.676	2.582	2.162	0.071	0.146
28.166	32.734	0.035	1.338	1.158	0.670	2.430	2.197	0.023	0.051
27.910	33.162	0.039	1.333	1.151	0.672	2.733	2.875	0.071	0.104
27.652	33.592	0.043	1.319	1.142	0.660	2.520	2.358	0.062	0.120
27.396	34.020	0.047	1.323	1.145	0.663	2.406	2.479	0.009	0.017
27.138	34.448	0.051	1.324	1.146	0.663	2.437	2.411	0.012	0.023
26.882	34.878	0.055	1.314	1.137	0.657	2.962	2.454	-0.020	-0.032
26.626	35.306	0.059	1.302	1.129	0.649	2.444	2.163	0.029	0.062
26.368	35.736	0.063	1.305	1.129	0.653	2.518	3.089	0.020	0.030
26.110	36.164	0.067	1.298	1.124	0.649	2.405	2.424	0.033	0.065
25.854	36.594	0.071	1.296	1.123	0.647	2.464	2.648	0.006	0.010
25.596	37.022	0.075	1.293	1.119	0.646	2.382	2.376	0.035	0.071
25.340	37.452	0.079	1.282	1.111	0.640	2.391	2.425	0.006	0.012
25.084	37.880	0.083	1.279	1.108	0.640	2.440	2.675	0.030	0.053
24.826	38.310	0.086	1.280	1.110	0.637	2.366	2.384	0.044	0.091
24.568	38.740	0.090	1.272	1.102	0.635	2.368	2.396	-0.002	-0.003
24.312	39.168	0.094	1.267	1.098	0.632	2.678	3.133	0.025	0.034
24.054	39.596	0.098	1.268	1.099	0.633	2.516	2.683	-0.003	-0.005
23.798	40.026	0.102	1.261	1.093	0.628	2.381	2.768	0.018	0.031
23.542	40.454	0.106	1.252	1.084	0.625	2.407	2.416	0.052	0.104
23.282	40.884	0.110	1.251	1.083	0.625	2.246	2.371	0.030	0.065
23.028	41.312	0.114	1.244	1.078	0.621	2.412	2.725	0.024	0.042
22.770	41.742	0.118	1.240	1.075	0.617	2.677	2.856	0.087	0.131
22.512	42.172	0.122	1.235	1.071	0.616	2.510	2.347	0.035	0.069
22.256	42.600	0.126	1.231	1.067	0.614	2.397	2.445	0.069	0.136
22.000	43.032	0.130	1.228	1.063	0.613	2.439	2.389	0.038	0.076
21.742	43.458	0.134	1.220	1.057	0.610	2.316	2.548	0.030	0.058
21.484	43.888	0.138	1.222	1.058	0.612	2.335	2.360	0.034	0.071
21.228	44.316	0.141	1.216	1.054	0.607	2.389	2.494	0.026	0.051
20.972	44.744	0.145	1.207	1.044	0.605	2.850	2.589	0.058	0.091

Survey Number 15 (Station 7 boundary layer)									
x(mm)	y(mm)	d/c	W/Vref	U/Vref	V/Vref	Tu	Tv	Re stress	Cuv
60.810	41.410	0.008	1.004	0.883	0.477	10.513	28.941	-4.377	-0.168
60.734	41.904	0.012	1.332	1.306	0.264	3.565	1.451	0.019	0.042
60.660	42.400	0.016	1.348	1.322	0.267	3.340	1.509	0.013	0.030
60.586	42.896	0.020	1.334	1.307	0.266	2.570	1.617	0.037	0.103
60.510	43.390	0.024	1.322	1.296	0.263	2.521	1.584	0.022	0.065
60.436	43.886	0.028	1.328	1.301	0.265	2.365	1.829	0.010	0.028
60.360	44.380	0.031	1.320	1.293	0.265	2.576	2.117	0.023	0.049
60.286	44.874	0.035	1.306	1.279	0.263	2.483	1.912	0.035	0.085
60.210	45.370	0.039	1.304	1.276	0.267	2.567	3.187	0.045	0.064
60.134	45.866	0.043	1.298	1.271	0.263	2.555	1.889	0.029	0.071
60.058	46.360	0.047	1.288	1.260	0.264	2.544	2.003	0.022	0.049
59.986	46.854	0.051	1.280	1.253	0.265	2.578	3.012	0.034	0.050
59.910	47.350	0.055	1.279	1.251	0.264	2.499	1.925	0.029	0.070
59.834	47.844	0.059	1.272	1.244	0.266	2.605	2.018	0.023	0.052
59.760	48.340	0.063	1.267	1.239	0.265	2.503	1.897	0.038	0.094
59.686	48.836	0.067	1.258	1.230	0.264	2.638	1.902	0.057	0.132
59.610	49.330	0.071	1.248	1.219	0.267	2.414	1.967	0.035	0.086
59.534	49.824	0.075	1.251	1.221	0.270	2.712	2.046	0.034	0.072
59.460	50.320	0.079	1.247	1.218	0.270	2.771	3.201	0.033	0.044
59.384	50.816	0.083	1.240	1.211	0.268	2.977	1.980	0.021	0.041
59.310	51.310	0.087	1.232	1.202	0.272	2.570	2.064	0.014	0.031
59.234	51.804	0.090	1.225	1.196	0.266	3.108	2.215	0.028	0.047
59.160	52.300	0.094	1.210	1.180	0.268	2.529	2.185	0.004	0.009
59.086	52.794	0.098	1.216	1.185	0.272	2.462	2.136	0.035	0.077
59.010	53.290	0.102	1.216	1.184	0.273	2.493	2.025	0.022	0.050
58.934	53.784	0.106	1.199	1.167	0.272	3.205	2.595	0.018	0.025
58.860	54.280	0.110	1.198	1.166	0.272	3.374	2.163	0.020	0.032
58.784	54.774	0.114	1.184	1.153	0.273	3.125	2.178	0.016	0.028
58.710	55.270	0.118	1.181	1.149	0.273	2.460	2.400	0.043	0.086
58.634	55.764	0.122	1.182	1.150	0.275	2.403	2.794	0.021	0.036
58.560	56.260	0.126	1.184	1.151	0.277	3.029	2.115	0.040	0.073
58.486	56.756	0.130	1.179	1.145	0.279	2.417	2.266	0.028	0.060
58.410	57.250	0.134	1.173	1.140	0.279	2.606	2.799	0.037	0.059
58.334	57.744	0.138	1.165	1.131	0.279	2.442	2.135	0.038	0.085
58.260	58.240	0.142	1.151	1.117	0.278	2.853	2.252	0.068	0.123
58.186	58.736	0.146	1.148	1.113	0.281	2.545	2.241	0.042	0.086

Survey Number 16 (Station 7 boundary layer)									
x (mm)	z (mm)	d/c	W/Vref	U/Vref	V/Vref	Tu	Tv	Re stress	Cuv
60.810	40.992	0.005	0.068	0.066	0.017	2.621	0.907	0.114	0.731
60.780	41.190	0.006	0.115	0.112	0.025	2.454	1.186	0.059	0.309
60.750	41.388	0.008	0.953	0.776	0.554	11.825	34.407	-0.763	-0.029
60.720	41.586	0.009	1.087	1.063	0.228	8.251	2.292	0.344	0.278
60.690	41.784	0.011	1.270	1.241	0.267	4.690	1.566	0.079	0.164
60.662	41.982	0.012	1.321	1.292	0.279	2.892	2.880	0.058	0.107
60.630	42.180	0.014	1.353	1.323	0.284	2.683	1.486	0.028	0.106
60.600	42.378	0.016	1.345	1.314	0.284	2.634	1.628	0.006	0.022
60.570	42.578	0.017	1.341	1.310	0.285	2.593	3.016	0.026	0.052
60.540	42.774	0.019	1.341	1.310	0.285	2.717	1.662	0.024	0.080
60.510	42.972	0.020	1.338	1.307	0.283	2.615	1.801	0.032	0.102
60.480	43.170	0.022	1.331	1.300	0.283	2.799	1.798	0.042	0.126
60.450	43.368	0.024	1.329	1.299	0.283	2.762	2.855	0.019	0.036
60.420	43.566	0.025	1.332	1.301	0.283	2.686	2.831	0.006	0.012
60.390	43.764	0.027	1.328	1.297	0.284	2.655	3.331	0.027	0.047
60.360	43.962	0.028	1.323	1.292	0.283	2.599	3.627	-0.018	-0.029
60.330	44.160	0.030	1.312	1.282	0.280	2.567	1.914	0.017	0.052
60.300	44.358	0.031	1.320	1.289	0.283	2.637	1.948	0.020	0.061
60.270	44.556	0.033	1.320	1.290	0.279	2.554	1.889	0.018	0.058
60.240	44.754	0.035	1.320	1.290	0.282	2.671	1.996	0.028	0.081

Survey Number 17 (Station 7.25 boundary layer)									
x (mm)	z (mm)	d/c	W/Vref	U/Vref	V/Vref	Tu	Tv	Re stress	C uv
68.542	41.764	0.005	-0.053	-0.047	-0.024	13.105	9.885	4.502	0.545
68.532	41.964	0.006	-0.031	-0.019	0.024	15.364	10.312	-0.833	-0.082
68.522	42.164	0.008	0.109	0.062	0.090	25.329	18.380	-4.461	-0.150
68.512	42.364	0.009	0.285	0.277	0.068	36.480	12.101	-3.887	-0.138
68.502	42.564	0.011	0.614	0.610	0.072	43.361	11.176	-7.152	-0.231
68.492	42.764	0.012	0.992	0.990	0.072	28.673	9.727	-3.502	-0.197
68.482	42.964	0.014	1.171	1.166	0.106	12.924	6.641	-0.766	-0.140
68.472	43.164	0.016	1.271	1.264	0.134	9.583	6.202	-0.922	-0.243
68.462	43.364	0.017	1.319	1.311	0.148	6.583	5.833	-0.266	-0.109
68.452	43.564	0.019	1.332	1.324	0.152	6.854	5.188	-0.068	-0.030
68.442	43.764	0.020	1.343	1.334	0.153	5.027	5.176	0.082	0.050
68.432	43.964	0.022	1.337	1.328	0.152	4.587	4.189	0.007	0.006
68.422	44.164	0.024	1.331	1.322	0.152	3.997	4.952	-0.020	-0.016
68.412	44.364	0.025	1.327	1.318	0.153	3.517	4.511	0.047	0.046
68.402	44.564	0.027	1.324	1.315	0.153	3.238	5.625	0.011	0.010
68.392	44.764	0.028	1.323	1.314	0.154	3.135	2.722	0.010	0.018
68.382	44.964	0.030	1.313	1.304	0.153	3.305	4.674	0.000	0.000
68.372	45.164	0.031	1.306	1.297	0.150	3.052	2.750	-0.021	-0.039

Survey Number 18 (Station 7.5 boundary layer)									
x (mm)	z (mm)	d/c	W/Vref	U/Vref	V/Vref	Tu	Tv	Re stress	Cuv
76.202	41.928	0.005	0.068	0.044	0.052	23.088	14.264	-2.731	-0.127
76.202	42.128	0.006	0.225	0.221	0.041	30.537	22.631	-14.457	-0.320
76.204	42.328	0.008	0.332	0.299	0.145	33.532	31.964	-12.049	-0.172
76.204	42.528	0.009	0.446	0.446	-0.007	33.950	25.140	-17.212	-0.309
76.206	42.728	0.011	0.580	0.577	-0.059	32.935	24.039	-20.858	-0.403
76.206	42.928	0.012	0.743	0.739	-0.070	30.572	22.679	-17.255	-0.381
76.208	43.128	0.014	0.835	0.832	-0.074	28.464	20.849	-11.739	-0.303
76.210	43.328	0.016	0.959	0.955	-0.086	23.811	19.279	-8.696	-0.290
76.210	43.528	0.017	1.033	1.030	-0.085	19.367	19.008	-4.900	-0.204
76.210	43.728	0.019	1.091	1.089	-0.062	18.418	17.015	-2.571	-0.126
76.212	43.928	0.020	1.143	1.142	-0.047	15.720	15.647	-2.955	-0.184
76.214	44.128	0.022	1.171	1.170	-0.041	13.820	14.746	-1.739	-0.131
76.214	44.328	0.023	1.207	1.206	-0.027	11.948	12.748	-1.107	-0.111
76.214	44.528	0.025	1.206	1.206	-0.020	11.429	11.746	-0.598	-0.068
76.216	44.728	0.027	1.214	1.214	0.000	8.957	10.322	-0.145	-0.024
76.218	44.928	0.028	1.213	1.213	-0.001	8.663	9.420	-0.447	-0.084
76.218	45.128	0.030	1.209	1.209	0.007	7.361	8.714	-0.077	-0.018
76.218	45.328	0.031	1.215	1.215	0.004	6.778	6.639	-0.228	-0.078
76.220	45.528	0.033	1.214	1.214	0.007	5.565	5.884	-0.143	-0.067
76.220	45.728	0.034	1.209	1.209	0.011	4.934	5.305	-0.032	-0.019

Survey Number 19 (Station 7.75 boundary layer)									
x (mm)	z (mm)	d/c	W/Vref	U/Vref	V/Vref	Tu	Tv	Re stress	Cuv
83.836	41.554	0.003	0.333	0.333	-0.003	17.545	13.442	6.613	0.433
83.842	41.754	0.004	0.471	0.469	-0.035	21.888	14.971	-4.278	-0.202
83.850	41.954	0.006	0.510	0.510	0.026	23.971	20.810	-5.618	-0.174
83.858	42.154	0.008	0.545	0.545	-0.005	23.477	19.084	-6.049	-0.209
83.864	42.354	0.009	0.581	0.581	-0.003	23.972	20.008	-6.952	-0.224
83.870	42.554	0.011	0.656	0.655	-0.023	25.098	20.316	-9.467	-0.287
83.878	42.754	0.012	0.682	0.681	-0.044	24.839	19.139	-7.939	-0.258
83.884	42.954	0.014	0.733	0.731	-0.050	23.670	20.225	-7.280	-0.235
83.892	43.154	0.015	0.778	0.777	-0.047	23.618	19.487	-8.329	-0.280
83.898	43.354	0.017	0.848	0.846	-0.058	22.008	18.339	-7.233	-0.277
83.908	43.554	0.019	0.869	0.867	-0.057	22.282	17.614	-6.504	-0.256
83.914	43.754	0.020	0.905	0.904	-0.050	20.419	17.824	-5.312	-0.226
83.920	43.954	0.022	0.939	0.937	-0.064	18.688	15.714	-3.188	-0.168
83.928	44.154	0.023	0.971	0.970	-0.056	17.159	15.156	-3.589	-0.213
83.934	44.354	0.025	1.006	1.005	-0.044	15.582	14.592	-2.925	-0.199
83.942	44.554	0.026	1.030	1.029	-0.045	13.051	13.054	-1.590	-0.144
83.948	44.754	0.028	1.053	1.053	-0.037	10.656	12.746	-1.082	-0.123
83.954	44.954	0.030	1.051	1.051	-0.020	11.652	12.690	-2.385	-0.249
83.964	45.154	0.031	1.060	1.060	-0.021	11.138	11.857	-1.688	-0.198
83.968	45.352	0.033	1.074	1.074	-0.021	9.291	11.008	-1.336	-0.202

Survey Number 20 (Station 8 boundary layer)									
x(mm)	y(mm)	d/c	W/Vref	U/Vref	V/Vref	Tu	Tv	Re stress	Cuv
91.490	41.506	0.006	0.612	0.612	0.002	18.304	15.325	-2.336	-0.097
91.522	42.004	0.010	0.679	0.679	-0.024	18.604	12.634	-4.037	-0.200
91.554	42.504	0.014	0.753	0.753	-0.023	18.599	13.529	-2.978	-0.138
91.588	43.004	0.018	0.807	0.806	-0.018	18.641	14.050	-4.117	-0.183
91.620	43.502	0.022	0.869	0.868	-0.028	16.451	13.235	-3.644	-0.195
91.654	44.002	0.026	0.925	0.924	-0.029	14.031	12.975	-2.749	-0.176
91.686	44.500	0.029	0.959	0.959	-0.026	12.441	10.989	-2.217	-0.189
91.720	44.998	0.033	0.986	0.985	-0.023	9.519	9.486	-1.650	-0.213
91.754	45.498	0.037	1.005	1.005	-0.021	6.491	7.817	-0.399	-0.092
91.786	45.998	0.041	1.015	1.014	-0.017	5.754	6.130	-0.473	-0.157
91.818	46.498	0.045	1.025	1.025	-0.017	4.909	5.297	-0.078	-0.035
91.852	46.994	0.049	1.024	1.024	-0.012	3.770	4.241	-0.085	-0.062
91.884	47.494	0.053	1.028	1.028	-0.006	3.208	3.650	0.120	0.119
91.918	47.994	0.057	1.025	1.025	-0.009	2.940	2.944	0.024	0.032
91.950	48.492	0.061	1.029	1.029	-0.003	2.656	2.226	0.023	0.045
91.984	48.992	0.065	1.025	1.025	-0.001	2.670	2.016	0.042	0.090
92.016	49.490	0.069	1.028	1.028	0.003	2.513	2.094	0.041	0.091
92.050	49.988	0.073	1.027	1.027	0.006	2.538	2.349	0.046	0.089
92.082	50.488	0.077	1.025	1.025	0.011	2.428	1.761	0.014	0.039
92.116	50.990	0.081	1.024	1.024	0.016	2.468	2.753	0.026	0.045
92.150	51.486	0.084	1.021	1.021	0.016	2.350	1.650	0.016	0.049
92.182	51.986	0.088	1.018	1.018	0.021	2.340	2.079	0.032	0.077
92.214	52.484	0.092	1.016	1.016	0.022	2.349	2.018	0.036	0.088
92.248	52.984	0.096	1.023	1.022	0.026	2.444	3.041	0.011	0.017
92.280	53.482	0.100	1.015	1.014	0.030	2.466	3.669	0.039	0.050
92.314	53.980	0.104	1.017	1.017	0.033	2.822	3.461	0.037	0.044
92.348	54.478	0.108	1.014	1.013	0.033	2.386	2.440	0.032	0.063
92.380	54.978	0.112	1.016	1.016	0.037	2.494	2.698	0.038	0.065
92.412	55.478	0.116	1.014	1.013	0.043	2.654	3.154	0.047	0.065
92.446	55.976	0.120	1.016	1.015	0.042	2.358	2.399	0.025	0.051
92.478	56.476	0.124	1.011	1.010	0.044	2.493	1.863	0.062	0.157
92.512	56.974	0.128	1.008	1.007	0.048	2.341	2.126	0.075	0.177
92.546	57.474	0.132	1.007	1.006	0.052	2.334	4.218	0.016	0.020
92.578	57.974	0.136	1.004	1.003	0.050	2.501	2.361	0.065	0.128
92.610	58.472	0.140	1.000	0.999	0.054	2.324	2.835	0.061	0.107
92.644	58.970	0.143	0.998	0.997	0.056	2.444	3.352	0.017	0.024

Survey Number 21 (Station 9 boundary layer)									
x(mm)	y(mm)	d/c	W/Vref	U/Vref	V/Vref	Tu	Tv	Re stress	Cuv
115.870	39.706	0.005	0.497	0.497	-0.013	13.058	9.720	-1.174	-0.124
115.910	40.206	0.009	0.560	0.559	-0.033	12.765	9.384	-1.447	-0.162
115.948	40.706	0.013	0.576	0.575	-0.030	13.261	9.717	-1.636	-0.170
115.988	41.204	0.017	0.622	0.621	-0.040	13.914	10.035	-2.103	-0.202
116.028	41.702	0.021	0.643	0.642	-0.043	13.699	10.285	-2.164	-0.206
116.066	42.202	0.025	0.667	0.666	-0.033	14.219	10.758	-2.350	-0.206
116.104	42.700	0.029	0.705	0.704	-0.036	13.831	11.106	-1.725	-0.151
116.144	43.200	0.032	0.712	0.712	-0.032	13.897	11.115	-2.077	-0.180
116.182	43.700	0.036	0.762	0.761	-0.040	13.246	10.773	-2.269	-0.213
116.222	44.198	0.040	0.787	0.786	-0.036	12.413	9.611	-1.856	-0.209
116.262	44.696	0.044	0.817	0.816	-0.035	11.125	9.395	-1.630	-0.209
116.300	45.196	0.048	0.832	0.831	-0.035	10.747	9.373	-1.095	-0.146
116.338	45.696	0.052	0.863	0.862	-0.032	9.178	8.955	-0.897	-0.146
116.378	46.194	0.056	0.874	0.874	-0.030	8.037	6.949	-0.788	-0.189
116.416	46.692	0.060	0.895	0.894	-0.026	6.960	9.320	-0.553	-0.114
116.456	47.192	0.064	0.905	0.904	-0.025	6.271	6.145	-0.475	-0.165
116.494	47.690	0.068	0.908	0.908	-0.027	4.882	5.422	-0.093	-0.047
116.534	48.190	0.072	0.917	0.916	-0.026	4.176	4.484	-0.046	-0.033
116.574	48.688	0.076	0.915	0.914	-0.020	3.733	3.977	-0.035	-0.032
116.612	49.188	0.080	0.918	0.918	-0.021	3.152	4.843	-0.016	-0.014
116.652	49.688	0.084	0.920	0.919	-0.016	2.914	5.546	0.033	0.027
116.690	50.186	0.088	0.919	0.919	-0.013	2.621	4.555	0.040	0.045
116.730	50.684	0.091	0.916	0.916	-0.012	2.665	2.667	0.057	0.108
116.770	51.184	0.095	0.918	0.918	-0.010	2.480	2.973	0.000	0.000
116.806	51.682	0.099	0.915	0.915	-0.008	2.610	4.414	0.047	0.055
116.846	52.182	0.103	0.914	0.914	-0.007	2.595	2.329	0.034	0.074
116.884	52.680	0.107	0.911	0.911	-0.002	2.495	4.201	0.068	0.088
116.924	53.180	0.111	0.912	0.912	-0.002	2.528	3.324	0.055	0.087
116.964	53.680	0.115	0.911	0.911	-0.001	2.549	2.267	0.024	0.057
117.002	54.178	0.119	0.912	0.912	0.001	2.363	1.827	0.050	0.155
117.040	54.676	0.123	0.916	0.916	0.004	2.607	4.178	0.068	0.084
117.080	55.176	0.127	0.911	0.911	0.005	2.237	2.659	0.031	0.070
117.118	55.674	0.131	0.907	0.907	0.011	2.502	3.868	0.055	0.076
117.160	56.174	0.135	0.910	0.910	0.009	2.438	1.726	0.035	0.112
117.196	56.672	0.139	0.907	0.907	0.015	2.423	5.324	0.010	0.011
117.236	57.172	0.143	0.906	0.906	0.014	2.353	3.734	0.040	0.061
117.274	57.672	0.147	0.906	0.906	0.016	2.356	1.910	0.049	0.145
117.316	58.170	0.150	0.906	0.905	0.022	2.407	2.743	0.052	0.106
117.354	58.668	0.154	0.909	0.909	0.020	2.276	2.140	0.051	0.140
117.392	59.168	0.158	0.908	0.908	0.020	2.292	4.989	0.041	0.048
117.430	59.668	0.162	0.909	0.908	0.027	2.263	4.694	0.032	0.040
117.470	60.166	0.166	0.907	0.907	0.029	2.411	3.200	0.047	0.081
117.510	60.664	0.170	0.899	0.899	0.030	2.297	5.653	0.058	0.060
117.548	61.164	0.174	0.908	0.907	0.032	2.514	5.393	0.028	0.028
117.586	61.662	0.178	0.902	0.902	0.031	2.350	2.073	0.046	0.127
117.626	62.162	0.182	0.905	0.904	0.032	2.146	3.338	0.039	0.073

Survey Number 22 (Station 13 wake)									
x (mm)	z (mm)	y/s	W/Vref	U/Vref	V/Vref	Tu	Tv	Re stress	Cuv
146.300	-14.222	-0.333	0.874	0.870	0.089	2.319	1.918	0.069	0.204
146.300	-6.720	-0.284	0.874	0.870	0.086	2.651	2.036	0.077	0.186
146.300	0.780	-0.235	0.875	0.872	0.078	2.313	2.134	0.097	0.257
146.300	8.280	-0.186	0.875	0.872	0.068	2.970	2.248	0.118	0.231
146.300	15.780	-0.136	0.861	0.860	0.055	2.560	2.538	0.114	0.228
146.300	23.280	-0.087	0.861	0.860	0.042	3.024	2.072	0.080	0.166
146.300	30.780	-0.038	0.858	0.858	0.038	3.499	3.018	0.053	0.065
146.300	38.280	0.011	0.496	0.495	0.029	10.520	11.033	-1.160	-0.130
146.300	45.780	0.060	0.846	0.846	0.011	5.578	4.714	-0.263	-0.131
146.300	53.280	0.110	0.876	0.875	0.023	3.166	1.779	0.056	0.131
146.300	60.780	0.159	0.883	0.882	0.038	3.028	2.475	0.069	0.119
146.300	68.280	0.208	0.885	0.884	0.051	2.939	2.613	0.103	0.175
146.300	75.780	0.257	0.877	0.876	0.056	2.715	1.929	0.071	0.176
146.300	83.280	0.306	0.876	0.874	0.061	2.783	1.897	0.047	0.115
146.300	90.780	0.356	0.878	0.875	0.071	2.568	1.803	0.074	0.209
146.300	98.280	0.405	0.882	0.878	0.085	3.008	2.334	0.083	0.154
146.300	105.780	0.454	0.874	0.870	0.086	3.313	2.529	0.116	0.180
146.300	113.280	0.503	0.873	0.869	0.089	2.872	2.178	0.085	0.176
146.300	120.780	0.552	0.870	0.865	0.092	2.501	1.985	0.060	0.159
146.300	128.280	0.602	0.868	0.863	0.089	2.235	1.763	0.043	0.143
146.300	135.780	0.651	0.868	0.864	0.084	2.241	1.864	0.060	0.188
146.300	143.280	0.700	0.868	0.865	0.070	2.145	1.847	0.052	0.171
146.300	150.780	0.749	0.865	0.863	0.063	2.185	2.036	0.073	0.213
146.300	158.280	0.799	0.859	0.857	0.052	2.555	2.812	0.102	0.186
146.300	165.780	0.848	0.855	0.855	0.039	2.236	1.983	0.064	0.189
146.300	173.280	0.897	0.860	0.859	0.034	2.483	1.987	0.091	0.240
146.300	180.780	0.946	0.859	0.859	0.027	2.419	2.149	0.059	0.147
146.300	188.280	0.995	0.579	0.578	0.037	11.928	12.719	2.331	0.200
146.300	195.780	1.045	0.697	0.697	0.003	11.501	8.693	-1.752	-0.229
146.300	203.280	1.094	0.881	0.881	0.017	3.055	2.889	-0.038	-0.057
146.300	210.780	1.143	0.891	0.891	0.030	2.292	1.547	0.041	0.150
146.300	218.280	1.192	0.898	0.897	0.044	2.193	1.553	0.039	0.149
146.300	225.780	1.241	0.901	0.899	0.056	2.231	1.559	0.054	0.204
146.300	233.280	1.291	0.899	0.896	0.070	2.219	2.060	0.037	0.105
146.300	240.778	1.340	0.899	0.896	0.079	2.140	1.657	0.039	0.144

Survey Number 23 (Station 7 boundary layer)									
x(mm)	y(mm)	d/c	W/Vref	U/Vref	V/Vref	Tu	Tv	Re stress	Cuv
60.470	41.942	0.013	0.345	0.262	0.224	15.360	5.886	-0.407	-0.016
60.318	42.422	0.017	0.369	0.285	0.234	15.053	2.469	0.801	0.075
60.164	42.894	0.020	0.366	0.281	0.235	15.496	2.434	0.756	0.070
60.010	43.372	0.024	0.375	0.290	0.238	15.770	2.636	-0.048	-0.004
59.858	43.846	0.028	0.365	0.275	0.240	15.092	2.758	0.595	0.049
59.704	44.322	0.032	0.378	0.292	0.241	15.809	3.186	0.028	0.002
59.552	44.798	0.036	0.376	0.288	0.243	15.364	2.911	0.411	0.032
59.400	45.274	0.040	0.365	0.270	0.245	16.036	2.752	-0.235	-0.018
59.246	45.750	0.044	0.354	0.253	0.247	16.592	2.729	0.509	0.038
59.094	46.226	0.048	0.360	0.263	0.246	16.645	3.010	0.260	0.018
58.940	46.702	0.052	0.354	0.254	0.247	15.968	2.706	-0.198	-0.016
58.786	47.178	0.056	0.381	0.289	0.248	14.940	2.972	0.222	0.017
58.634	47.654	0.060	0.366	0.266	0.252	16.120	2.637	0.339	0.027
58.482	48.130	0.064	0.363	0.259	0.254	17.125	2.777	0.554	0.040
58.328	48.604	0.068	0.373	0.273	0.255	16.755	2.630	-0.438	-0.034
58.176	49.082	0.072	0.391	0.297	0.255	15.911	2.649	-0.641	-0.053
58.022	49.558	0.075	0.396	0.301	0.258	16.077	2.989	1.051	0.076
57.868	50.034	0.079	0.394	0.296	0.260	15.896	2.613	-0.041	-0.003
57.716	50.510	0.083	0.404	0.307	0.263	16.008	2.752	-0.107	-0.008
57.562	50.986	0.087	0.388	0.284	0.265	17.150	2.647	0.332	0.025
57.408	51.462	0.091	0.394	0.291	0.266	18.912	3.255	1.363	0.076
57.256	51.940	0.095	0.385	0.277	0.267	19.047	2.682	0.397	0.027
57.104	52.414	0.099	0.394	0.290	0.267	20.463	2.823	0.100	0.006
56.950	52.890	0.103	0.425	0.328	0.271	26.156	4.765	0.713	0.020
56.798	53.366	0.107	0.450	0.359	0.271	29.248	3.242	-0.792	-0.030
56.646	53.842	0.111	0.559	0.488	0.272	38.360	3.964	0.126	0.003
56.492	54.318	0.115	0.683	0.626	0.274	41.842	4.734	-0.331	-0.008
56.340	54.794	0.119	0.812	0.764	0.275	41.894	5.939	-1.663	-0.036
56.184	55.270	0.123	0.944	0.903	0.278	37.181	6.647	-0.590	-0.014
56.032	55.746	0.127	1.032	0.993	0.281	30.933	6.876	-2.073	-0.063

Survey Number 24 (Station 7.5 boundary layer)									
x(mm)	y(mm)	d/c	W/Vref	U/Vref	V/Vref	Tu	Tv	Re stress	Cuv
76.202	42.340	0.008	0.631	0.630	0.032	12.669	5.513	-6.491	-0.162
76.202	42.840	0.012	0.911	0.911	0.033	12.796	5.476	-5.045	-0.126
76.204	43.340	0.016	1.103	1.102	0.023	4.742	3.610	-0.566	-0.058
76.204	43.840	0.020	1.136	1.136	0.027	2.215	2.030	-0.231	-0.090
76.206	44.340	0.024	1.137	1.137	0.031	2.487	1.318	-0.209	-0.111
76.206	44.840	0.028	1.135	1.135	0.033	3.043	1.563	-0.332	-0.122
76.208	45.340	0.031	1.134	1.134	0.037	2.077	1.288	-0.146	-0.095
76.208	45.840	0.035	1.134	1.133	0.041	2.369	1.331	-0.015	-0.008
76.210	46.340	0.039	1.131	1.130	0.045	4.033	1.364	0.018	0.006
76.210	46.840	0.043	1.127	1.126	0.050	4.387	1.383	0.083	0.024
76.212	47.340	0.047	1.128	1.127	0.053	2.316	1.452	-0.092	-0.048
76.212	47.840	0.051	1.121	1.119	0.058	2.775	1.530	-0.108	-0.044
76.214	48.340	0.055	1.120	1.118	0.061	3.176	1.512	-0.244	-0.089
76.214	48.840	0.059	1.117	1.115	0.065	3.018	1.665	0.025	0.009
76.216	49.340	0.063	1.115	1.113	0.067	2.979	1.511	-0.031	-0.012
76.216	49.840	0.067	1.112	1.110	0.071	2.379	1.592	-0.007	-0.003
76.218	50.340	0.071	1.111	1.109	0.073	2.104	1.548	-0.001	0.000
76.218	50.840	0.075	1.105	1.102	0.078	2.029	1.603	-0.113	-0.061
76.220	51.340	0.079	1.107	1.104	0.079	2.817	1.561	-0.026	-0.010
76.220	51.840	0.083	1.101	1.098	0.084	2.362	1.681	-0.009	-0.004
76.222	52.340	0.086	1.102	1.099	0.086	2.068	1.841	0.056	0.026
76.222	52.842	0.090	1.100	1.096	0.090	2.397	1.601	0.179	0.082
76.224	53.340	0.094	1.096	1.092	0.093	2.410	1.654	0.042	0.019
76.224	53.840	0.098	1.090	1.086	0.095	3.203	1.643	0.096	0.032
76.226	54.340	0.102	1.087	1.082	0.100	3.328	1.686	-0.064	-0.020
76.226	54.842	0.106	1.085	1.081	0.102	2.616	1.691	0.032	0.013
76.228	55.340	0.110	1.083	1.078	0.105	3.114	1.668	0.075	0.025
76.226	55.840	0.114	1.079	1.074	0.108	2.496	1.648	-0.111	-0.047
76.230	56.340	0.118	1.080	1.074	0.109	3.061	1.683	-0.030	-0.010
76.230	56.840	0.122	1.073	1.068	0.112	2.674	1.725	-0.008	-0.003

Survey Number 25 (Station 6 boundary layer)									
x(mm)	y(mm)	d/c	W/Vref	U/Vref	V/Vref	Tu	Tv	Re stress	Cuv
29.708	30.160	0.010	1.347	1.157	0.689	1.736	1.266	0.244	0.196
29.452	30.588	0.013	1.344	1.158	0.682	1.486	1.602	0.042	0.031
29.196	31.016	0.017	1.340	1.155	0.678	1.619	1.528	0.103	0.073
28.938	31.446	0.020	1.335	1.153	0.674	1.659	1.504	-0.037	-0.026
28.680	31.874	0.024	1.330	1.149	0.669	1.933	1.673	0.007	0.004
28.424	32.304	0.027	1.325	1.146	0.663	1.708	1.706	0.111	0.067
28.168	32.734	0.030	1.321	1.145	0.659	1.916	1.680	0.131	0.072
27.908	33.160	0.034	1.316	1.141	0.656	1.630	1.721	0.001	0.001
27.652	33.590	0.037	1.313	1.141	0.649	1.643	1.628	-0.029	-0.019
27.396	34.020	0.040	1.306	1.136	0.645	1.920	1.729	-0.047	-0.025
27.138	34.448	0.044	1.302	1.133	0.642	1.761	1.574	0.037	0.023
26.882	34.878	0.047	1.300	1.131	0.641	1.720	1.600	0.025	0.016
26.624	35.306	0.051	1.293	1.126	0.635	1.959	1.527	-0.008	-0.005
26.368	35.736	0.054	1.288	1.123	0.632	1.916	1.569	0.079	0.047
26.110	36.164	0.057	1.283	1.118	0.629	1.714	1.375	-0.054	-0.040
25.856	36.594	0.061	1.280	1.116	0.627	1.719	1.434	0.123	0.088
25.596	37.022	0.064	1.274	1.112	0.623	1.777	1.348	0.049	0.036
25.340	37.452	0.067	1.268	1.105	0.622	1.756	1.305	0.076	0.059
25.084	37.880	0.071	1.262	1.101	0.617	1.795	1.427	0.086	0.059
24.824	38.310	0.074	1.260	1.099	0.616	1.819	1.388	-0.005	-0.004
24.570	38.738	0.078	1.256	1.096	0.613	1.991	1.516	0.011	0.007
24.312	39.168	0.081	1.251	1.093	0.609	1.881	1.649	0.029	0.016
24.054	39.598	0.084	1.247	1.089	0.607	1.911	1.633	0.028	0.016
23.798	40.026	0.088	1.245	1.087	0.608	1.656	1.415	0.142	0.107
23.542	40.454	0.091	1.241	1.084	0.606	1.638	1.667	0.065	0.042
23.284	40.884	0.094	1.236	1.079	0.603	1.855	1.627	0.020	0.012
23.026	41.312	0.098	1.234	1.077	0.602	1.754	1.471	-0.024	-0.016
22.770	41.742	0.101	1.228	1.073	0.597	1.962	1.540	0.062	0.036
22.514	42.170	0.104	1.224	1.070	0.595	2.006	1.536	0.025	0.015
22.256	42.600	0.108	1.221	1.066	0.596	1.903	1.623	0.015	0.008

Survey Number 26 (Station 8 boundary layer)									
x(mm)	y(mm)	d/c	W/Vref	U/Vref	V/Vref	Tu	Tv	Re stress	Cuv
91.506	41.754	0.008	0.665	0.636	0.196	15.160	12.098	4.934	0.047
91.538	42.254	0.012	0.801	0.800	0.035	15.901	6.326	-8.002	-0.139
91.572	42.754	0.016	0.963	0.963	0.004	9.946	5.288	-5.260	-0.175
91.604	43.252	0.020	1.029	1.029	-0.015	4.938	3.830	-0.691	-0.064
91.636	43.750	0.024	1.038	1.037	-0.026	4.601	2.437	0.218	0.034
91.670	44.250	0.027	1.038	1.037	-0.031	4.314	2.022	0.198	0.040
91.702	44.748	0.031	1.037	1.037	-0.029	3.618	1.710	-0.007	-0.002
91.736	45.248	0.035	1.035	1.035	-0.027	4.493	1.865	0.018	0.004
91.768	45.746	0.039	1.034	1.034	-0.024	4.320	2.323	0.022	0.004
91.802	46.246	0.043	1.033	1.033	-0.022	3.894	1.571	0.120	0.034
91.836	46.744	0.047	1.027	1.027	-0.019	5.843	1.696	0.050	0.009
91.868	47.244	0.051	1.025	1.025	-0.016	6.339	2.061	-0.005	-0.001
91.902	47.744	0.055	1.027	1.026	-0.013	5.459	1.540	0.058	0.012
91.934	48.242	0.059	1.027	1.027	-0.011	5.157	1.508	0.096	0.022
91.966	48.740	0.063	1.018	1.018	-0.007	6.878	2.142	0.335	0.040
91.998	49.240	0.067	1.023	1.023	-0.004	4.885	1.644	0.035	0.008
92.034	49.738	0.071	1.021	1.021	-0.003	4.766	1.535	0.190	0.045
92.066	50.238	0.075	1.021	1.021	0.000	4.228	1.462	0.036	0.010
92.100	50.738	0.078	1.020	1.020	0.003	4.676	1.740	-0.033	-0.007
92.132	51.238	0.082	1.019	1.019	0.005	4.191	1.521	0.091	0.025
92.164	51.734	0.086	1.013	1.013	0.007	5.107	1.581	0.393	0.085
92.198	52.234	0.090	1.008	1.008	0.011	6.969	1.541	-0.202	-0.033
92.232	52.732	0.094	1.010	1.010	0.013	4.538	1.569	0.131	0.032
92.264	53.232	0.098	1.006	1.006	0.016	5.799	1.546	0.014	0.003
92.298	53.730	0.102	1.006	1.006	0.018	5.686	1.503	0.213	0.044
92.330	54.230	0.106	1.000	1.000	0.022	7.192	1.686	0.206	0.030
92.362	54.728	0.110	1.003	1.002	0.024	5.433	1.588	0.005	0.001
92.398	55.228	0.114	0.999	0.999	0.025	6.439	1.996	-0.016	-0.002
92.428	55.728	0.118	1.000	0.999	0.027	5.062	1.563	0.094	0.021
92.462	56.226	0.122	0.996	0.996	0.028	5.570	1.562	0.120	0.024

Survey Number 27 (Station 1 inlet)									
x (mm)	z (mm)	y/s	W/Vref	U/Vref	V/Vref	Tu	Tv	Re stress	Cuv
-36.578	-76.200	-0.500	1.088	0.870	0.654	2.773	2.264	0.106	0.087
-36.578	-68.700	-0.451	1.076	0.860	0.647	2.330	2.372	0.151	0.140
-36.576	-61.200	-0.402	1.063	0.849	0.640	2.295	2.603	0.095	0.082
-36.576	-53.700	-0.352	1.046	0.833	0.633	2.181	2.444	0.100	0.096
-36.576	-46.200	-0.303	1.040	0.824	0.634	2.390	2.211	0.042	0.041
-36.576	-38.700	-0.254	1.038	0.819	0.639	2.501	2.503	-0.002	-0.002
-36.576	-31.200	-0.205	1.030	0.805	0.642	2.150	2.443	0.066	0.064
-36.576	-23.700	-0.156	1.030	0.802	0.646	2.157	2.174	0.086	0.094
-36.576	-16.200	-0.106	1.030	0.795	0.655	2.203	2.337	0.139	0.139
-36.576	-8.700	-0.057	1.033	0.790	0.666	2.290	2.226	0.110	0.111
-36.574	-1.200	-0.008	1.043	0.793	0.677	2.347	2.209	0.110	0.109
-36.576	6.300	0.041	1.055	0.800	0.687	2.031	2.254	0.051	0.057
-36.576	13.800	0.091	1.065	0.810	0.691	2.505	2.214	0.095	0.088
-36.576	21.300	0.140	1.086	0.836	0.694	2.175	2.174	0.059	0.064
-36.576	28.800	0.189	1.095	0.850	0.691	2.194	2.078	0.146	0.164
-36.574	36.300	0.238	1.099	0.859	0.685	2.036	2.579	0.100	0.098
-36.574	43.800	0.287	1.100	0.866	0.679	2.112	1.928	0.046	0.058
-36.576	51.300	0.337	1.100	0.871	0.671	2.251	2.377	0.083	0.080
-36.576	58.800	0.386	1.097	0.873	0.663	1.869	2.035	0.100	0.134
-36.576	66.300	0.435	1.090	0.871	0.656	1.922	2.052	0.101	0.131
-36.576	73.800	0.484	1.082	0.865	0.650	2.017	2.167	0.091	0.107
-36.576	81.300	0.533	1.076	0.862	0.645	2.142	2.293	0.084	0.088
-36.576	88.800	0.583	1.066	0.852	0.640	2.031	2.247	0.088	0.099
-36.576	96.300	0.632	1.053	0.842	0.633	1.958	2.238	0.061	0.072
-36.576	103.800	0.681	1.048	0.839	0.628	2.035	1.986	0.032	0.040
-36.576	111.300	0.730	1.043	0.830	0.631	1.939	2.145	0.042	0.052
-36.576	118.800	0.780	1.038	0.819	0.637	1.956	2.152	0.033	0.040
-36.576	126.300	0.829	1.037	0.812	0.646	2.091	2.747	0.072	0.065
-36.576	133.800	0.878	1.037	0.806	0.653	2.091	2.408	0.096	0.097
-36.576	141.300	0.927	1.040	0.802	0.661	2.054	2.281	0.085	0.093
-36.578	148.800	0.976	1.050	0.806	0.674	1.971	2.307	0.108	0.121
-36.578	156.300	1.026	1.067	0.816	0.688	2.005	1.908	0.040	0.053
-36.576	163.800	1.075	1.078	0.826	0.693	1.986	2.641	0.117	0.114
-36.576	171.300	1.124	1.091	0.839	0.698	2.050	3.724	0.049	0.033
-36.576	178.800	1.173	1.107	0.857	0.700	2.081	2.217	0.083	0.092
-36.574	186.300	1.222	1.115	0.872	0.695	2.181	2.478	0.075	0.071
-36.578	193.800	1.272	1.111	0.880	0.678	2.101	2.636	0.069	0.064
-36.576	201.300	1.321	1.109	0.884	0.669	2.079	2.163	0.076	0.087
-36.576	208.800	1.370	1.108	0.890	0.661	2.102	2.194	0.044	0.049
-36.574	216.300	1.419	1.106	0.891	0.655	2.253	2.946	0.075	0.058
-36.576	223.800	1.469	1.106	0.895	0.650	2.297	2.269	0.069	0.068
-36.578	231.300	1.518	1.098	0.888	0.647	2.176	2.299	0.074	0.076

Survey Number 28 (Station 3 inlet)									
x (mm)	z (mm)	y/s	W/Vref	U/Vref	V/Vref	Tu	Tv	Re stress	Cuv
-6.094	-76.200	-0.500	1.096	0.914	0.604	2.097	2.652	-0.017	-0.016
-6.098	-71.200	-0.467	1.081	0.900	0.599	1.956	2.298	0.060	0.068
-6.096	-66.200	-0.434	1.070	0.892	0.591	2.171	2.079	0.100	0.112
-6.096	-61.200	-0.402	1.058	0.880	0.587	2.228	2.340	0.067	0.065
-6.098	-56.200	-0.369	1.045	0.867	0.584	2.176	1.973	0.050	0.059
-6.094	-51.200	-0.336	1.035	0.856	0.582	2.133	2.329	0.127	0.130
-6.094	-46.200	-0.303	1.021	0.838	0.583	2.160	2.202	0.161	0.172
-6.096	-41.200	-0.270	1.002	0.818	0.578	2.111	2.288	0.185	0.195
-6.094	-36.200	-0.238	0.989	0.801	0.579	1.951	2.540	0.147	0.151
-6.096	-31.200	-0.205	0.967	0.778	0.575	2.162	2.162	0.159	0.173
-6.096	-26.200	-0.172	0.954	0.758	0.578	2.042	1.974	0.128	0.162
-6.098	-21.200	-0.139	0.941	0.734	0.588	1.891	2.081	0.095	0.123
-6.098	-16.200	-0.106	0.927	0.707	0.599	1.941	2.227	0.050	0.059
-6.096	-11.200	-0.073	0.917	0.677	0.619	2.171	2.156	0.105	0.114
-6.096	-6.200	-0.041	0.914	0.638	0.656	1.981	2.367	0.066	0.072
-6.096	-1.200	-0.008	0.950	0.600	0.737	2.132	2.383	0.080	0.080
-6.096	8.800	0.058	1.162	0.755	0.883	2.160	2.273	0.016	0.016
-6.098	13.800	0.091	1.201	0.835	0.863	2.064	2.507	0.068	0.067
-6.098	18.800	0.123	1.205	0.877	0.826	2.136	2.288	0.186	0.194
-6.098	23.804	0.156	1.202	0.905	0.791	2.035	2.120	0.075	0.089
-6.096	28.800	0.189	1.200	0.925	0.766	2.022	2.039	0.043	0.053
-6.096	33.800	0.222	1.187	0.932	0.736	2.041	2.163	0.009	0.010
-6.096	38.800	0.255	1.180	0.939	0.714	1.989	1.938	0.057	0.076
-6.096	43.800	0.287	1.167	0.942	0.690	2.101	2.008	0.056	0.067
-6.096	48.800	0.320	1.156	0.941	0.671	2.170	2.050	0.088	0.100
-6.098	53.800	0.353	1.145	0.940	0.653	2.277	2.169	0.134	0.138
-6.094	58.800	0.386	1.133	0.936	0.638	2.009	2.045	0.095	0.117
-6.096	63.800	0.419	1.117	0.926	0.624	2.018	2.018	0.107	0.133
-6.098	68.800	0.451	1.105	0.920	0.613	2.073	2.000	0.081	0.100
-6.096	73.800	0.484	1.091	0.910	0.603	2.202	1.909	0.010	0.012
-6.096	78.800	0.517	1.074	0.898	0.589	2.074	1.983	0.067	0.083
-6.096	83.800	0.550	1.066	0.891	0.585	2.644	1.968	0.120	0.117
-6.096	88.800	0.583	1.048	0.874	0.577	2.123	2.033	0.062	0.072
-6.096	93.800	0.615	1.037	0.864	0.573	2.557	2.012	0.131	0.130
-6.096	98.800	0.648	1.025	0.851	0.572	2.377	1.988	0.115	0.124
-6.094	103.800	0.681	1.016	0.839	0.572	2.185	2.097	0.102	0.114
-6.094	108.800	0.714	1.003	0.826	0.569	2.261	2.260	0.091	0.090
-6.094	113.800	0.747	0.989	0.809	0.570	2.299	2.220	0.126	0.125
-6.094	118.800	0.780	0.974	0.791	0.568	2.033	1.964	0.090	0.115
-6.096	123.800	0.812	0.961	0.775	0.568	2.020	1.969	0.058	0.074
-6.096	128.800	0.845	0.951	0.757	0.576	2.515	2.163	0.150	0.140
-6.096	133.800	0.878	0.941	0.735	0.587	2.069	1.940	0.044	0.056
-6.096	138.800	0.911	0.931	0.709	0.604	2.024	1.999	0.053	0.067
-6.096	143.800	0.944	0.927	0.676	0.634	2.464	1.927	0.091	0.098
-6.096	148.800	0.976	0.932	0.637	0.680	2.205	2.019	0.069	0.078
-6.098	153.800	1.009	1.002	0.629	0.780	2.470	2.477	-0.030	-0.025
-6.096	158.800	1.042	1.123	0.716	0.865	2.261	2.477	0.131	0.119
-6.098	163.800	1.075	1.187	0.807	0.870	2.212	2.711	0.075	0.063
-6.096	168.800	1.108	1.215	0.866	0.853	2.089	2.220	0.021	0.023
-6.096	173.800	1.140	1.215	0.898	0.818	3.786	2.467	0.155	0.084
-6.096	178.800	1.173	1.220	0.932	0.788	2.498	2.018	0.020	0.020
-6.094	183.800	1.206	1.215	0.947	0.762	2.144	1.955	0.040	0.049
-6.098	188.800	1.239	1.209	0.959	0.737	1.955	2.045	0.032	0.040
-6.096	193.800	1.272	1.200	0.963	0.716	1.978	2.219	0.028	0.032
-6.096	198.800	1.304	1.186	0.961	0.695	1.954	1.962	0.043	0.058
-6.098	203.800	1.337	1.178	0.963	0.678	2.171	1.981	0.053	0.063
-6.096	208.800	1.370	1.165	0.960	0.659	2.053	2.063	0.083	0.100
-6.096	213.800	1.403	1.150	0.954	0.643	2.501	2.132	0.093	0.089
-6.096	218.800	1.436	1.132	0.944	0.625	2.132	2.179	0.066	0.072
-6.096	223.800	1.469	1.115	0.934	0.610	1.962	2.019	0.098	0.126
-6.094	228.800	1.501	1.100	0.924	0.597	1.943	2.194	0.062	0.074

Survey Number 29 (Station 5 boundary layer)									
x(mm)	y(mm)	d/c	W/Vref	U/Vref	V/Vref	Tu	Tv	Re stress	Cuv
4.972	10.674	0.012	1.299	0.913	0.925	2.062	20.440	0.305	0.037
4.596	11.006	0.016	1.349	0.907	0.999	3.070	2.665	0.110	0.069
4.222	11.336	0.020	1.335	0.902	0.984	3.933	2.768	0.133	0.062
3.846	11.666	0.024	1.323	0.897	0.972	2.766	2.854	0.066	0.043
3.470	11.998	0.028	1.318	0.896	0.966	2.901	3.065	0.034	0.019
3.096	12.328	0.031	1.310	0.893	0.959	3.471	2.175	0.181	0.123
2.722	12.660	0.035	1.300	0.890	0.947	2.788	2.787	0.118	0.077
2.346	12.992	0.039	1.294	0.891	0.939	3.268	3.060	0.059	0.030
1.970	13.322	0.043	1.281	0.886	0.926	2.358	3.230	-0.054	-0.036
1.598	13.652	0.047	1.284	0.888	0.927	2.997	2.571	0.109	0.072
1.222	13.984	0.051	1.271	0.881	0.916	2.817	1.967	0.034	0.031
0.844	14.314	0.055	1.263	0.879	0.906	2.751	3.365	0.095	0.053
0.470	14.646	0.059	1.253	0.874	0.897	2.212	3.021	0.133	0.102
0.096	14.976	0.063	1.251	0.876	0.892	2.210	2.075	0.071	0.079
-0.280	15.308	0.067	1.247	0.878	0.886	2.175	2.398	0.069	0.067
-0.654	15.640	0.071	1.236	0.873	0.875	2.199	2.962	0.097	0.076
-1.030	15.970	0.075	1.232	0.874	0.869	2.199	2.626	0.034	0.030
-1.406	16.300	0.079	1.225	0.870	0.863	2.416	2.115	0.109	0.110
-1.780	16.632	0.083	1.226	0.872	0.862	2.141	2.430	0.030	0.029
-2.154	16.962	0.086	1.216	0.870	0.850	3.547	2.113	0.103	0.070
-2.528	17.294	0.090	1.209	0.865	0.844	2.142	2.245	0.062	0.066
-2.904	17.626	0.094	1.206	0.867	0.839	2.093	2.913	0.016	0.014
-3.278	17.956	0.098	1.204	0.868	0.834	2.156	2.576	0.045	0.041
-3.652	18.288	0.102	1.197	0.864	0.828	2.227	2.305	0.026	0.026
-4.030	18.618	0.106	1.193	0.865	0.821	2.159	2.727	0.095	0.083
-4.406	18.948	0.110	1.194	0.867	0.820	2.046	2.067	0.078	0.094
-4.782	19.280	0.114	1.189	0.867	0.814	2.024	2.621	0.091	0.087
-5.156	19.610	0.118	1.177	0.860	0.804	2.385	2.292	0.094	0.088
-5.530	19.942	0.122	1.183	0.866	0.806	2.012	2.596	0.141	0.138
-5.902	20.272	0.126	1.175	0.861	0.800	2.016	2.538	0.031	0.031
-6.280	20.604	0.130	1.166	0.857	0.791	2.375	2.627	0.016	0.013
-6.652	20.934	0.134	1.167	0.861	0.787	2.074	2.280	0.089	0.097
-7.028	21.266	0.138	1.167	0.863	0.785	2.058	2.312	0.049	0.053
-7.402	21.596	0.141	1.159	0.861	0.775	2.010	2.449	0.124	0.129
-7.778	21.928	0.145	1.153	0.855	0.774	2.060	2.121	0.023	0.027
-8.154	22.260	0.149	1.157	0.859	0.776	2.047	2.324	0.126	0.135

Survey Number 30 (Station 6 boundary layer)									
x(mm)	y(mm)	d/c	W/Vref	U/Vref	V/Vref	Tu	Tv	Re stress	Cuv
29.968	29.730	0.008	1.248	1.083	0.620	9.357	5.352	0.796	0.081
29.708	30.158	0.012	1.394	1.203	0.705	6.139	2.854	0.180	0.053
29.452	30.588	0.016	1.411	1.219	0.711	2.514	2.189	0.166	0.154
29.194	31.016	0.020	1.401	1.211	0.705	2.916	1.950	0.066	0.059
28.936	31.446	0.024	1.389	1.201	0.699	3.166	1.883	0.068	0.058
28.680	31.874	0.028	1.385	1.198	0.695	2.696	2.015	0.089	0.084
28.424	32.304	0.031	1.381	1.194	0.695	2.441	2.192	0.120	0.115
28.168	32.734	0.035	1.376	1.190	0.690	2.896	2.160	0.122	0.100
27.908	33.162	0.039	1.373	1.189	0.687	2.318	2.278	0.083	0.080
27.652	33.592	0.043	1.369	1.184	0.687	2.283	2.012	-0.022	-0.025
27.396	34.020	0.047	1.362	1.179	0.682	2.359	2.237	0.036	0.035
27.140	34.448	0.051	1.353	1.171	0.677	2.413	2.168	0.027	0.027
26.882	34.878	0.055	1.355	1.175	0.676	2.413	2.467	0.062	0.053
26.624	35.306	0.059	1.341	1.161	0.672	2.719	2.263	0.037	0.031
26.370	35.736	0.063	1.341	1.161	0.671	2.463	2.254	0.147	0.136
26.110	36.164	0.067	1.333	1.154	0.668	2.229	2.329	0.084	0.082
25.854	36.594	0.071	1.322	1.144	0.663	2.584	2.005	0.060	0.060
25.598	37.022	0.075	1.325	1.148	0.661	2.623	2.258	0.118	0.102
25.338	37.452	0.079	1.321	1.144	0.660	2.623	2.292	0.091	0.077
25.084	37.880	0.083	1.317	1.141	0.657	2.102	2.427	0.089	0.090
24.824	38.310	0.086	1.312	1.136	0.655	2.076	2.145	0.055	0.063
24.572	38.738	0.090	1.302	1.128	0.651	2.062	2.124	0.090	0.105
24.312	39.168	0.094	1.299	1.126	0.648	2.110	2.384	0.070	0.071
24.054	39.596	0.098	1.297	1.124	0.647	2.524	2.135	0.084	0.080
23.798	40.026	0.102	1.296	1.123	0.646	2.327	2.667	0.055	0.045
23.540	40.454	0.106	1.288	1.115	0.644	2.562	2.091	0.089	0.085
23.284	40.884	0.110	1.284	1.112	0.641	2.069	2.115	0.006	0.007
23.028	41.314	0.114	1.273	1.103	0.635	2.585	2.575	0.080	0.062
22.768	41.742	0.118	1.275	1.103	0.638	2.448	2.263	0.074	0.068
22.514	42.170	0.122	1.267	1.097	0.634	2.086	2.238	0.104	0.114
22.256	42.600	0.126	1.264	1.094	0.632	2.483	2.220	0.105	0.098
21.998	43.030	0.130	1.258	1.089	0.629	3.178	2.176	0.159	0.118
21.740	43.458	0.134	1.253	1.085	0.626	2.098	2.692	0.045	0.041
21.484	43.886	0.138	1.250	1.083	0.624	2.387	2.169	0.041	0.041
21.228	44.316	0.141	1.245	1.078	0.623	2.123	2.442	0.031	0.030
20.972	44.744	0.145	1.239	1.073	0.619	2.559	2.373	0.084	0.071

Survey Number 31 (Station 7 boundary layer)									
x(mm)	y(mm)	d/c	W/Vref	U/Vref	V/Vref	Tu	Tv	Re stress	Cuv
60.848	41.164	0.006	0.970	0.961	0.131	13.892	5.099	-1.422	-0.103
60.774	41.658	0.010	1.222	1.202	0.218	10.884	10.615	0.208	0.009
60.698	42.152	0.014	1.331	1.314	0.210	3.912	2.771	0.008	0.004
60.624	42.648	0.018	1.331	1.314	0.215	2.795	1.757	0.012	0.013
60.546	43.142	0.022	1.328	1.310	0.219	2.731	1.550	0.044	0.053
60.474	43.638	0.026	1.330	1.312	0.222	2.473	1.609	0.093	0.120
60.398	44.132	0.030	1.313	1.294	0.225	2.745	1.826	-0.003	-0.003
60.322	44.628	0.033	1.307	1.287	0.229	2.740	1.727	0.014	0.015
60.248	45.122	0.037	1.310	1.290	0.231	2.883	2.288	-0.015	-0.012
60.174	45.618	0.041	1.297	1.275	0.235	2.672	1.684	-0.023	-0.026
60.096	46.114	0.045	1.296	1.274	0.235	2.235	1.727	-0.007	-0.009
60.024	46.608	0.049	1.294	1.273	0.237	2.279	1.867	0.026	0.031
59.948	47.102	0.053	1.278	1.254	0.244	2.398	1.756	0.028	0.034
59.872	47.598	0.057	1.280	1.257	0.242	2.343	1.816	0.035	0.042
59.798	48.092	0.061	1.259	1.235	0.246	3.354	1.863	-0.061	-0.050
59.724	48.588	0.065	1.260	1.235	0.250	2.911	2.014	-0.055	-0.048
59.650	49.082	0.069	1.254	1.229	0.251	3.120	1.939	-0.013	-0.011
59.572	49.578	0.073	1.251	1.225	0.255	2.369	1.862	-0.005	-0.006
59.498	50.072	0.077	1.255	1.230	0.253	2.187	1.801	0.052	0.068
59.424	50.568	0.081	1.238	1.211	0.257	2.152	1.846	0.013	0.017
59.346	51.062	0.085	1.230	1.203	0.256	2.252	1.801	0.071	0.090
59.274	51.558	0.089	1.227	1.200	0.259	2.765	1.975	0.066	0.062
59.200	52.052	0.092	1.214	1.186	0.262	2.382	2.087	0.001	0.001
59.122	52.548	0.096	1.221	1.193	0.261	2.380	1.904	0.072	0.081
59.046	53.042	0.100	1.212	1.183	0.264	2.643	2.062	0.057	0.053
58.974	53.538	0.104	1.203	1.174	0.265	2.758	1.884	0.051	0.050
58.896	54.034	0.108	1.199	1.169	0.267	2.568	1.971	-0.068	-0.069
58.822	54.528	0.112	1.197	1.167	0.267	2.376	1.946	0.018	0.020
58.746	55.022	0.116	1.188	1.157	0.272	2.351	1.952	-0.014	-0.016
58.672	55.518	0.120	1.184	1.152	0.273	2.381	2.076	-0.013	-0.013
58.598	56.014	0.124	1.181	1.150	0.272	2.479	1.992	-0.088	-0.092
58.522	56.508	0.128	1.182	1.150	0.271	2.236	2.082	0.115	0.127
58.448	57.002	0.132	1.172	1.139	0.274	2.122	1.984	0.005	0.006
58.372	57.498	0.136	1.166	1.132	0.278	2.725	1.940	-0.038	-0.037
58.298	57.992	0.140	1.157	1.123	0.276	2.108	2.355	-0.009	-0.009
58.222	58.488	0.144	1.151	1.116	0.279	2.207	2.052	0.075	0.085

Survey Number 32 (Station 8 boundary layer)									
x(mm)	y(mm)	d/c	W/ref	U/ref	V/ref	Tu	Tv	Re stress	Cuv
91.490	41.506	0.006	0.338	0.338	0.003	15.854	8.064	-3.631	-0.146
91.520	42.004	0.010	0.482	0.482	0.004	17.427	8.599	-5.551	-0.191
91.556	42.504	0.014	0.658	0.658	-0.011	18.455	8.691	-6.362	-0.204
91.586	43.002	0.018	0.836	0.836	-0.017	15.024	7.838	-5.171	-0.226
91.618	43.502	0.022	0.927	0.927	-0.006	13.710	6.607	-4.123	-0.234
91.654	44.002	0.026	1.020	1.020	-0.007	9.762	4.566	-1.977	-0.228
91.688	44.500	0.029	1.034	1.034	-0.001	12.907	3.912	-2.955	-0.301
91.720	44.998	0.033	1.052	1.052	-0.003	2.982	2.473	-0.157	-0.109
91.754	45.498	0.037	1.044	1.044	0.008	8.144	3.278	-2.173	-0.419
91.786	45.998	0.041	1.058	1.058	-0.002	2.413	1.855	-0.019	-0.022
91.820	46.496	0.045	1.053	1.052	0.015	2.647	2.157	-0.187	-0.168
91.850	46.994	0.049	1.051	1.051	0.024	2.654	2.945	-0.470	-0.310
91.884	47.494	0.053	1.051	1.051	0.013	2.437	2.880	-0.087	-0.064
91.918	47.992	0.057	1.055	1.055	0.010	2.596	1.916	0.062	0.064
91.948	48.492	0.061	1.050	1.050	0.017	2.361	2.066	-0.058	-0.061
91.984	48.992	0.065	1.046	1.046	0.031	2.397	2.149	-0.120	-0.120
92.016	49.490	0.069	1.045	1.045	0.032	2.288	2.169	-0.129	-0.134
92.050	49.988	0.073	1.039	1.039	0.039	2.485	3.294	-0.465	-0.292
92.082	50.488	0.077	1.040	1.039	0.046	2.318	2.373	-0.140	-0.131
92.116	50.988	0.081	1.045	1.044	0.046	2.282	2.301	0.016	0.016
92.150	51.486	0.084	1.044	1.044	0.040	2.151	2.660	-0.071	-0.064
92.182	51.984	0.088	1.042	1.041	0.053	2.718	4.183	-0.940	-0.426
92.218	52.484	0.092	1.040	1.039	0.048	2.198	2.758	0.020	0.017
92.248	52.984	0.096	1.039	1.038	0.043	2.205	1.807	0.013	0.017
92.282	53.482	0.100	1.035	1.034	0.047	2.197	2.027	-0.007	-0.008
92.314	53.982	0.104	1.037	1.035	0.061	2.199	3.169	-0.004	-0.003
92.344	54.480	0.108	1.032	1.030	0.065	2.156	2.138	-0.049	-0.054
92.380	54.978	0.112	1.033	1.031	0.068	2.225	2.494	-0.032	-0.029
92.412	55.478	0.116	1.031	1.029	0.066	2.172	2.580	-0.002	-0.002
92.446	55.978	0.120	1.032	1.031	0.060	1.994	2.479	0.060	0.062
92.480	56.476	0.124	1.033	1.031	0.065	2.154	2.363	0.021	0.021
92.510	56.974	0.128	1.028	1.026	0.067	2.078	3.119	0.033	0.026
92.544	57.474	0.132	1.024	1.022	0.073	2.157	2.245	-0.027	-0.028
92.578	57.972	0.136	1.024	1.021	0.069	2.113	2.547	0.133	0.128
92.610	58.472	0.140	1.024	1.022	0.075	2.108	2.249	0.099	0.108
92.646	58.970	0.143	1.020	1.017	0.083	2.189	2.946	0.077	0.062

Survey Number 33 (Station 9 boundary layer)									
x(mm)	y(mm)	d/c	W/Vref	U/Vref	V/Vref	Tu	Tv	Re stress	Cuv
115.880	39.832	0.006	0.229	0.226	0.033	16.563	11.974	-5.044	-0.131
115.920	40.330	0.010	0.314	0.313	-0.010	20.500	7.996	-8.095	-0.255
115.960	40.830	0.014	0.451	0.451	-0.019	20.327	8.400	-6.090	-0.184
115.996	41.328	0.018	0.568	0.568	-0.022	20.352	8.886	-8.310	-0.238
116.036	41.826	0.022	0.609	0.608	-0.021	21.089	9.059	-8.876	-0.240
116.074	42.326	0.026	0.663	0.663	-0.020	21.064	8.704	-9.407	-0.265
116.114	42.826	0.029	0.755	0.755	-0.024	20.417	8.513	-9.374	-0.279
116.152	43.324	0.033	0.838	0.837	-0.028	13.934	7.673	-5.280	-0.255
116.192	43.824	0.037	0.899	0.898	-0.027	9.192	6.544	-3.520	-0.303
116.228	44.322	0.041	0.919	0.918	-0.033	9.276	5.404	-2.163	-0.223
116.272	44.820	0.045	0.927	0.926	-0.020	8.613	5.464	-2.108	-0.232
116.306	45.320	0.049	0.949	0.949	-0.026	4.141	4.111	0.154	0.047
116.348	45.820	0.053	0.952	0.952	-0.015	3.544	4.887	-0.464	-0.139
116.386	46.318	0.057	0.955	0.954	-0.033	2.676	2.441	0.041	0.032
116.426	46.816	0.061	0.953	0.952	-0.030	2.537	2.269	0.109	0.098
116.464	47.316	0.065	0.958	0.958	-0.016	2.765	2.637	-0.022	-0.016
116.504	47.816	0.069	0.955	0.955	-0.020	2.385	3.366	0.137	0.088
116.544	48.314	0.073	0.954	0.954	-0.020	2.398	3.864	0.044	0.025
116.582	48.814	0.077	0.951	0.951	-0.018	2.182	1.871	0.030	0.038
116.620	49.312	0.081	0.955	0.955	-0.009	2.518	2.278	0.171	0.154
116.660	49.810	0.085	0.953	0.953	-0.010	2.208	2.962	0.150	0.119
116.698	50.310	0.088	0.950	0.950	-0.010	2.185	2.088	0.099	0.112
116.738	50.810	0.092	0.957	0.957	-0.004	2.392	2.381	0.105	0.095
116.776	51.308	0.096	0.951	0.951	-0.001	2.454	2.772	0.129	0.098
116.816	51.806	0.100	0.952	0.952	-0.002	2.136	2.060	0.129	0.152
116.854	52.306	0.104	0.949	0.949	0.001	2.327	2.305	0.237	0.229
116.894	52.804	0.108	0.949	0.949	0.001	2.179	1.974	0.133	0.160
116.936	53.304	0.112	0.948	0.948	0.003	2.188	1.907	0.121	0.150
116.972	53.804	0.116	0.947	0.947	0.008	2.102	1.868	0.140	0.185
117.012	54.302	0.120	0.947	0.947	0.009	2.268	2.199	0.079	0.082
117.050	54.800	0.124	0.948	0.948	0.010	2.236	1.900	0.198	0.241
117.088	55.300	0.128	0.945	0.945	0.010	2.497	1.757	0.115	0.135
117.126	55.800	0.132	0.948	0.947	0.020	2.220	3.522	0.234	0.155
117.166	56.298	0.136	0.947	0.947	0.017	2.655	2.389	0.272	0.222
117.204	56.796	0.140	0.943	0.943	0.014	2.191	2.253	0.147	0.154
117.246	57.296	0.144	0.946	0.946	0.018	2.444	1.713	0.156	0.193
117.284	57.794	0.147	0.946	0.946	0.027	2.165	2.350	0.176	0.179
117.322	58.294	0.151	0.941	0.941	0.021	2.059	1.801	0.107	0.149
117.362	58.794	0.155	0.939	0.938	0.021	2.135	2.502	0.092	0.089
117.400	59.292	0.159	0.939	0.938	0.025	2.124	1.747	0.138	0.193
117.440	59.790	0.163	0.942	0.941	0.029	2.006	1.795	0.152	0.218
117.480	60.290	0.167	0.939	0.939	0.029	2.298	1.795	0.158	0.198
117.518	60.790	0.171	0.942	0.941	0.037	2.103	1.939	0.160	0.203
117.558	61.288	0.175	0.937	0.936	0.033	2.177	2.737	0.148	0.128
117.596	61.788	0.179	0.939	0.939	0.037	2.153	1.791	0.186	0.249
117.636	62.286	0.183	0.940	0.939	0.040	2.177	1.921	0.272	0.336

Survey Number 34 (Station 13 wake)									
x (mm)	z (mm)	y/s	W/Vref	U/Vref	V/Vref	Tu	Tv	Re stress	Cuv
146.300	-14.220	-0.333	0.900	0.894	0.106	2.058	2.954	0.173	0.145
146.302	-9.220	-0.301	0.900	0.894	0.104	2.005	2.019	0.171	0.216
146.298	-4.220	-0.268	0.902	0.896	0.102	2.033	2.084	0.188	0.227
146.300	0.780	-0.235	0.901	0.896	0.099	2.138	3.047	0.185	0.145
146.300	5.780	-0.202	0.899	0.893	0.100	2.183	2.850	0.241	0.198
146.300	10.780	-0.169	0.895	0.890	0.090	2.152	2.323	0.341	0.349
146.300	15.780	-0.136	0.892	0.888	0.090	2.207	2.543	0.332	0.302
146.300	20.780	-0.104	0.891	0.886	0.094	2.256	2.729	0.318	0.264
146.300	25.780	-0.071	0.887	0.882	0.091	2.602	3.163	0.278	0.173
146.300	30.780	-0.038	0.887	0.881	0.101	5.138	5.717	0.628	0.109
146.300	35.780	-0.005	0.743	0.727	0.156	15.802	13.218	8.710	0.213
146.300	40.782	0.028	0.309	0.286	0.115	15.687	19.870	13.410	0.220
146.298	45.780	0.060	0.540	0.540	0.018	29.541	14.882	-23.707	-0.275
146.300	50.782	0.093	0.822	0.822	0.013	15.838	8.643	-5.348	-0.199
146.300	55.780	0.126	0.878	0.877	0.029	8.006	5.919	-1.867	-0.201
146.300	60.780	0.159	0.896	0.895	0.041	3.591	3.543	-0.335	-0.134
146.300	65.780	0.192	0.899	0.897	0.048	2.452	2.188	0.032	0.030
146.300	70.780	0.224	0.899	0.897	0.060	2.354	2.058	0.181	0.191
146.300	75.780	0.257	0.895	0.892	0.064	2.254	1.936	0.167	0.196
146.300	80.780	0.290	0.893	0.890	0.072	1.952	1.877	0.123	0.171
146.300	85.780	0.323	0.889	0.886	0.076	2.045	1.705	0.148	0.217
146.300	90.780	0.356	0.890	0.887	0.083	2.024	1.759	0.138	0.198
146.300	95.780	0.388	0.890	0.886	0.081	2.199	1.695	0.184	0.252
146.300	100.780	0.421	0.892	0.888	0.084	2.061	1.780	0.145	0.202
146.300	105.780	0.454	0.894	0.889	0.089	2.113	1.769	0.190	0.259
146.300	110.780	0.487	0.891	0.886	0.091	2.114	1.735	0.180	0.250
146.300	115.780	0.520	0.887	0.882	0.093	2.017	2.448	0.217	0.224
146.300	120.780	0.552	0.883	0.878	0.092	1.873	1.670	0.108	0.176
146.300	125.780	0.585	0.883	0.878	0.092	1.935	1.662	0.115	0.182
146.300	130.780	0.618	0.880	0.875	0.088	1.807	1.764	0.114	0.182
146.300	135.780	0.651	0.880	0.876	0.087	1.786	1.764	0.156	0.253
146.300	140.780	0.684	0.881	0.877	0.080	1.998	1.916	0.154	0.206
146.300	145.780	0.717	0.881	0.878	0.075	2.025	2.106	0.202	0.242
146.300	150.780	0.749	0.879	0.877	0.070	2.001	1.981	0.222	0.286
146.300	155.780	0.782	0.880	0.878	0.064	1.900	2.028	0.232	0.308
146.300	160.780	0.815	0.878	0.876	0.059	1.867	2.042	0.194	0.260
146.300	165.780	0.848	0.875	0.874	0.052	1.966	2.187	0.225	0.268
146.300	170.780	0.881	0.873	0.872	0.045	1.819	2.099	0.182	0.244
146.300	175.780	0.913	0.870	0.870	0.038	1.813	2.082	0.173	0.233
146.300	180.780	0.946	0.874	0.873	0.035	2.063	2.716	0.100	0.091
146.300	185.780	0.979	0.841	0.840	0.056	7.939	6.835	0.592	0.056
146.300	190.780	1.012	0.499	0.496	0.053	11.750	12.714	-0.285	-0.010
146.300	195.780	1.045	0.843	0.843	0.000	7.375	6.029	-1.544	-0.177
146.298	200.780	1.077	0.892	0.892	0.007	2.383	1.757	0.062	0.075
146.300	205.780	1.110	0.901	0.901	0.016	2.187	1.467	0.076	0.121
146.300	210.780	1.143	0.906	0.906	0.027	2.057	1.461	0.076	0.129
146.300	215.780	1.176	0.911	0.910	0.037	2.020	1.525	0.108	0.179
146.300	220.780	1.209	0.914	0.913	0.046	1.913	1.476	0.054	0.097
146.298	225.780	1.241	0.913	0.912	0.053	2.012	1.471	0.075	0.129
146.300	230.780	1.274	0.914	0.912	0.060	2.284	1.500	0.109	0.163
146.300	235.780	1.307	0.916	0.914	0.067	1.965	1.604	0.061	0.099
146.300	240.780	1.340	0.914	0.911	0.074	1.960	1.496	0.092	0.161

APPENDIX B. REFERENCE VELOCITY INPUT AND OUTPUT DATA FILES

FORTRAN INPUT FILE "CALIB1"

REFERENCE CONDITIONS FOR EACH RUN

AMBIENT PRESSURE	PLENUM PRESSURE	PLENUM TEMPERATURE	RUN NAME
INCHES MERCURY	INCHES WATER	DEGREES CELCIUS	

29.8070	12.0000	26.6667	1027bs7
29.8478	11.8000	22.2222	1031bs6
29.8478	11.9000	22.2222	1031bs8
29.9699	12.0000	22.2222	1102bs75
29.9699	11.8500	22.2222	1102bs8
29.9500	12.0000	21.1111	0108s1a
29.9500	12.0500	21.1111	0108s2a
30.0510	12.0000	22.7780	0109s3a
30.1124	12.0500	23.3333	0110s4a
30.1328	11.9500	23.3333	0110s13a
30.1328	12.0500	23.3333	0110s12a
30.1330	12.1500	19.4440	0114s4a
30.1330	11.9500	20.0000	0114s11a
30.1330	11.9500	20.0000	0114s10a
30.1530	11.9000	21.6666	0115s5a
30.1530	12.0000	22.2222	0115s6a
30.1530	12.0000	22.2222	0115s7a
30.1530	12.0000	22.2222	0115s8a
30.1530	12.0500	22.2222	0115s9a
29.7660	11.8500	22.2222	0116bs5a
29.7660	12.0500	22.7778	0116bs6a
29.8070	12.1000	22.7778	0116bs7a
29.8070	12.1000	23.3333	0116bs8a
29.8070	12.1000	23.3333	0116bs9a
30.2142	12.1000	20.5556	0120bs9a
30.1328	12.0000	21.6667	0120s11a
30.1328	12.1500	22.2222	0120s4a
30.0921	11.9500	21.1111	0120s1a
30.1735	11.9500	17.7778	0122s8a
30.1735	12.1000	18.3333	0122bs8a
30.2142	12.0500	18.3333	0123s11a
29.9699	01.7500	16.6667	0203bs5a
29.9699	01.7500	16.6667	0203bs6a
29.9699	01.7300	16.6667	0203bs7a
29.9699	01.7300	16.6667	0203bs8a
29.9699	01.4900	16.6667	0203bs9a
29.9292	04.0000	18.8889	0203bs9b
29.9292	04.0000	20.0000	0203bs8b
29.9292	04.0000	21.1111	0203bs7b
29.9292	04.0000	21.6667	0203bs6b

29.9292	04.0000	22.2222	0203bs5b_____
29.9699	01.5200	19.4444	0210s1a_____
29.9699	01.5200	19.4444	0210s2a_____
29.9699	01.5200	19.4444	0210s3a_____
29.9699	01.5200	19.4444	0210s11a_____
29.9699	01.5200	19.4444	0210s12a_____
29.9699	01.5200	19.4444	0210s13a_____
30.0514	04.0000	22.7778	0213s1a_____
30.0514	03.9800	23.8889	0213s2a_____
30.0514	04.0000	25.0000	0213s3a_____
30.0514	03.9800	25.5556	0213s11a_____
30.0514	03.9600	26.1111	0213s12a_____
30.0514	03.9600	26.6667	0213s13a_____
29.8274	01.2500	18.8889	0303s10a_____
29.8274	03.5300	20.0000	0303s10b_____
29.9903	01.2900	17.7778	0319bs7a_____
29.9903	01.2800	19.4444	0319bs75_____
29.9292	01.2700	18.3333	0321BS77_____
29.9292	01.2500	18.3333	0321BS72_____

FORTRAN OUTPUT FILE "CALIB.OUT"

EXPERIMENT NUMBER	REFERENCE VELOCITY	NAME
-------------------	--------------------	------

1	76.5357	1027bs7_____
2	75.2889	1031bs6_____
3	75.6026	1031bs8_____
4	75.7625	1102bs75_____
5	75.6446	0108s1a_____
6	75.7328	0109s3a_____
7	75.5467	0110s13a_____
8	75.1206	0114s10a_____
9	75.1538	0115s5a_____
10	75.5354	0115s8a_____
11	75.5480	0116bs5a_____
12	76.3493	0116bs7a_____
13	75.5552	0120bs9a_____
14	75.3132	0120s1a_____
15	29.4427	0203bs5a_____
16	29.4427	0203bs6a_____
17	29.2835	0203bs7a_____
18	29.2835	0203bs8a_____
19	27.3011	0203bs9a_____
20	43.9813	0203bs9b_____
21	44.0649	0203bs8b_____
22	44.1483	0203bs7b_____
23	44.1900	0203bs6b_____
24	44.2316	0203bs5b_____

25	27.6884	0210s1a_____
26	27.6884	0210s3a_____
27	27.6884	0210s13a_____
28	44.1855	0213s1a_____
29	44.3511	0213s3a_____
30	44.2581	0213s13a_____
31	25.5721	0319bs7a_____
32	25.5531	0319bs75_____
33	25.4362	0321BS77_____
34	25.2504	0321BS72_____

APPENDIX C. INVESTIGATION AT DESIGN INCIDENCE

A preliminary investigation at design incidence was performed in the vicinity of the blade mid-chord to confirm the initiation of flow separation at station 7 as reported in Reference 3.

A. FLOW VISUALIZATION

A laser-sheet flow visualization of the mid span flow was photographed through the acrylic window using a 300 milli-Watt argon laser and a hand-held VHS camera. Reference 7 contains a description of the laser-sheet setup. The cascade was run at a plenum pressure of 305 mm (12 inches) H₂O, corresponding to a Reynolds number of 640,000. The filming was performed at night to reduce glare and optimize the flow field image contrast. Analysis of the video at normal and slow speeds showed no indications of flow separation.

Further flow visualization via dye injection was performed by injecting dye through static pressure ports 11, 12 and 13 (Figure 3) in the vicinity of stations 6, 7 and 8 on blade 6 (Figure 4). The resulting blade surface stream patterns were visually observed through the acrylic window at the Reynolds number of 640,000. Again, no indications of flow separation were noted.

B. LDV MEASUREMENTS

LDV measurements were repeated at station 7 for comparison with previous measurements. In addition, boundary layer surveys were performed at stations 6 and 8 on the blade suction side as well as at station 7.5 (corresponding to $0.67 C_{ac}$) in an attempt to capture additional indications of flow separation.

The station 7 boundary layer profiles, shown in Figure 37a, matched those previously recorded by Hansen (Figure 37b) [Ref. 3]. The results indicated a large flat region in the velocity profiles throughout the apparent boundary layer. The station 7.5

boundary layer profiles, shown in Figure 38, did not give any indication of separated flow. Due to the absence of a plateau type perturbation on the previously recorded C_p distribution (defined in chapter III A), as would be associated with a separated flow region [Ref. 9], it was concluded that the velocity ratio profiles alone did not lend credence to the presence of separated flow. The station 6 and station 8 boundary layer results are shown in Figures 39 and 40, respectively. Neither boundary layer profile gave any indications of separated flow.

A possible explanation for the anomaly at station 7 is that the LDV measurements were contaminated by reflections from the brass shims which had been inserted between the blades and the far end wall. The shims had been inserted so as to ensure that the blades were perpendicular to the end walls. This anomaly in the measurements was not present just on blade number 3, but was also present in measurements performed on blade number 4.

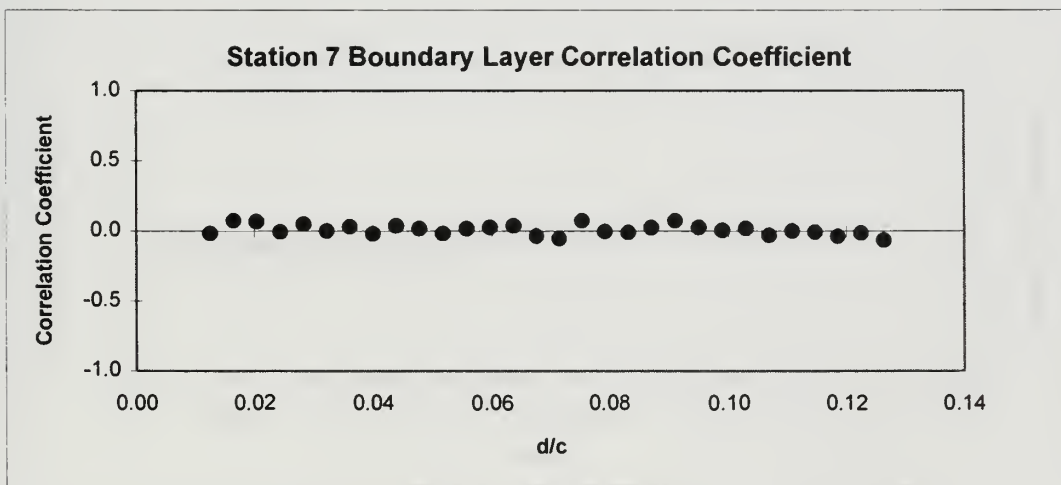
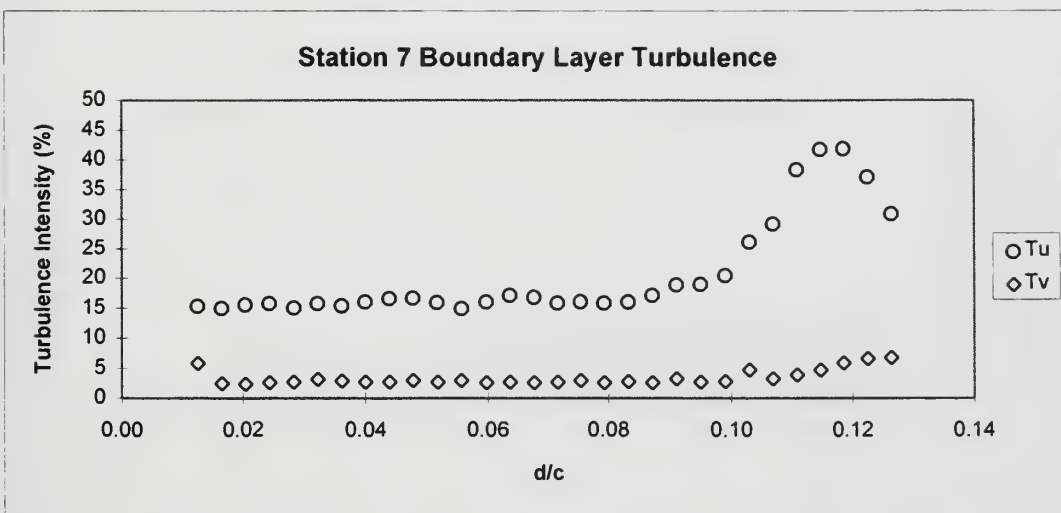
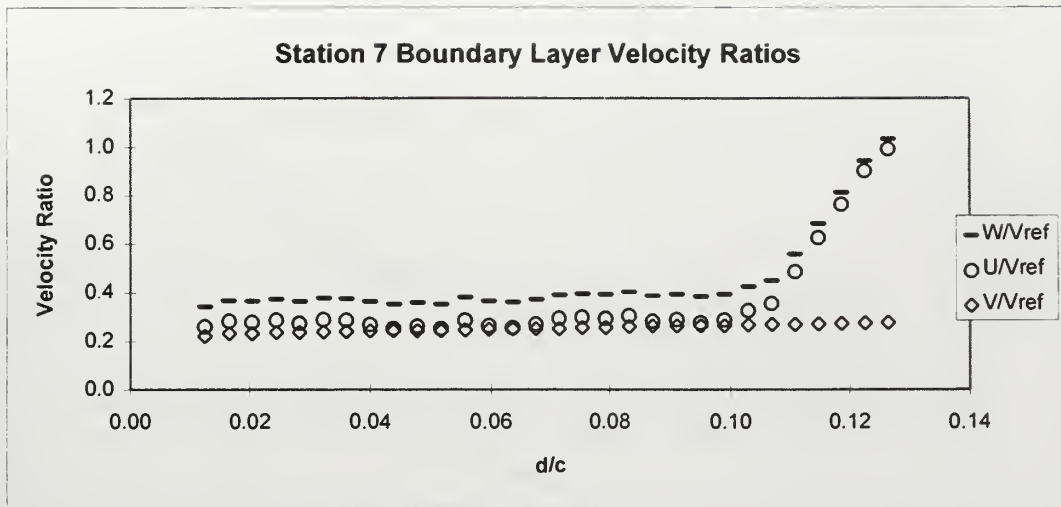


Figure 37a. Station 7 Boundary Layer Survey Results at Design Incidence.
(Present Study)

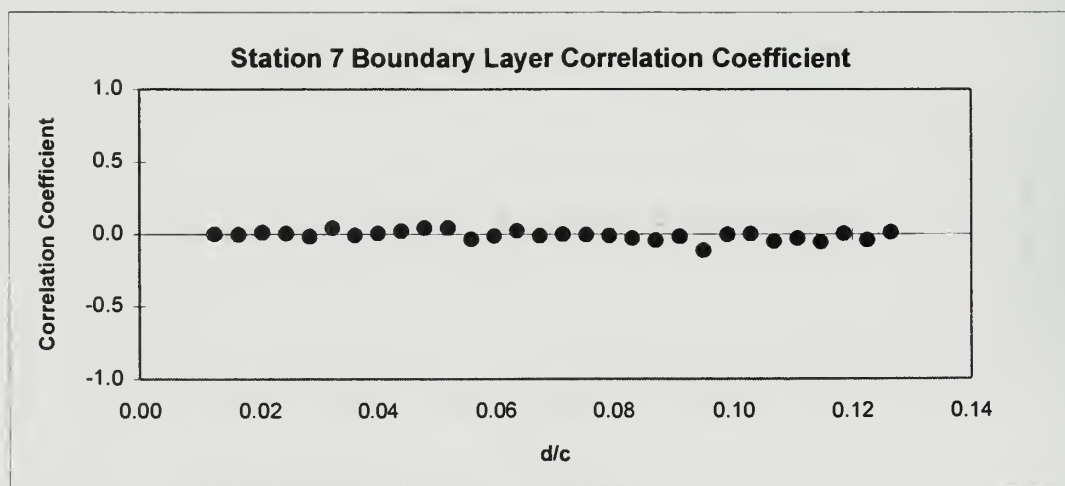
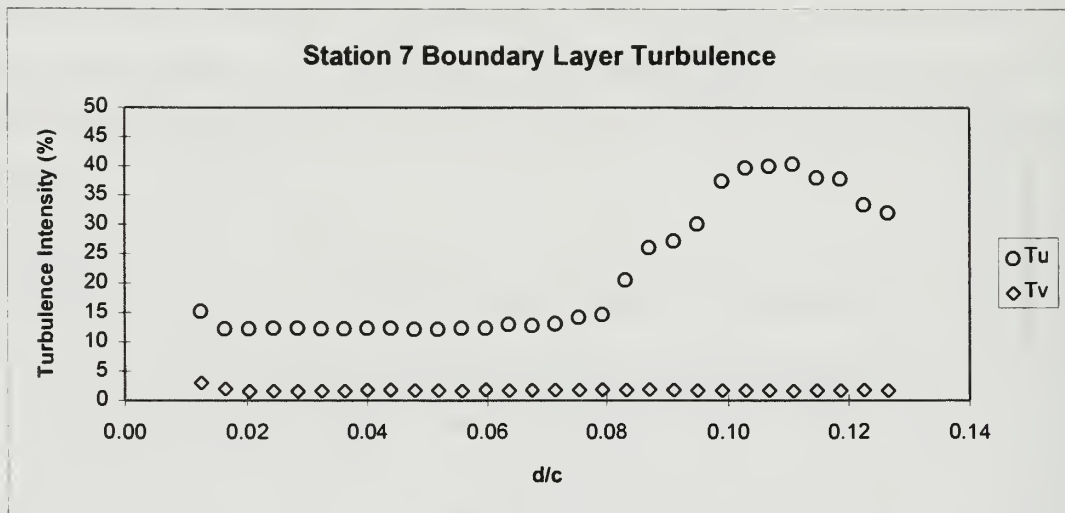
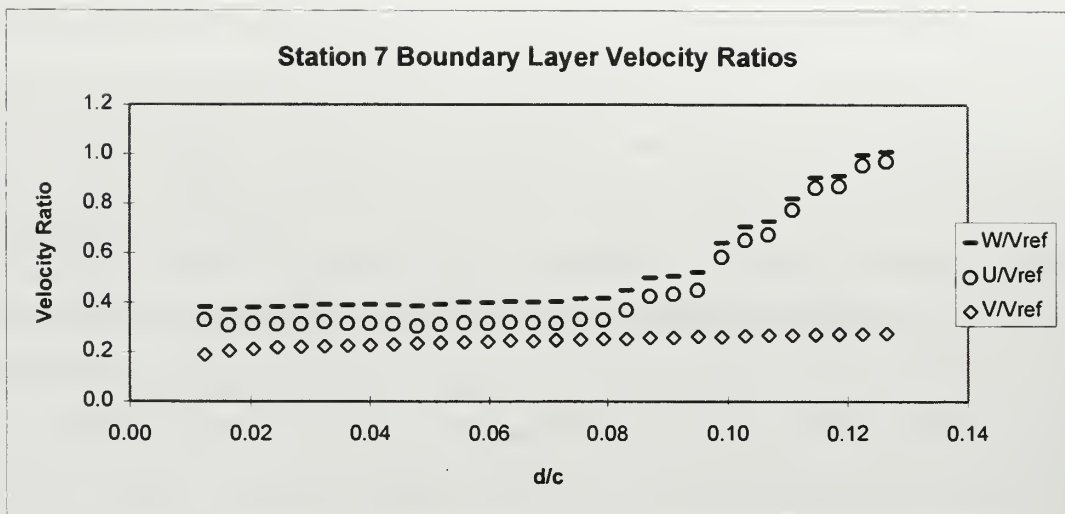


Figure 37b. Station 7 Boundary Layer Survey Results at Design Incidence.
(From Ref. 3)

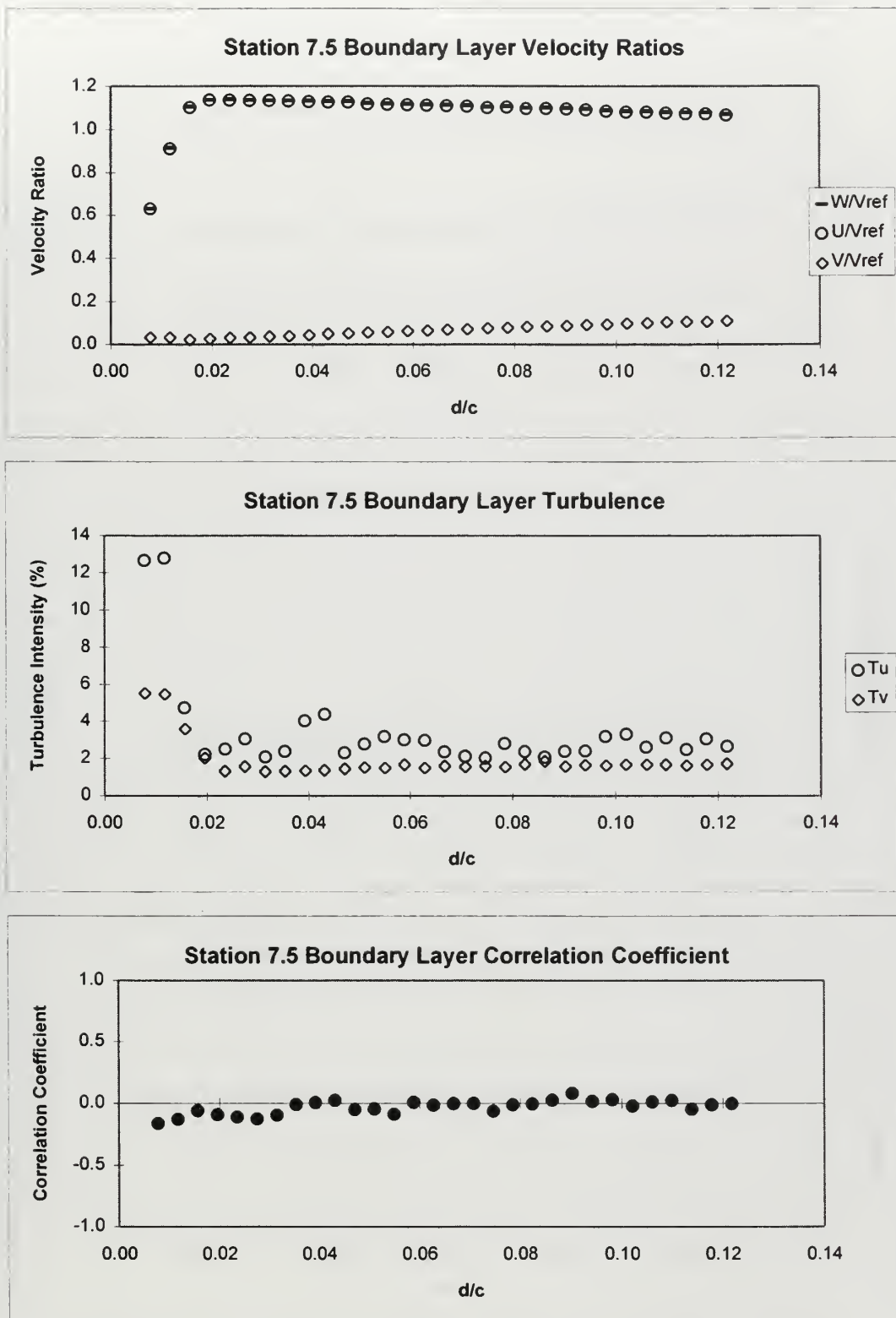


Figure 38. Station 7.5 Boundary Layer Survey Results at Design Incidence.

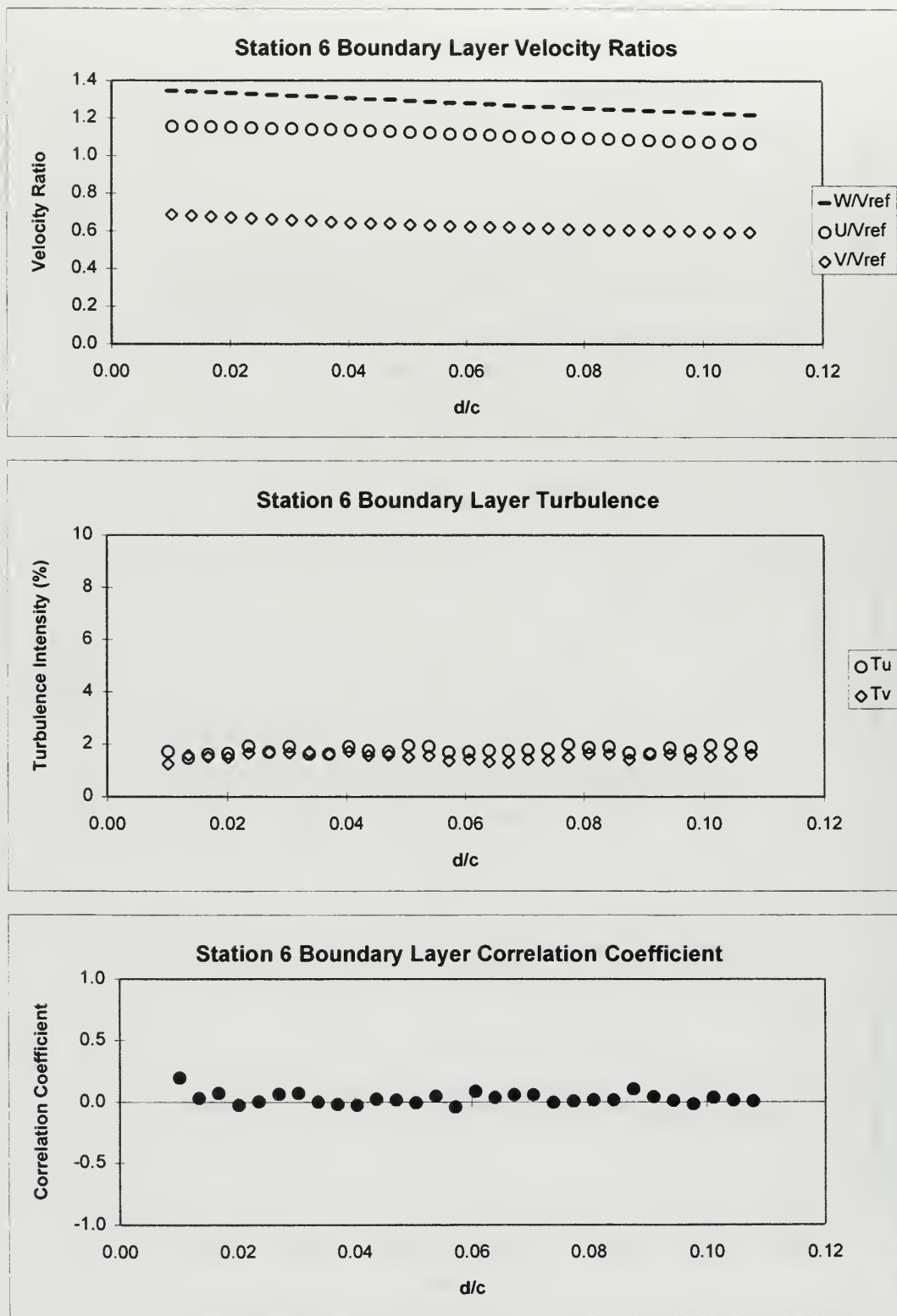


Figure 39. Station 6 Boundary Layer Survey Results at Design Incidence.

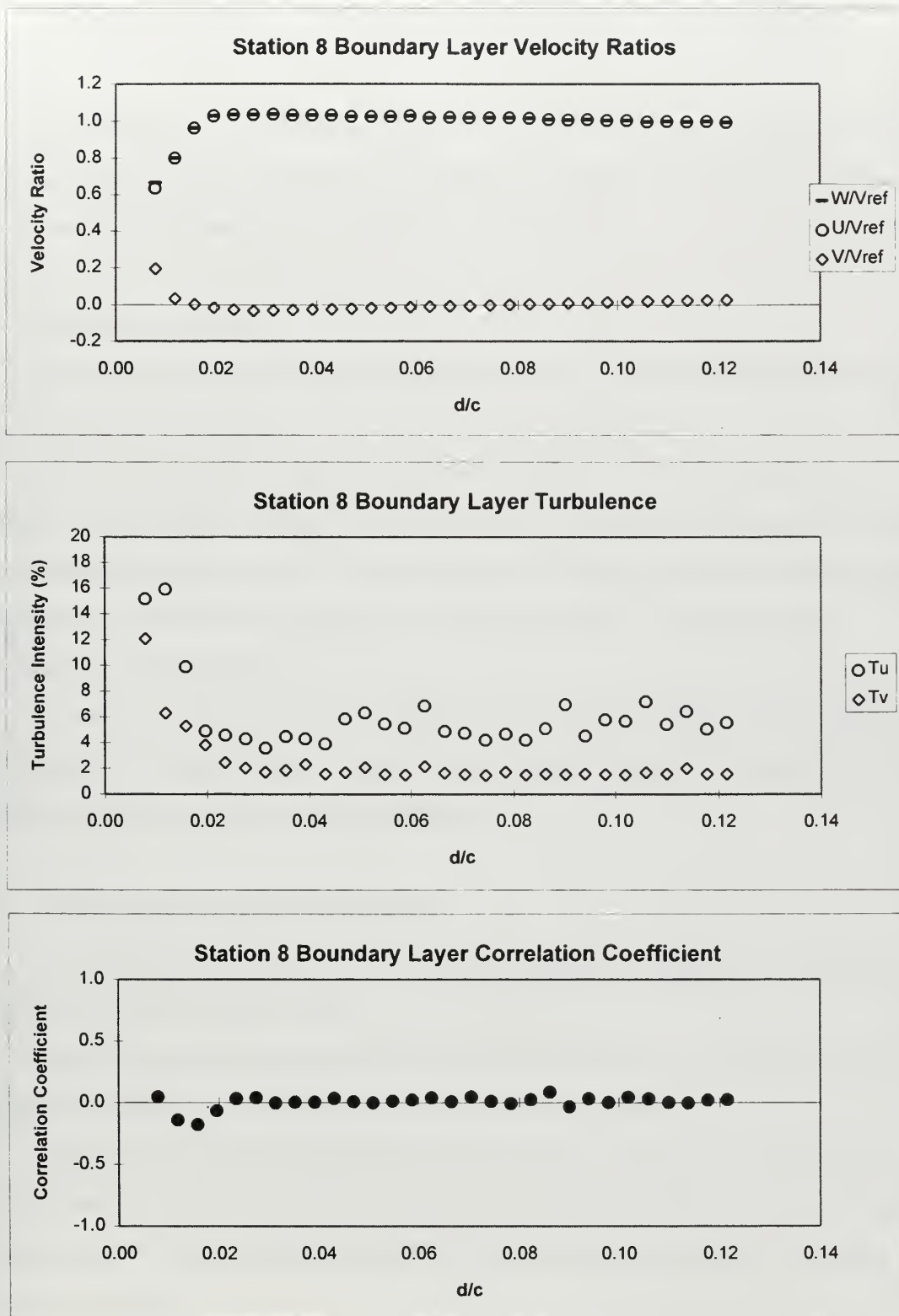


Figure 40. Station 8 Boundary Layer Survey Results at Design Incidence.

APPENDIX D. LDV MEASUREMENTS AT $Re=380,000$

The surface flow visualization indicated two dimensional flow along most of the bladespan section. LDV surveys were performed to characterize the behavior of the separation region as compared to the low Reynolds number.

A. INLET SURVEYS

Inlet surveys were performed at stations 1, 2 and 3. The station 1 and 3 surveys are discussed and compared to those at the slow tunnel setting.

Station 1 inlet survey results are shown in Figure 41. The velocity profiles matched those at the slow setting. Both the axial and tangential turbulence profiles were nearly steady between 2 and 3%. The decrease in the tangential turbulence from the slow setting was expected due to the increase in Reynolds number. The correlation coefficients remained below 0.1.

Station 3 results are shown in Figure 42. The velocity profiles matched well with those at the slow tunnel setting. A slight decrease in the turbulence was again noted, and the correlation coefficients remained below 0.2.

B. BOUNDARY LAYER SURVEYS

Boundary layer surveys were performed at stations 5 through 9 for comparison with those at the slow tunnel setting.

Station 5 boundary layer results are shown in Figure 43. The boundary layer profiles matched nearly identically with those at the slow setting.

Station 6 boundary layer results are shown in Figure 44. The boundary layer velocity profiles indicated that the boundary layer had grown slightly with the increase in Reynolds number. The turbulence had also increased slightly over that at the lower Reynolds number

Station 7 boundary layer results are shown in Figure 45. The boundary layer thickness was nearly the same as that of the slow setting. The velocity gradient was less steep and the peak turbulence less than at the lower Reynolds number.

Station 8 boundary layer results are shown in Figure 46. The boundary layer was thinner and the turbulence slightly less than at the lower Reynolds number. The general shape of the profiles indicated fully turbulent attached flow at this position.

Station 9 boundary layer results are shown in Figure 47. As at station 8, the boundary layer was thinner than at the lower Reynolds number; however, the turbulence level was slightly higher.

In general, the boundary layer profiles suggested transition from laminar to fully turbulent flow in the region between stations 7 and 8, which was similar to the results at the lower Reynolds number. Additional LDV surveys would more fully characterize the separation bubble, as were performed at the lower Reynolds number. However, both the C_p distribution and surface flow visualization confirmed that the separation point has moved downstream and the separation region had decreased in size as a result of increased Reynolds number. The surface flow visualization further indicated transitional vice laminar separation with the increase in Reynolds number.

C. WAKE SURVEYS

Wake surveys were performed at stations 11, 12 and 13. The station 13 farfield wake results are shown in Figure 48. The velocity profiles were uniform in the freestream, with depressions in the vicinity of the blade trailing edge position. The turbulence profiles were also relatively constant in the freestream, ranging between 2 and 3%, with peaks of 30 and 20% for the axial and tangential turbulence, respectively, at the trailing edge position of blade 3. The turbulence was slightly lower for blade 4 than blade 3, which indicated a slight degradation in periodicity.

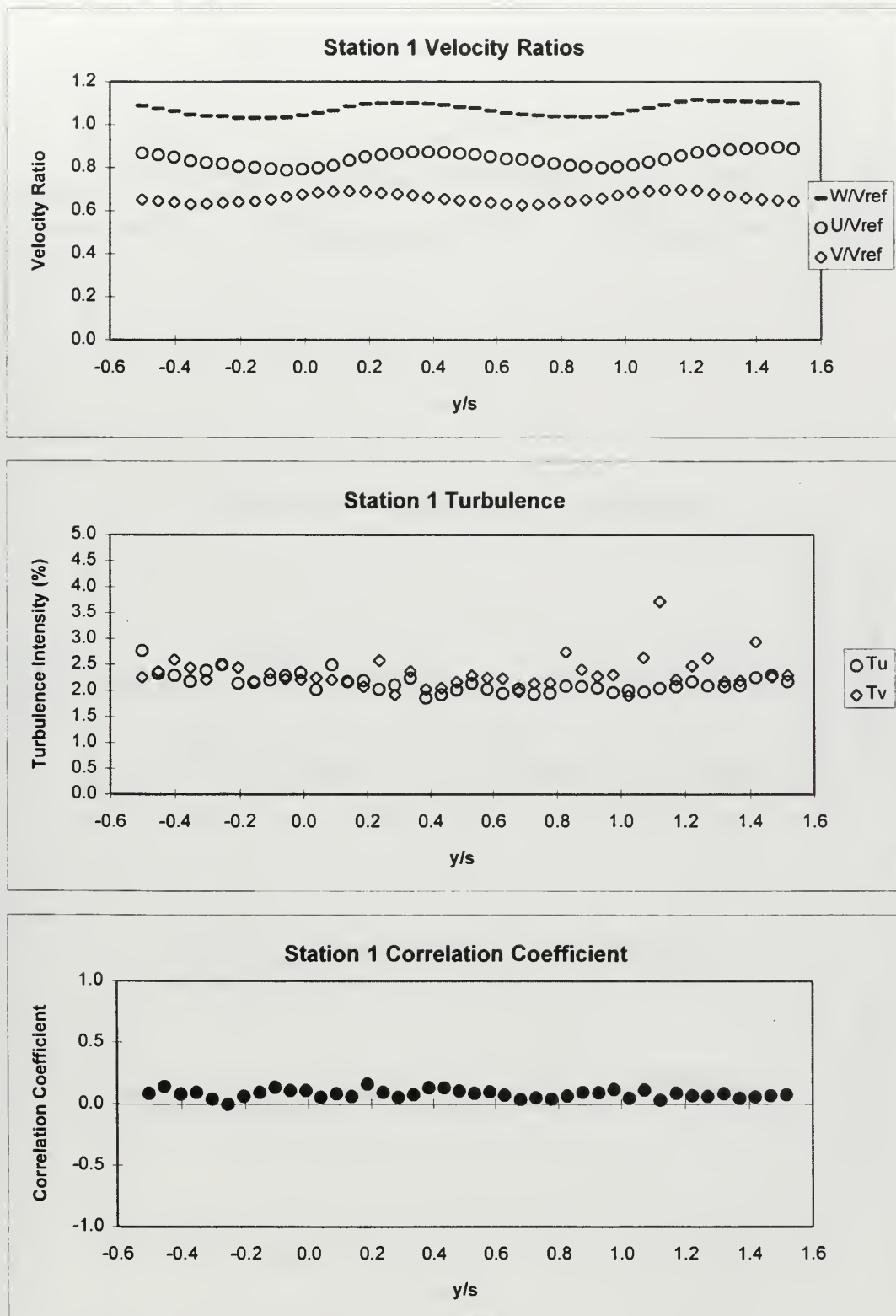


Figure 41. Station 1 Inlet Survey Results at $Re=380,000$.

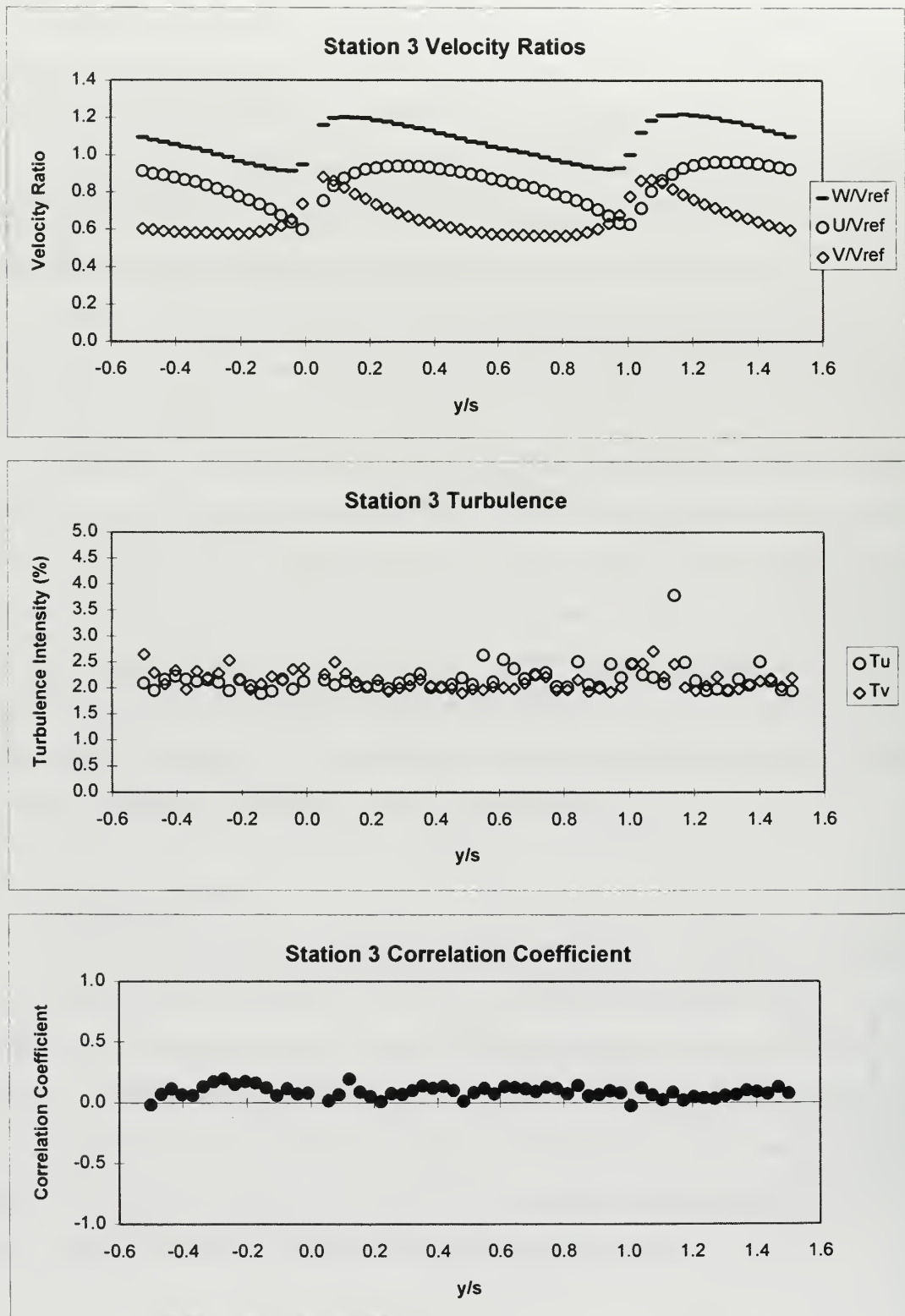


Figure 42. Station 3 Inlet Survey Results at $Re=380,000$.

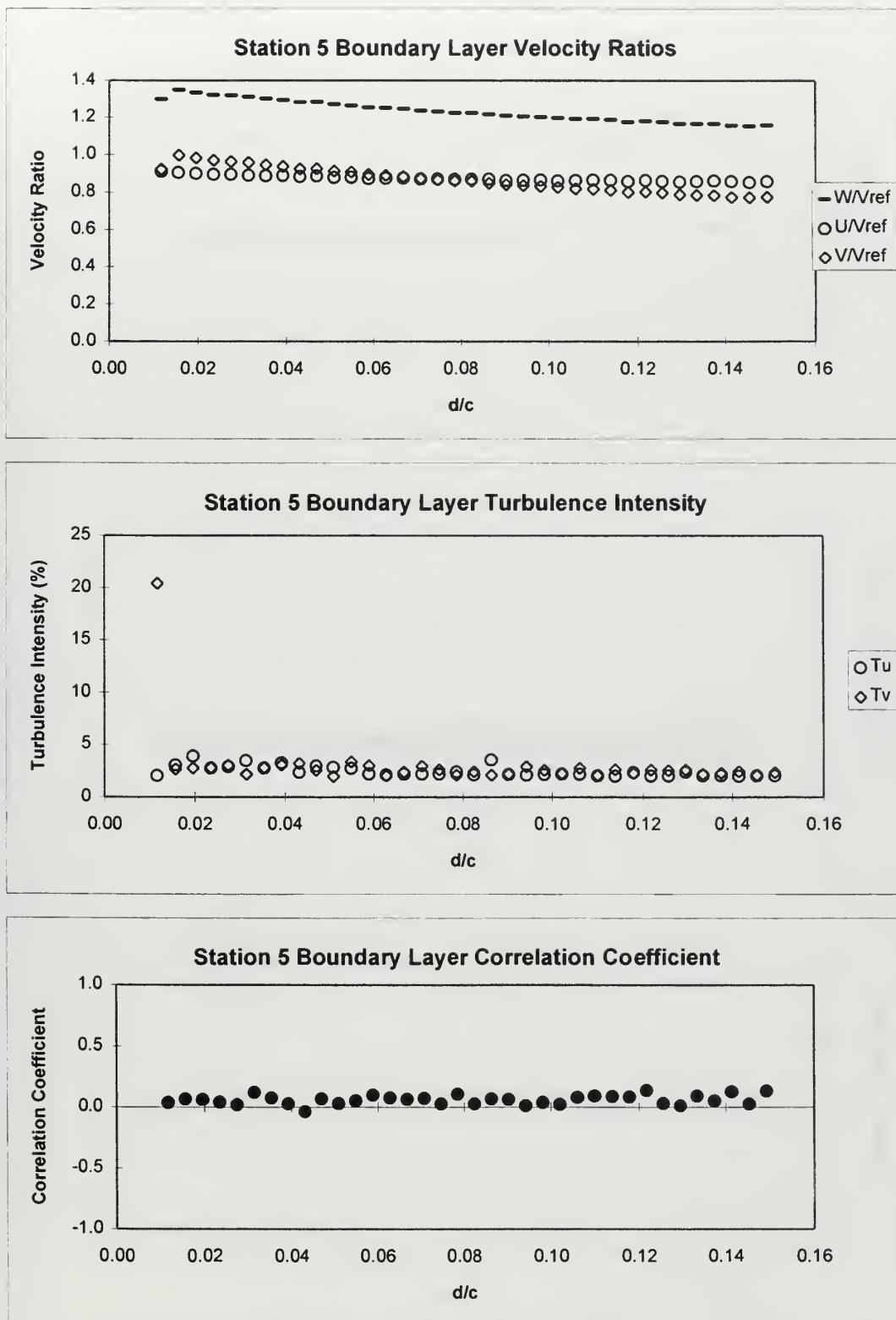


Figure 43. Station 5 Boundary Layer Survey Results at $Re=380,000$.

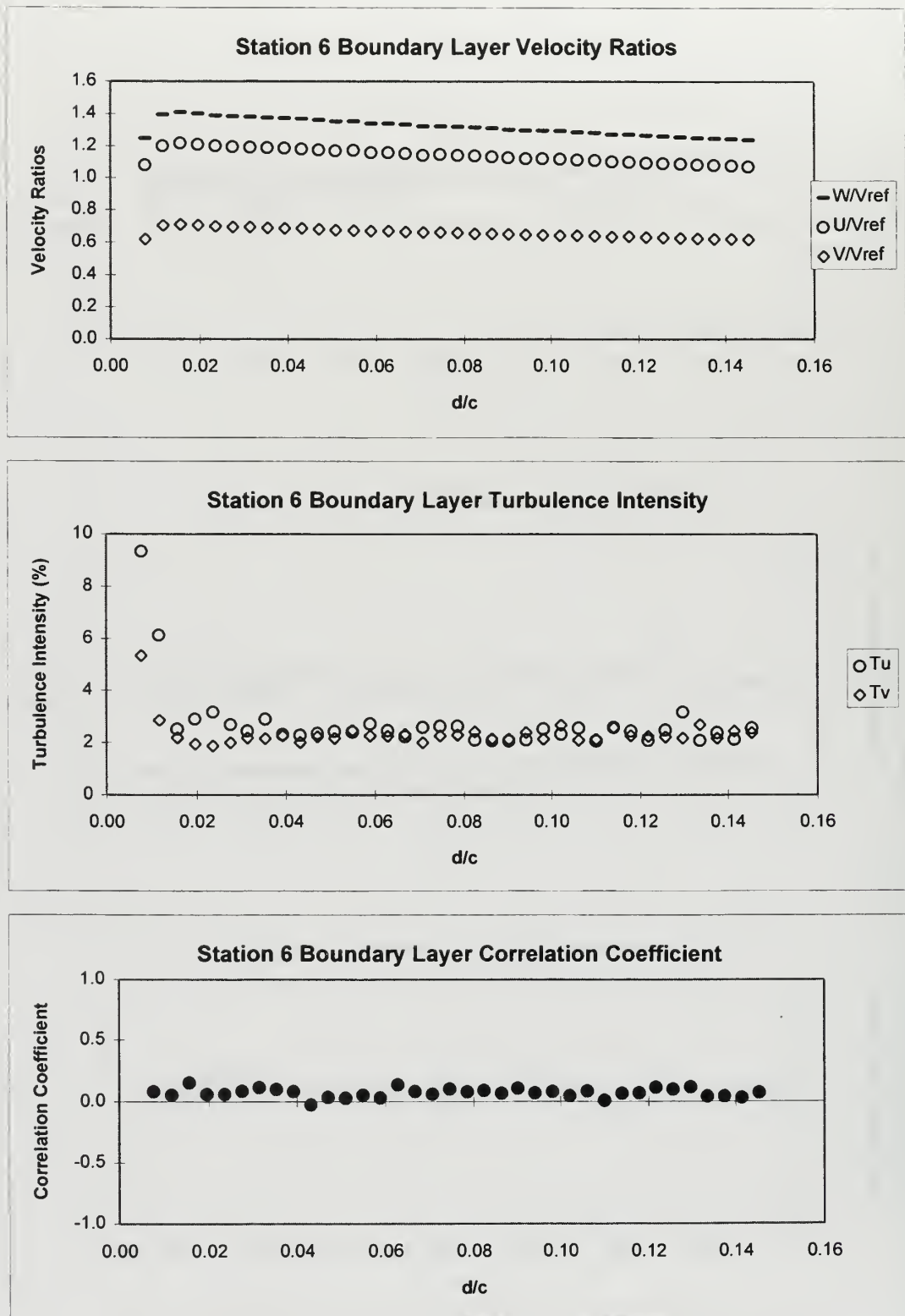


Figure 44. Station 6 Boundary Layer Survey Results at $Re=380,000$.

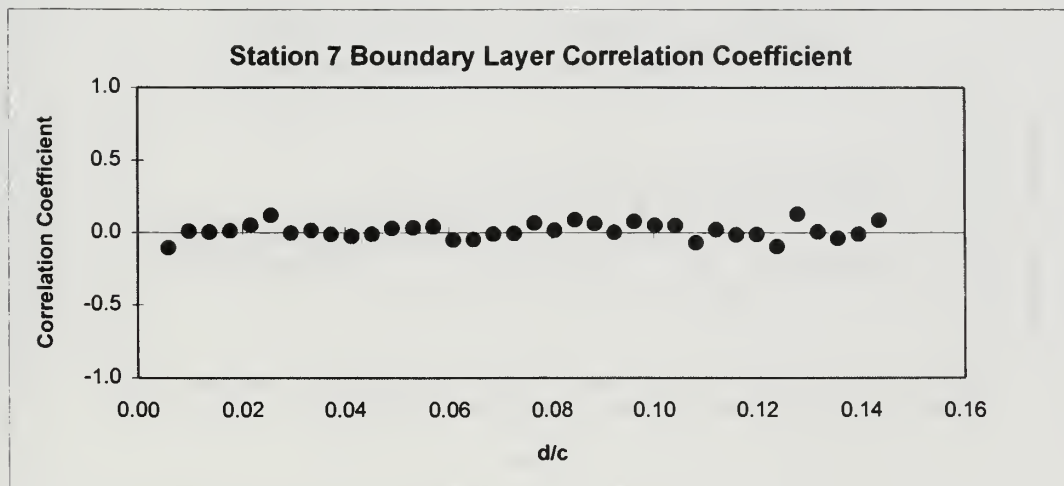
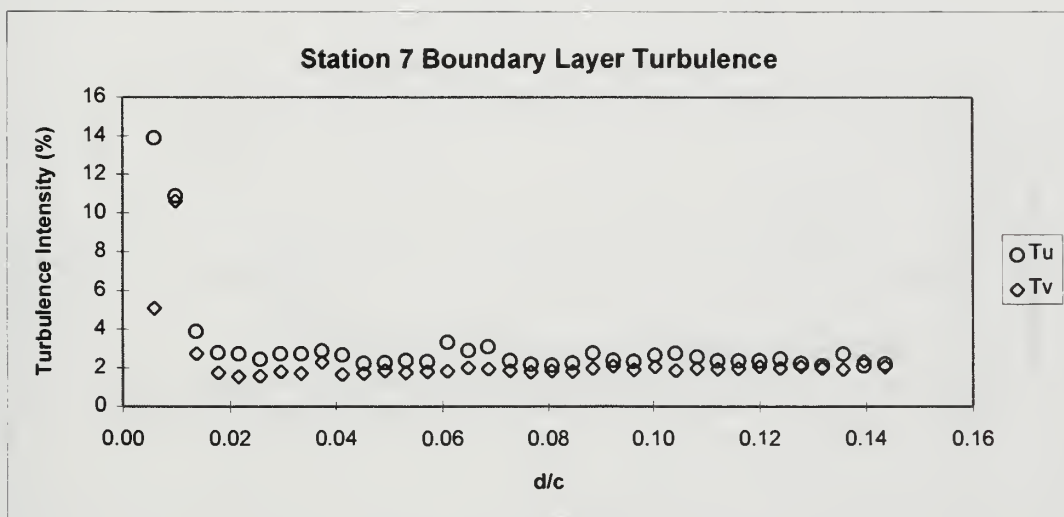
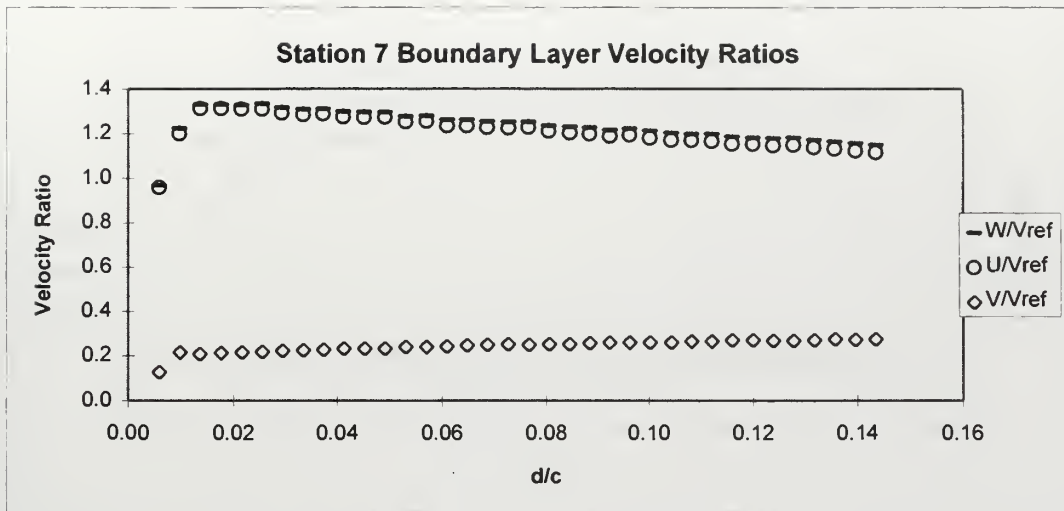


Figure 45. Station 7 Boundary Layer Survey Results at $Re=380,000$.

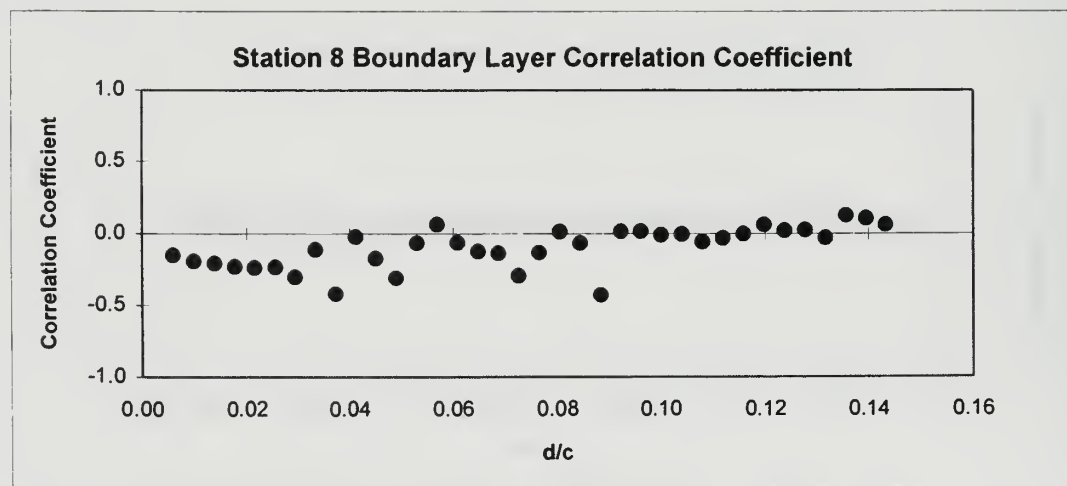
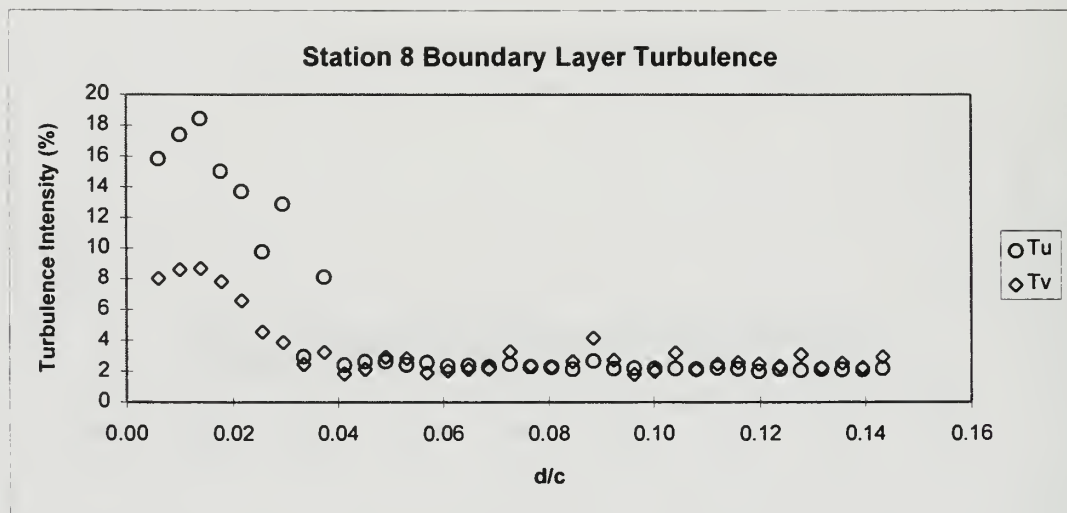
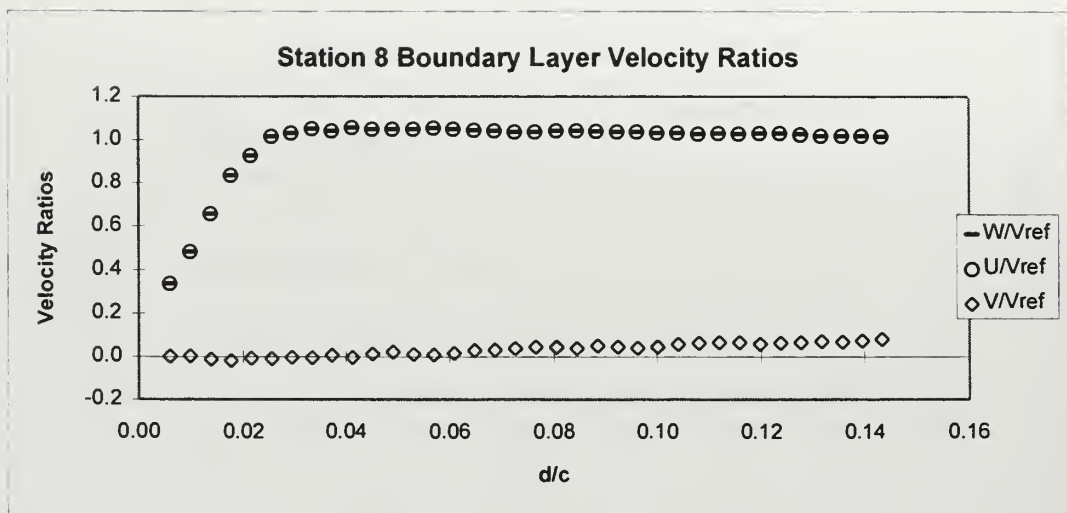


Figure 46. Station 8 Boundary Layer Survey Results at $Re=380,000$.

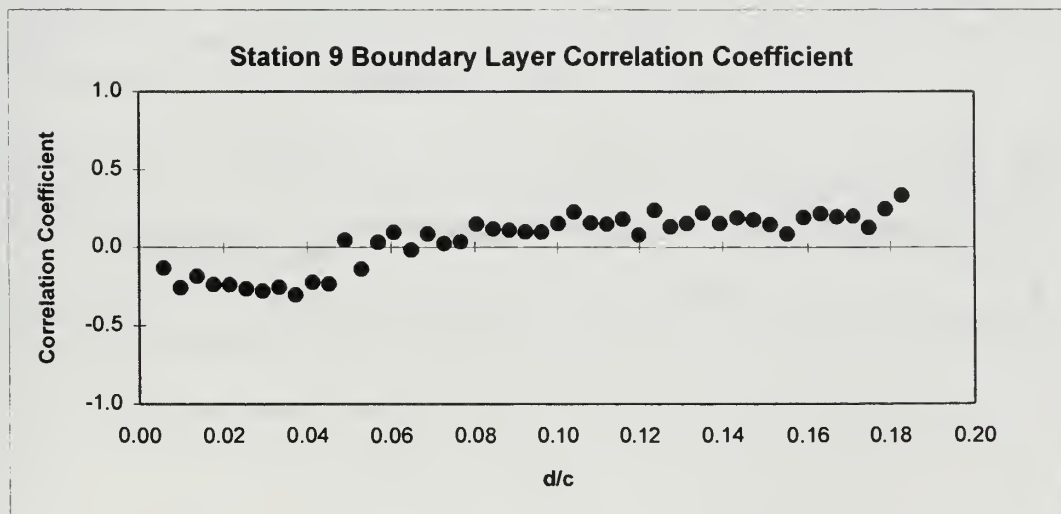
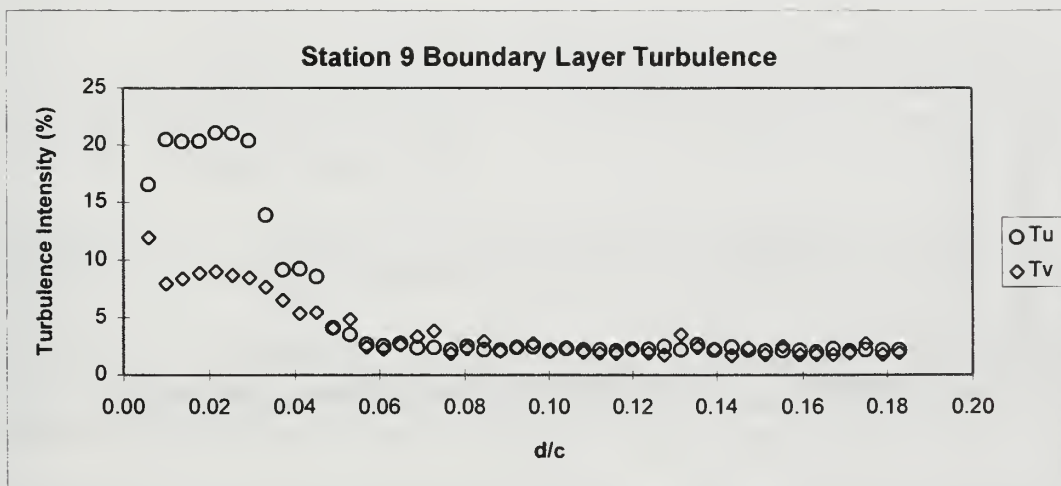
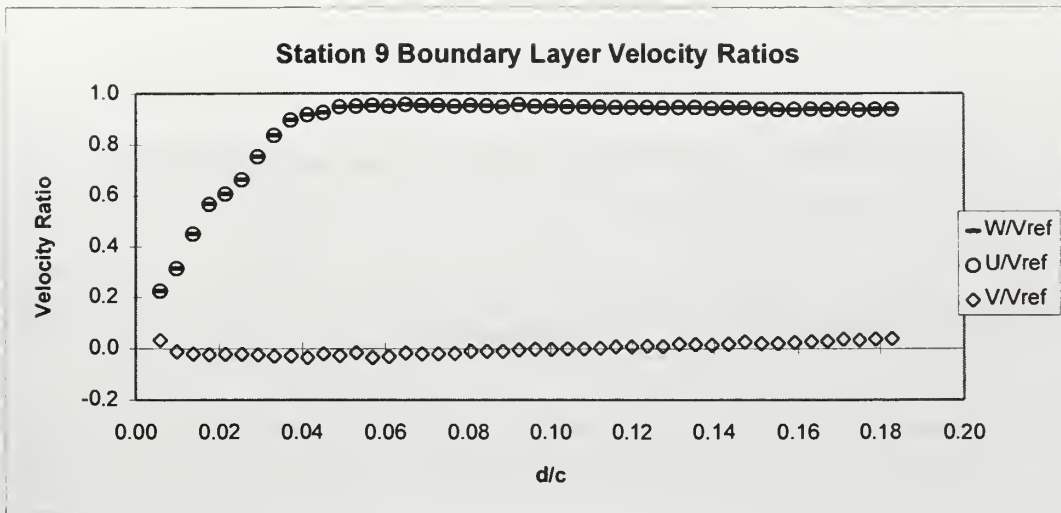


Figure 47. Station 9 Boundary Layer Survey Results at $Re=380,000$.

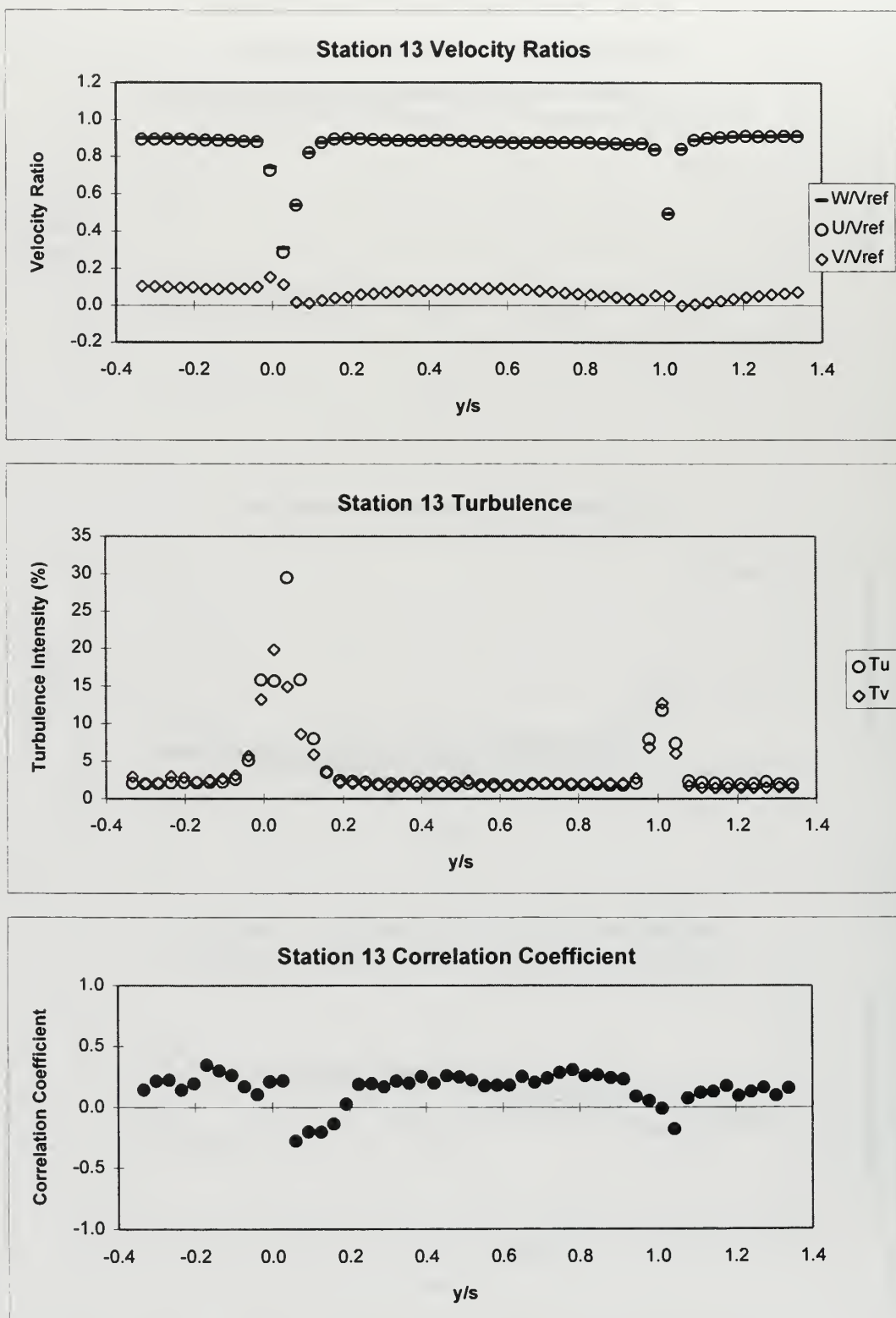


Figure 48. Station 13 Wake Survey Results at $Re=380,000$.

LIST OF REFERENCES

1. Gelder, T. F., Schmidt, J. F., Suder, K. L., and Hathaway, M. D., "Design and Performance of Controlled-Diffusion Stator Compared With Original Double-Circular-Arc Stator", NASA Technical Paper 2852, March, 1989.
2. Sanger, N. L., "The Use of Optimization Techniques to Design Controlled-Diffusion Compressor Blading", *ASME Journal of Engineering for Power*, Vol. 105, 1986.
3. Hansen, D. J., "Investigation of Second Generation Controlled-Diffusion Compressor Blades in Cascade", Master's Thesis, Naval Postgraduate School, Monterey, California, September, 1995.
4. Elazar, Y., "A Mapping of the Viscous Flow Behavior in a Controlled Diffusion Compressor Cascade Using Laser Doppler Velocimetry and Preliminary Evaluation of Codes for the Prediction of Stall", Ph.D. Dissertation, Naval Postgraduate School, Monterey, California, March, 1988.
5. Classick, M. A., "Off-Design Loss Measurements in a Compressor Cascade", Master's Thesis, Naval Postgraduate School, Monterey, California, September, 1989.
6. Murray, K. D., "Automation and Extension of LDV Measurements of Off-Design Flow in a Subsonic Cascade Wind Tunnel", Master's Thesis, Naval Postgraduate School, Monterey, California, June, 1989.
7. Williams, A. J. H., "Laser-Doppler Velocimetry and Viscous Flow Computation of the Flow Through A Compressor Cascade Near Stall", Master's Thesis, Naval Postgraduate School, June, 1995.
8. Hobson, G. V., and Shreeve, R. P., "Inlet Turbulence Distortion and Viscous Flow Development in a Controlled-Diffusion Compressor Cascade at Very High Incidence", *Journal of Propulsion and Power*, Vol. 9, No. 3, May-June, 1993.
9. Roberts, W. B., "The Effect of Reynolds Number and Laminar Separation on Axial Cascade Performance", *Journal of Engineering for Power*, April, 1975.

10. Webber, M. A., "Determining the Effect of Endwall Boundary Layer Suction in a Large Scale Subsonic Compressor Cascade", Master's Thesis, Naval Postgraduate School, Monterey, California, March, 1993.
11. Fitzgerald, E. J., and Mueller, T. J., "Measurements in a Separation Bubble on an Airfoil Using Laser Velocimetry", *AIAA Journal*, Vol. 28, No. 4, April, 1990.

INITIAL DISTRIBUTION LIST

1. Defense Technical Information Center 2
8725 John J. Kingman Rd., STE 0944
Ft. Belvoir, VA 22060-6218
2. Dudley Knox Library 2
Naval Postgraduate School
411 Dyer Rd.
Monterey, CA 93943-5101
3. Department Chairman 1
Department of Aeronautics and Astronautics
Code AA
Naval Postgraduate School
699 Dyer Road Room 137
Monterey, CA 93943-5106
4. Professor R. P. Shreeve 1
Department of Aeronautics and Astronautics
Code AA/Sf
Naval Postgraduate School
699 Dyer Road Room 137
Monterey, CA 93943-5106
5. Assoc. Prof. G. V. Hobson 7
Department of Aeronautics and Astronautics
Code AA/Hg
Naval Postgraduate School
699 Dyer Road Room 137
Monterey, CA 93943-5106
6. Naval Air Systems Command 1
AIR-4.4T (Attn: Mr. C. Gordon)
Washington, DC 20361-5360
7. Naval Air Warfare Center 1
Propulsion and Power Engineering
AIR-4.4.3.1 (Attn: S. McAdams)
Building 106, Sears Rd.
Patuxent River, MD 20670-5304

- | | |
|---|---|
| 8. Naval Air Systems Command
AIR-4.1.1 (Attn: Mr. S. Carson)
Arlington, VA 22243 | 1 |
| 9. Director, Marine Corps Research Center
MCCDC
Code C40RC
2040 Broadway Street
Quantico, VA 22134-5107 | 2 |
| 10. Director, Studies and Analysis Division
MCCDC
Code C45
3300 Russell Road
Quantico, VA 22134-5130 | 1 |
| 11. T. Gelder
211 44 Aberdeen
Rocky River, OH 44116 | 1 |
| 12. N. L. Sanger
752 Elmwood Rd.
Rocky River, OH 44116 | 1 |
| 13. David G. Schnorenberg
%James P. Schnorenberg
3425 High Road
Hartford, WI 53027 | 3 |

QUIDLEY KNOX LIBRARY
NAVAL POSTGRADUATE SCHOOL
MONTEREY CA 93943-5101

DUDLEY KNOX LIBRARY



3 2768 00323878 3